

สารออกฤทธิ์ทางชีวภาพจากใบแก้ว *Murraya paniculata* (L.) Jack



บทคัดย่อและแฟ้มข้อมูลฉบับเต็มของวิทยานิพนธ์ตั้งแต่ปีการศึกษา 2554 ที่ให้บริการในคลังปัญญาจุฬาฯ (CUIR)
เป็นแฟ้มข้อมูลของนิสิตเจ้าของวิทยานิพนธ์ ที่ส่งผ่านทางบัณฑิตวิทยาลัย

The abstract and full text of theses from the academic year 2011 in Chulalongkorn University Intellectual Repository (CUIR)
are the thesis authors' files submitted through the University Graduate School.

วิทยานิพนธ์นี้เป็นส่วนหนึ่งของการศึกษาตามหลักสูตรปริญญาวิทยาศาสตรมหาบัณฑิต
สาขาวิชาเคมี ภาควิชาเคมี
คณะวิทยาศาสตร์ จุฬาลงกรณ์มหาวิทยาลัย
ปีการศึกษา 2559
ลิขสิทธิ์ของจุฬาลงกรณ์มหาวิทยาลัย

BIOACTIVE COMPOUNDS FROM THE LEAVES OF *Murraya paniculata* (L.) Jack

Miss Nawara Samritsakulchai



A Thesis Submitted in Partial Fulfillment of the Requirements
for the Degree of Master of Science Program in Chemistry

Department of Chemistry

Faculty of Science

Chulalongkorn University

Academic Year 2016

Copyright of Chulalongkorn University

Thesis Title	BIOACTIVE COMPOUNDS FROM THE LEAVES OF <i>Murraya paniculata</i> (L.) Jack
By	Miss Nawara Samritsakulchai
Field of Study	Chemistry
Thesis Advisor	Assistant Professor Warinthorn Chavasiri, Ph.D.
Thesis Co-Advisor	Assistant Professor Preecha Lertpratchya, Ph.D.

Accepted by the Faculty of Science, Chulalongkorn University in Partial
Fulfillment of the Requirements for the Master's Degree

.....Dean of the Faculty of Science
(Associate Professor Polkit Sangvanich, Ph.D.)

THESIS COMMITTEE

.....Chairman
(Associate Professor Vudhichai Parasuk, Ph.D.)

.....Thesis Advisor
(Assistant Professor Warinthorn Chavasiri, Ph.D.)

.....Thesis Co-Advisor
(Assistant Professor Preecha Lertpratchya, Ph.D.)

.....Examiner
(Nawaporn Vinayavekhin, Ph.D.)

.....External Examiner
(Assistant Professor Veena Nukoolkarn, Ph.D.)

นวาระ สัมฤทธิ์สกุลชัย : สารออกฤทธิ์ทางชีวภาพจากใบแก้ว *Murraya paniculata* (L.) Jack (BIOACTIVE COMPOUNDS FROM THE LEAVES OF *Murraya paniculata* (L.) Jack) อ.ที่ปรึกษาวิทยานิพนธ์หลัก: ผศ. ดร.วรินทร์ ชวศิริ, อ.ที่ปรึกษาวิทยานิพนธ์ร่วม: ผศ. ดร.ปรีชา เลิศปรัชญา, 183 หน้า.

แก้วเป็นพืชเขตร้อนที่มีลักษณะเป็นไม้พุ่มกลมสีเขียวช่อ พบในภูมิภาคเอเชียใต้ เอเชียตะวันออกเฉียงใต้ จีนและออสเตรเลีย การศึกษาทางพฤกษเคมีเมื่อไม่นานมานี้ยืนยันความสัมพันธ์เชิงบวกระหว่างการใช้งานแบบดั้งเดิมกับสารออกฤทธิ์ที่หลากหลายขององค์ประกอบในกลุ่มคูมาริน ซินนาเมต ฟลาโวนและพอลิฟีนอล ในงานวิจัยนี้ ได้แยกสารสามสิบสามตัวจากใบแก้ว 2,6,2',6'-เทระเมทอกซี-4,4'-บิส-(1,2-แทรนส์-2,3-อีพอกซี-1-ไฮดรอกซีโพรพิล)ไบเฟนิล (20) และเมดิโอเรซินอล (21) ถูกรายงานครั้งแรกว่าเป็นส่วนประกอบในพืชชนิดนี้ ได้ทดสอบฤทธิ์ด้านการกินของแมลง ฤทธิ์ฆ่าแมลง ฤทธิ์ไล่แมลง ฤทธิ์ต้านแบคทีเรีย ฤทธิ์ต้านอนุมูลอิสระ ฤทธิ์ต้านการอักเสบและฤทธิ์ต้านฮิวแมนคาร์บอนิกแอนไฮเดรส II ของสารบางชนิด สารสกัดจากเมทานอลมีฤทธิ์ด้านการกินของหนอนกระทู้ผักด้วยดัชนีด้านการกิน 62% ฤทธิ์ฆ่าแมลงของสารหลัก 3 ชนิด ได้แก่ เมอแรงกทินแอสเทท (5), ออแรปทีน (2) และพีบาโลซิน (3) แสดงให้เห็นถึงอัตราการตายของตัวอ่อนในช่วง 80-93% ร่วมกับฤทธิ์การไล่ที่ดี มีเพียงสโกโปเลทิน (12) มีฤทธิ์ต้านอนุมูลอิสระปานกลางด้วยค่า IC_{50} 289 ไมโครกรัมต่อมิลลิลิตร อย่างไรก็ตามสารทั้งหมดไม่แสดงฤทธิ์ต้านเชื้อแบคทีเรียและต้านการอักเสบ เป็นที่น่าสนใจว่าเมอพานิคูอล (17) และออกทาทาโนอิลคูมาริน (35) สามารถยับยั้งการทำงานของเอนไซม์ฮิวแมนคาร์บอนิกแอนไฮเดรส II ที่ความเข้มข้นต่ำสุด (<0.032 ไมโครโมลาร์)

จุฬาลงกรณ์มหาวิทยาลัย
CHULALONGKORN UNIVERSITY

ภาควิชา เคมี
สาขาวิชา เคมี
ปีการศึกษา 2559

ลายมือชื่อนิสิต
ลายมือชื่อ อ.ที่ปรึกษาหลัก
ลายมือชื่อ อ.ที่ปรึกษาร่วม

5772025623 : MAJOR CHEMISTRY

KEYWORDS: MURRAYA PANICULATA / ANTIFEEDANT / INSECTICIDAL / REPELLENT / ANTIOXIDANT / ANTIBACTERIAL / ANTI-INFLAMMATORY / ANTI-HUMAN CARBONIC ANHYDRASE II

NAWARA SAMRITSAKULCHAI: BIOACTIVE COMPOUNDS FROM THE LEAVES OF *Murraya paniculata* (L.) Jack. ADVISOR: ASST. PROF. WARINTHORN CHAVASIRI, Ph.D., CO-ADVISOR: ASST. PROF. PREECHA LERTPRATCHYA, Ph.D., 183 pp.

Murraya paniculata (L.) Jack is a tropical evergreen rounded shrub found in South and Southeast Asia, China and Australia. Recent phytochemical studies revealed a positive correlation between the traditional usage and several groups of active constituents in the class of coumarin, cinnamate, flavone and polyphenol. In this work, thirty-three compounds were isolated from the leaves of *M. paniculata*. 2,6,2',6'-Tetramethoxy-4,4'-bis-(1,2-*trans*-2,3-epoxy-1-hydroxypropyl) biphenyl (20) and medioresinol (21) were reported for the first time as constituents in this plant. Antifeedant, insecticidal, repellent, antibacterial, antioxidant, anti-inflammatory and antihuman carbonic anhydrase II activities of some isolated compounds were investigated. The MeOH extract exhibited antifeedant activity against *S. litura* larva with 62% antifeedant index. Insecticidal activity of three main compounds, murrangatin acetate (5), auraptene (2) and phebalosin (3) exhibited the high percentage of larval mortality in range of 80-93%, together with good repellent activity. Only scopoletin (12) displayed moderate antioxidant activity with IC₅₀ 289 µg/mL. Nonetheless, all compounds did not show antibacterial and anti-inflammatory activity. Interestingly, murpaniculol (17) and octanoyl coumarin (35) inhibited the activity of human carbonic anhydrase II at the lowest concentration of <0.032 µM.

Department: Chemistry

Field of Study: Chemistry

Academic Year: 2016

Student's Signature

Advisor's Signature

Co-Advisor's Signature

ACKNOWLEDGEMENTS

The author would like to prompt her highest acknowledgment to her advisor, Assistant Professor Dr. Warinthorn Chavasiri and her co-advisor, Assistant Professor Dr. Preecha Lertpratchya for their valuable advices, very kind assistance, generous guidance and encouragement throughout the course of this research. Furthermore sincere thanks are extended to NPRU, Department of Chemistry, Chulalongkorn University.

The author wishes to express appreciation to Associate Professor Dr. Vudhichai Parasuk, Dr. Nawaporn Vinayavekhin and Assistant Professor Dr. Veena Nukoolkarn serving as a chairman and members of this thesis committee, respectively, for their valuable suggestions and comments.

The author express her gratitude toward Professor Dr. Jun Wu, Marine Drugs Research Center, College of Pharmacy, Jinan University, P. R. China for providing the knowledge in HPLC separation, Associate Professor Dr. Chulee Yompakdee, Department of Microbiology, Faculty of Science, Chulalongkorn University for the testing on antihuman carbonic anhydrase II activity and Associate Professor Dr. Tanapat Palaga, Department of Microbiology, Faculty of Science, Chulalongkorn University for his help in anti-inflammatory testing.

Further acknowledgement is extended to her parents, sister and friends for their love, inspiration, friendliness, understanding, helpful advice, great support and encouragement throughout her entire education. Finally, the author would like to thank all members of NPRU for their assistance in her experiments and their kind suggestion during research.

CONTENTS

	Page
THAI ABSTRACT	iv
ENGLISH ABSTRACT	v
ACKNOWLEDGEMENTS	vi
CONTENTS	vii
LIST OF TABLES	xi
LIST OF FIGURES	xv
LIST OF SCHEMES	xix
LIST OF ABBREVIATIONS	xx
CHAPTER I INTRODUCTION.....	1
1.1 Botanical characteristics of <i>Murraya paniculata</i> (L.) Jack.....	2
1.2 Chemical constituent studies on <i>Murraya paniculata</i>	2
1.3 Biological activity studies on <i>Murraya paniculata</i>	6
1.4 Insect bioassay	10
1.4.1 Antifeedant activity.....	10
1.4.2 Insecticidal activity.....	10
1.4.3 Repellent activity.....	10
1.5 Antibacterial activity.....	11
1.6 Anti-inflammatory activity.....	11
1.7 Antioxidant activity	12
1.8 Anti-human carbonic anhydrase isozyme II activity	13
1.9 The goal of this research.....	13
CHAPTER II MATERIAL AND METHODS	14

	Page
2.1 Plant materials	14
2.2 Instrument and equipment	14
2.3 Extraction procedure.....	15
2.4 Isolation and purification procedure.....	16
2.4.1 Separation of Fraction I	16
2.4.1.1 Separation of Fraction I-8	17
2.4.2 Separation of Fraction II	18
2.4.2.1 Separation of Fraction II-4.....	18
2.4.2.2 Separation of Fraction II-8.....	19
2.4.3 Separation of Fraction III.....	20
2.4.3.1 Separation of Fraction III-4.....	20
2.4.3.1 Separation of Fraction III-9.....	21
2.4.4 Separation of Fraction VI.....	21
2.4.4.1 Separation of Fraction VI-I	22
2.4.4.2 Separation of Fraction VI-II.....	23
2.4.4.3 Further Separation of Fraction VI-II.....	25
2.5 Synthesis of Coumarin Derivatives	35
2.5.1 General Esterification Procedure	35
2.5.2 General Alkylation Procedure	37
2.6 Bioassay.....	39
2.6.1 Exploration for insect control agent	39
2.6.1.1 Antifeedant activity	39
2.6.1.2 Insecticide activity	40

	Page
2.6.1.3 Repellent activity.....	40
2.6.2 Antibacterial activity.....	41
2.6.3 Anti-inflammatory activity.....	42
2.6.3.1 Cell culture.....	42
2.6.3.2 Cell viability assay.....	42
2.6.3.3 Nitrite assay.....	43
2.6.4 Antioxidant activity.....	43
2.6.5 Anti-human carbonic anhydrase activity.....	44
CHAPTER III RESULTS AND DISCUSSION.....	46
3.1 Extraction of <i>M. paniculata</i> leaves.....	46
3.2 Chemical constituents of <i>M. paniculata</i> leaves.....	47
3.2.1 Separation of Fraction I and structural elucidation of its constituents.....	47
3.2.2 Separation of Fraction II and structural elucidation of its constituents.....	49
3.2.3 Separation of Fraction III and structural elucidation of its constituents.....	53
3.2.4 Separation of Fraction VI and structural elucidation of its constituents.....	57
3.2.4.1 Separation of Fraction VI-I and structural elucidation of its constituents.....	57
3.2.4.2 Separation of Fraction VI-II (Part 1) and structural elucidation of its constituents.....	60
3.2.4.3 Separation of Fraction VI-II (Part 2) and structural elucidation of its constituents.....	69
3.3 Synthesis of coumarin derivatives.....	115
3.3.1 Ester derivatives.....	115
3.3.2 Ether derivatives.....	117

3.4 Biological activities of isolated compounds from <i>M. paniculata</i> leaves and related compounds.....	119
3.4.1 Exploration for insect control agent.....	119
3.4.1.1 Antifeedant activity.....	119
3.4.1.2 Insecticidal activity.....	122
3.4.1.3 Repellent activity.....	123
3.4.2 Antibacterial activity.....	126
3.4.3 Anti-inflammatory activity.....	127
3.4.4 Antioxidant activity.....	130
3.4.5 Anti-Human carbonic anhydrase II activity.....	132
3.5 Structure-Activity Relationship (SAR) study.....	135
CHAPTER IV CONCLUSION.....	137
REFERENCES.....	140
APPENDIX.....	146
VITA.....	183

LIST OF TABLES

	Page
Table 1.1 Chemical constituents of <i>Murraya paniculata</i>	3
Table 2.1 The synthesis of ester analogues of 7-hydroxycoumarin from carboxylic acids	36
Table 2.2 Alkylation of 7-hydroxycoumarin from alkyl halides	38
Table 3.1 The comparison of ^1H NMR spectral assignment of compound 1 and murraxocin acetate	48
Table 3.2 The comparison of ^1H and ^{13}C NMR spectral assignment of compound 2 and auraptene	50
Table 3.3 The comparison of ^1H and ^{13}C NMR spectral assignment of compound 3 and phebalosin	52
Table 3.4 The comparison of ^1H NMR spectral assignment of compound 4 and hainanmurpanin	54
Table 3.5 The comparison of ^1H and ^{13}C NMR spectral assignment of compound 5 and murrangatin acetate	55
Table 3.6 The comparison of ^1H and ^{13}C NMR spectral assignment of compound 6 and methyl ferulate	58
Table 3.7 The comparison of ^1H NMR spectral assignment of compound 7 and 3,4- <i>O</i> -dimethylcaffeic acid methyl ester	60
Table 3.8 The comparison of ^1H and ^{13}C NMR spectra assignment of compound 8 and minumicrolin	62
Table 3.9 The comparison of ^1H and ^{13}C NMR spectra assignment of compound 9 and murracarpin	64
Table 3.10 The comparison of ^1H and ^{13}C NMR spectral assignment of compound 10 and omphalocarpin	66

LIST OF TABLES

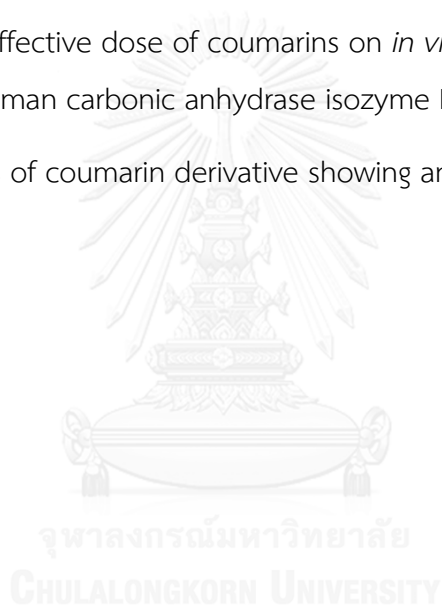
	Page
Table 3.11 The comparison of ^{13}C NMR spectral assignment of compound 11 and 3,5,7,3',4',5'-hexamethoxyflavone	68
Table 3.12 The comparison of ^1H and ^{13}C NMR spectral assignment of compound 12 and scopoletin	71
Table 3.13 The comparison of ^1H and ^{13}C NMR spectral assignment of compound 13 and meranzin hydrate	73
Table 3.14 The comparison of ^1H and ^{13}C NMR spectral assignment of compound 14 and albiflorin 3.....	75
Table 3.15 The comparison of ^1H and ^{13}C NMR spectral assignment of compound 15 and (-)-murrangatin	77
Table 3.16 The comparison of ^1H and ^{13}C NMR spectral assignment of compound 16 and muralatin K.....	79
Table 3.17 The comparison of ^1H and ^{13}C NMR spectral assignment of compound 17 and murpaniculol.....	81
Table 3.18 The comparison of ^1H and ^{13}C NMR spectral assignment of compound 18 and murralongin	83
Table 3.19 The comparison of ^1H and ^{13}C NMR spectral assignment of compound 19 and murrangatin acetate	85
Table 3.20 The comparison of ^1H and ^{13}C NMR spectral assignment of compound 20 and 2,6,2',6'-tetramethoxy-4,4'-bis(1,2- <i>trans</i> -2,3-epoxy-1-hydroxypropyl)biphenyl	87
Table 3.21 The comparison of ^1H and ^{13}C NMR spectral assignment of compound 21 and medioresinol	88

LIST OF TABLES

	Page
Table 3.22 The comparison of ^1H and ^{13}C NMR spectral assignment of compound 22 and albiflorin 2.....	91
Table 3.23 The comparison of ^1H and ^{13}C NMR spectral assignment of compound 23 and (+)murrangatin	93
Table 3.24 The comparison of ^1H and ^{13}C NMR spectral assignment of compound 24 and murpaninulol senecioate	95
Table 3.25 ^1H and ^{13}C NMR spectral assignment of compound 25	98
Table 3.26 The comparison of ^1H and ^{13}C NMR spectral assignment of compound 26 and auraptenol	100
Table 3.27 The comparison of ^{13}C NMR spectral assignment of compound 27 and 3,5,7,8,3',4'-hexamethoxyflavone	102
Table 3.28 The comparison of ^1H and ^{13}C NMR spectral assignment of compound 28 and 3,5,7,8,3',4',5'-heptamethoxyflavone	103
Table 3.29 The comparison of ^1H NMR spectral assignment of compound 29 and 3,5,6,7,3',4',5'-heptamethoxyflavone	105
Table 3.30 The comparison of ^1H NMR spectral assignment of compound 30 and 3,6,7,8,2',5'-hexamethoxyflavone	108
Table 3.31 The comparison of ^{13}C NMR spectral assignment of compound 31 and 5,6,7,3',4',5'-hexamethoxyflavone	110
Table 3.32 The ^1H and ^{13}C NMR spectral assignment of compound 32	112
Table 3.33 The comparison of ^{13}C NMR spectral assignment of compound 33 and 5,6,7,8,3',4',5'-heptamethoxyflavone	114
Table 3.34 The ^1H NMR spectral assignment of compounds 34-37	117
Table 3.35 The ^1H NMR spectral assignment of compounds 38 and 39	118

LIST OF TABLES

	Page
Table 3.36 The PR values of isolated compounds on <i>Ferrisia virgate</i> adults	124
Table 3.37 The PR values of phebalosin (3) on <i>F. virgate</i> adults	125
Table 3.38 Antibacterial activity of compounds 2 , 3 and 5	126
Table 3.39 Antioxidant activity of selected isolated compounds from the leaves of <i>M. paniculata</i>	131
Table 3.40 Minimal effective dose of coumarins on <i>in vivo</i> inhibitory activity against human carbonic anhydrase isozyme II	133
Table 3.41 Structures of coumarin derivative showing anti-hCA II activity	136



LIST OF FIGURES

	Page
Figure 1.1 All parts of <i>Murraya paniculata</i> a) tree b) leaves c) flowers d) fruits.....	2
Figure 1.2 The chemical constituents of <i>Murraya</i> plants	4
Figure 3.1 The structures of compounds 34, 35, 36 and 37	116
Figure 3.2 The structures of compounds 38 and 39	117
Figure 3.3 Antifeedant index (%) of the crude extracts from <i>M. paniculata</i> leaves.	119
Figure 3.4 Antifeedant index (%) of compounds 2, 3 and 5	120
Figure 3.5 Insecticidal activity of compounds from <i>M. paniculata</i> on larvae of <i>S. litura</i>	122
Figure 3.6 Repellent activity of phebalosin (3) on adults of <i>Ferrisia virgate</i> (Cockerell).....	126
Figure 3.7 Effect of compounds 1, 2, 3, 5, 6, 8, 9, 10, 11, 12, 15, 17, 18, 25, 26, 28, 29 and 33 on the viability of RAW 264.7 cells by the MTT assay.....	128
Figure 3.8 The inhibitory activity on NO production when treated with compounds 1, 2, 3, 5, 6, 8, 9, 10, 11, 12, 15, 17, 18, 25, 26, 28, 29 and 33	129
Figure A-1 The ¹ H NMR spectrum (CDCl ₃) of compound 1	147
Figure A-2 The ¹³ C NMR spectrum (CDCl ₃) of compound 1	147
Figure A-3 The ¹ H NMR spectrum (CDCl ₃) of compound 2	148
Figure A-4 The ¹³ C NMR spectrum (CDCl ₃) of compound 2	148
Figure A-5 The ¹ H NMR spectrum (CDCl ₃) of compound 3	149
Figure A-6 The ¹³ C NMR spectrum (CDCl ₃) of compound 3	149
Figure A-7 The ¹ H NMR spectrum (CDCl ₃) of compound 4	150
Figure A-8 The ¹ H NMR spectrum (CDCl ₃) of compound 5	151

LIST OF FIGURES

	Page
Figure A-9 The ^{13}C NMR spectrum (CDCl_3) of compound 5	151
Figure A-10 The ^1H NMR spectrum (CDCl_3) of compound 6	152
Figure A-11 The ^{13}C NMR spectrum (CDCl_3) of compound 6	152
Figure A-12 The ^1H NMR spectrum (CDCl_3) of compound 7	153
Figure A-13 The ^{13}C NMR spectrum (CDCl_3) of compound 7	153
Figure A-14 The ^1H NMR spectrum (CDCl_3) of compound 8	154
Figure A-15 The ^{13}C NMR spectrum (CDCl_3) of compound 8	154
Figure A-16 The ^1H NMR spectrum (CDCl_3) of compound 9	155
Figure A-17 The ^{13}C NMR spectrum (CDCl_3) of compound 9	155
Figure A-18 The ^1H NMR spectrum (CDCl_3) of compound 10	156
Figure A-19 The ^{13}C NMR spectrum (CDCl_3) of compound 10	156
Figure A-20 The ^1H NMR spectrum (CDCl_3) of compound 11	157
Figure A-21 The ^{13}C NMR spectrum (CDCl_3) of compound 11	157
Figure A-22 The ^1H NMR spectrum (CDCl_3) of compound 12	158
Figure A-23 The ^{13}C NMR spectrum (CDCl_3) of compound 12	158
Figure A-24 The ^1H NMR spectrum (CDCl_3) of compound 13	159
Figure A-25 The ^{13}C NMR spectrum (CDCl_3) of compound 13	159
Figure A-26 The ^1H NMR spectrum (CDCl_3) of compound 14	160
Figure A-27 The ^{13}C NMR spectrum (CDCl_3) of compound 14	160
Figure A-28 The ^1H NMR spectrum (CDCl_3) of compound 15	161
Figure A-29 The ^{13}C NMR spectrum (CDCl_3) of compound 15	161

LIST OF FIGURES

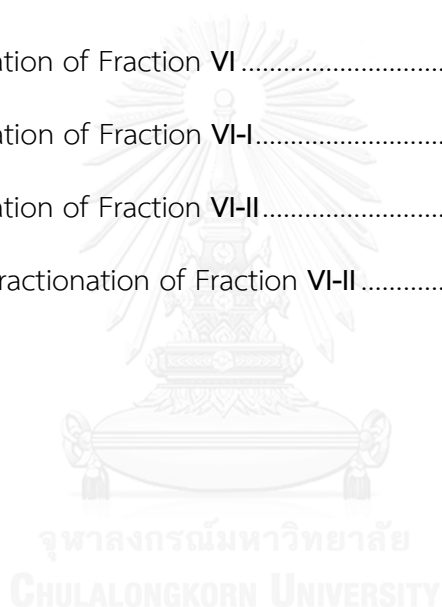
	Page
Figure A-30 The ^1H NMR spectrum (CDCl_3) of compound 16	162
Figure A-31 The ^{13}C NMR spectrum (CDCl_3) of compound 16	162
Figure A-32 The ^1H NMR spectrum (CDCl_3) of compound 17	163
Figure A-33 The ^{13}C NMR spectrum (CDCl_3) of compound 17	163
Figure A-34 The ^1H NMR spectrum (CDCl_3) of compound 18	164
Figure A-35 The ^{13}C NMR spectrum (CDCl_3) of compound 18	164
Figure A-36 The ^1H NMR spectrum (CDCl_3) of compound 19	165
Figure A-37 The ^{13}C NMR spectrum (CDCl_3) of compound 19	165
Figure A-38 The ^1H NMR spectrum (CDCl_3) of compound 20	166
Figure A-39 The ^{13}C NMR spectrum (CDCl_3) of compound 20	166
Figure A-40 The ^1H NMR spectrum (CDCl_3) of compound 21	167
Figure A-41 The ^{13}C NMR spectrum (CDCl_3) of compound 21	167
Figure A-42 The ^1H NMR spectrum (CDCl_3) of compound 22	168
Figure A-43 The ^{13}C NMR spectrum (CDCl_3) of compound 22	168
Figure A-44 The ^1H NMR spectrum (CDCl_3) of compound 23	169
Figure A-45 The ^{13}C NMR spectrum (CDCl_3) of compound 23	169
Figure A-46 The ^1H NMR spectrum (CDCl_3) of compound 24	170
Figure A-47 The ^{13}C NMR spectrum (CDCl_3) of compound 24	170
Figure A-48 The ^1H NMR spectrum (CDCl_3) of compound 25	171
Figure A-49 The ^{13}C NMR spectrum (CDCl_3) of compound 25	171
Figure A-50 The ^1H NMR spectrum (CDCl_3) of compound 26	172

LIST OF FIGURES

	Page
Figure A-51 The ^{13}C NMR spectrum (CDCl_3) of compound 26	172
Figure A-52 The ^1H NMR spectrum (CDCl_3) of compound 27	173
Figure A-53 The ^{13}C NMR spectrum (CDCl_3) of compound 27	173
Figure A-54 The ^1H NMR spectrum (CDCl_3) of compound 28	174
Figure A-55 The ^{13}C NMR spectrum (CDCl_3) of compound 28	174
Figure A-56 The ^1H NMR spectrum (CDCl_3) of compound 29	175
Figure A-57 The ^{13}C NMR spectrum (CDCl_3) of compound 29	175
Figure A-58 The ^1H NMR spectrum (CDCl_3) of compound 30	176
Figure A-59 The ^{13}C NMR spectrum (CDCl_3) of compound 30	176
Figure A-60 The ^1H NMR spectrum (CDCl_3) of compound 31	177
Figure A-61 The ^{13}C NMR spectrum (CDCl_3) of compound 31	177
Figure A-62 The ^1H NMR spectrum (CDCl_3) of compound 32	178
Figure A-63 The ^{13}C NMR spectrum (CDCl_3) of compound 32	178
Figure A-64 The ^1H NMR spectrum (CDCl_3) of compound 33	179
Figure A-65 The ^{13}C NMR spectrum (CDCl_3) of compound 33	179
Figure A-66 The ^1H NMR spectrum (CDCl_3) of compound 34	180
Figure A-67 The ^1H NMR spectrum (CDCl_3) of compound 35	180
Figure A-68 The ^1H NMR spectrum (CDCl_3) of compound 36	181
Figure A-69 The ^1H NMR spectrum (CDCl_3) of compound 37	181
Figure A-70 The ^1H NMR spectrum (CDCl_3) of compound 38	182
Figure A-71 The ^1H NMR spectrum (CDCl_3) of compound 39	182

LIST OF SCHEMES

	Page
Scheme 2.1 The extraction procedure for <i>M. paniculata</i> leaves	15
Scheme 2.2 The further extraction procedure for Fraction IV	16
Scheme 2.3 Fractionation of Fraction I	17
Scheme 2.4 Fractionation of Fraction II	18
Scheme 2.5 Fractionation of Fraction III	20
Scheme 2.6 Fractionation of Fraction VI	22
Scheme 2.7 Fractionation of Fraction VI-I	22
Scheme 2.8 Fractionation of Fraction VI-II	24
Scheme 2.9 Further fractionation of Fraction VI-II	26



LIST OF ABBREVIATIONS

CH ₃ CN	acetonitrile
conc.	concentrated
CO ₂	carbondioxide
CHCl ₃	chloroform
CDCl ₃	chloroform-D
J	coupling constant (NMR)
δ	chemical shift
DSS	dextran sulfate sodium
°C	degree of Celsius
CH ₂ Cl ₂	dichloromethane
d	doublet (NMR)
dd	doublet of doublets (NMR)
DMEM	dulbecco's modified eagle medium
DMSO	dimethylsulfoxide
DPPH	2,2-diphenyl-1-picrylhydrazyl
dt	doublet of triplets (NMR)
ERK	extracellular signal-regulated kinases

LIST OF ABBREVIATIONS

equiv.	equivalent (s)
EtOAc	ethyl acetate
EtOH	ethanol
FBS	fetal bovine serum
g	gram (s)
Hz	hertz
h	hour (s)
HCl	hydrochloric acid
HPLC	high performance liquid chromatography
hCA	human carbonic anhydrase
IFN	Interferon
IL	Interleukin
IC ₅₀	inhibition concentration 50 %
IZ	inhibition zone
LPS	lipopolysaccharide
m	multiplet (NMR)
MeOH	methanol

LIST OF ABBREVIATIONS

μg	microgram (s)
μM	micromolar (s)
mg	milligram (s)
mm	millimeter (s)
min	minute (s)
mL	milliliter (s)
mmol	millimole (s)
MHz	megahertz
NF- κ B	nuclear factor-kappaB
NO	nitric oxide
nm	nanometer
MTT	3-(4,5-dimethylthiazol-2-yl)-2,5-diphenyltetrazolium bromide
NADH	β -nicotinamide adenine dinucleotide
NMR	nuclear magnetic resonance
K_2CO_3	potassium carbonate
%	percent
Ph	phenyl

LIST OF ABBREVIATIONS

pH	potential of Hydrogen ion
PMS	phenazine methosulfate
ppm	part per million
q	quartet (NMR)
qui	quintet (NMR)
R _f	retention factor
rt	room temperature
Na ₂ SO ₄	sodium sulfate
s	singlet (NMR)
sEH	soluble epoxide hydrolase
TNBS	2,4,6-trinitrobenzenesulfonic acid
PPh ₃	triphenylphosphine
TNF	tumor necrosis factor
t	triplet (NMR)
CCl ₃ CN	trichloroacetonitrile
TLC	thin layer chromatograph
UV	ultraviolet

LIST OF ABBREVIATIONS

v/v	volume per volume
H ₂ O	water
w/w	weight per weight
w/v	weight per volume



CHAPTER I

INTRODUCTION

Many plants in Thailand are medicinal potent. Various medicinal plants have long been used as the primary source of medicine. Nowadays, certain diseases have no drug for treatment. Although some diseases have drug to treat but there are many disadvantages such as toxic, tissue distribution, central nervous system penetration, and high cost. Thus, the study on chemical constituents from medicinal plants together with their pharmacological activities and toxicity are important for development of new medicinal drugs.

The genus *Murraya* belongs to family Rutaceae. There are many species in this genus such as *M. alata*, *M. crenulata*, *M. euchrestifolia*, *M. koenigii*, *M. kwangsiensis*, *M. microphylla*, *M. ovatifoliolata*, *M. paniculata*, *M. stenocarpa* and *M. tetramera*. *Murraya* species are used in landscaping. Some species can be grafted onto citrus rootstocks. Many species have been used in traditional medicine, with various parts of the plants used to treat fever, pain, and dysentery. *M. paniculata*, known in Thai as Kaew, has traditionally found wide medicinal uses in Southeast Asia and China. Several reports on chemical constituents of this plant including flavonoids, flavones, indole alkaloids, coumarins, monoterpenes, sesquiterpenes and cinnamates were addressed.

1.1 Botanical characteristics of *Murraya paniculata* (L.) Jack

M. paniculata (L.) Jack is a small, smooth tree, growing from 3 to 8 m in height, and having very hard wood (Figure 1.1). Leaves are 8 to 15 cm long, with usually 7 to 9 leaflets on each side, oblong to ovate, elliptic or sub rhomboid, and 2 to 7 cm. Stems are hairy. Flowers are few, white, very fragrant, 1.5 to 2 cm long, and borne on short, terminal or axillary cymes. Fruits are fleshy, red when ripe, pointed or oval-shaped, 1 to 1.5 cm



Figure 1.1 All parts of *Murraya paniculata* a) tree b) leaves c) flowers d) fruits

1.2 Chemical constituent studies on *Murraya paniculata*

From literature review, the chemical constituents of *Murraya* plants were investigated as collected in Table 1.1.

Table 1.1 Chemical constituents of *Murraya paniculata*

Plant parts	Crude extract	Substance	Reference
Flowers	MeOH	omphalocarpin, (-)-murracarpin, murrayacarpin-A and murrayacarpin-B	[1]
Leaves	acetone	peroxyauraptanol, <i>cis</i> -dehydroosthol, murraol, murranganon, isomurranganon senecioate, murrangatin acetate, isomurralonginol acetate and chlitolol	[2]
Leaves	EtOH	murrangatin and murracarpin	[3]
Leaves	chloroform	5,7,3',4',5'-pentamethoxyflavone, 5,7,8,3',4',5'-hexamethoxyflavone, 3,5,7,3',4',5'-hexamethoxyflavone, 3,5,7,8,3',4',5'-heptamethoxyflavone, 3-hydroxy-5,7,3',4',5'-pentamethoxyflavone	[4]
Leaves	benzene	auraptanol	[5]
Leaves	MeOH	murrayanone and murraculatin	[6]
Leaves	acetone	peroxymurraol and paniculonol isovalerate	[7]
Leaves	chloroform	paniculin, coumurrin and murpaniculol	[8]
Leaves	acetone	omphamurrayin	[9]
Leaves	EtOH	murrmeranzin and murralonginal	[10]
Leaves	Petroleum ether, chloroform and MeOH	auraptene, trans-gleinadiene, and toddalenone	[11]
Leaves	MeOH	kimcuongin and murracarpin	[12]

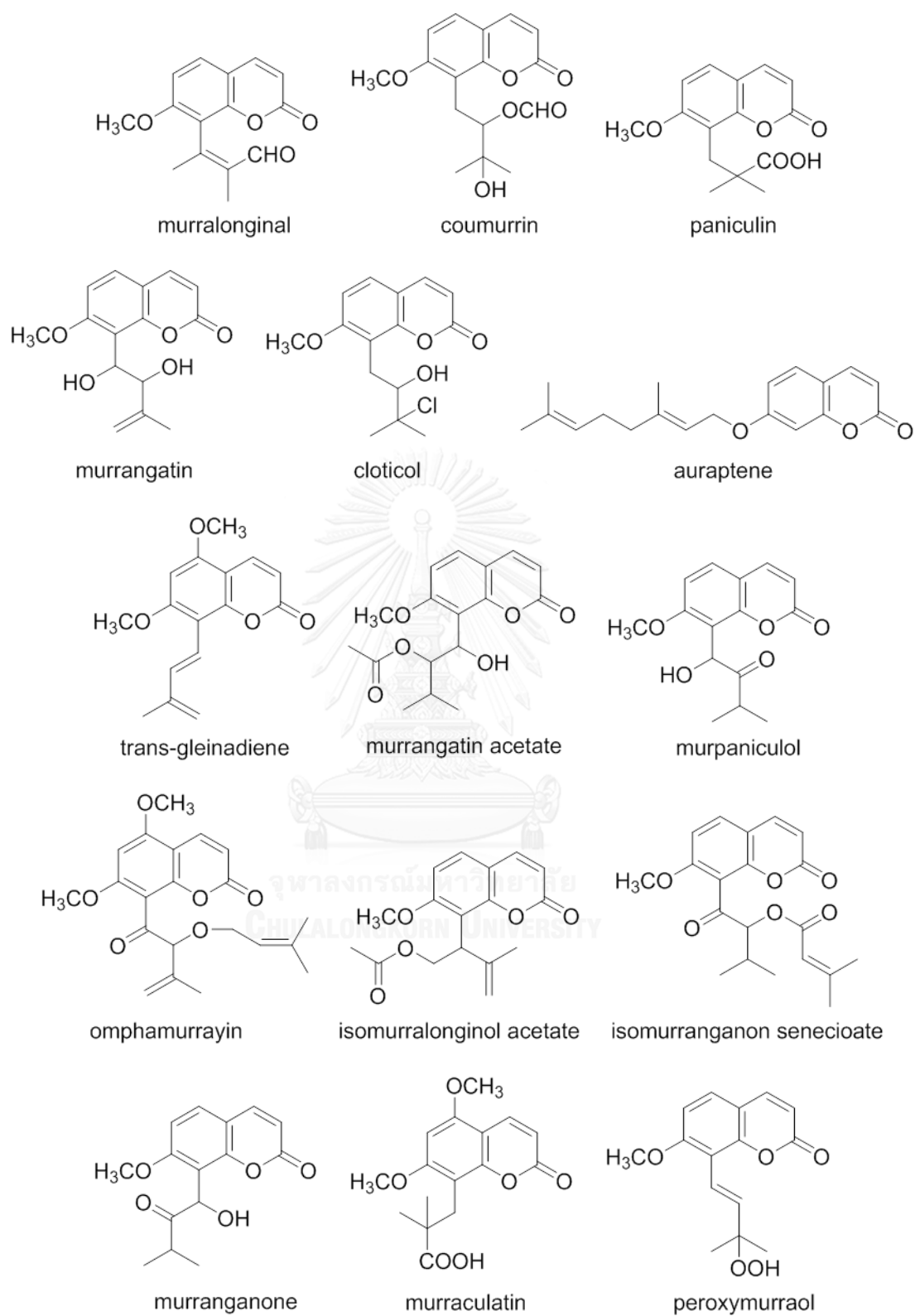


Figure 1.2 The chemical constituents of *Murraya* plants

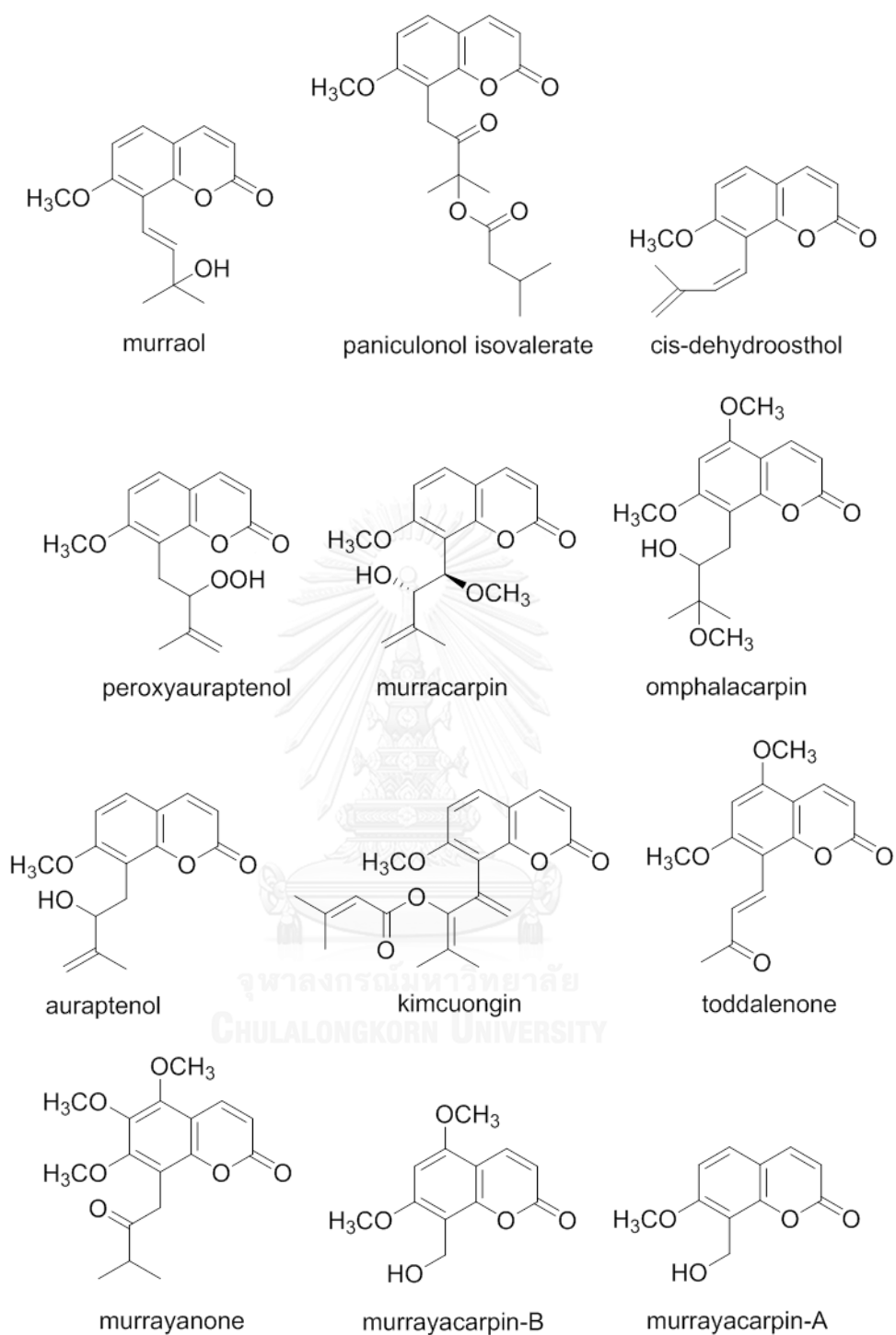


Figure 1.2 The chemical constituents of *Murraya* plants (cont)

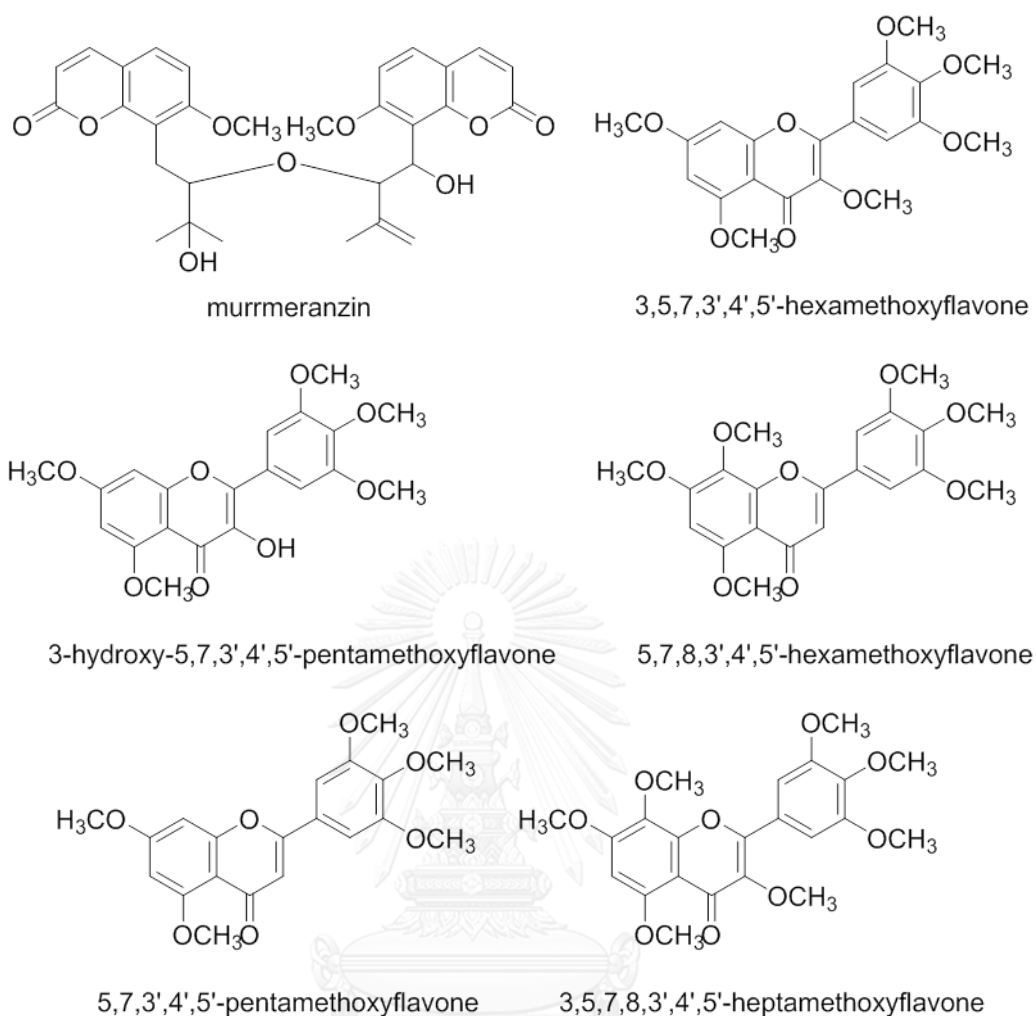


Figure 1.2 The chemical constituents of *Murraya* plants (cont)

1.3 Biological activity studies on *Murraya paniculata*

In 2010, Sukari and co-workers studied on CHCl_3 extract from the leaves of *M. paniculata*. Four coumarins such as auraptene, *trans*-gleinadiene which was firstly reported from this plant, 5,7-dimethoxy-8-(3-methyl-2-oxo-butyl)coumarin and toddalenone were isolated using chromatographic methods. Investigation of antimicrobial activity on the crude extracts and pure compounds indicated that the

CHCl₃ extract from the leaves exhibited moderate activity and only gleinadiene showed moderate activity against *Bacillus cereus*. [11]

In 2010, Wu and co-workers investigated *in vivo* antinociceptive and anti-inflammatory activities of the 70% EtOH extract and six isolated compounds from the leaves of *M. exotica*. The antinociceptive activities were evaluated with the methods of acetic acid-induced writhing response and hot-plate latent pain response test. Carrageenan induced hind paw edema, xylene induced ear edema, and a rat knee osteoarthritis model was employed to measure anti-inflammatory activities. The EtOH extract significantly decreased in the acetic acid-induced writhing response; increased in hot-plate latency; suppressed xylene induced ear swelling and the carrageenan-induced paw edema effectively. In the rat knee osteoarthritis model, the treatment of the 70% EtOH extract resulted in significant increase in the activity of superoxide dismutase, an inhibition on inducible nitric oxide synthase activity, and a decrease in the contents of interleukin-1 β and tumor necrosis factor- α of the rat serum. Following this, an isolated coumarin namely murracarpin exhibited the most potential in antinociceptive and anti-inflammatory activities. [13]

In 2013, Rohan and co-workers assembled a natural product library comprising 24 plant coumarins and 3 ascidian coumarins include lamellarins E, lamellarins B and lamellarins G 8-sulfate. Those compounds were evaluated for inhibition of six human CA isozymes (CAs I, II, VII, IX, XII and XIII). [14]

In 2014, Nguyen and coworkers reported four coumarins isolated from the chloroform fraction from the MeOH extract of *M. paniculata* leaves. All compounds were assessed for its effects on sEH inhibitory effects. Two coumarins: (-)-murracarpin and murrangatin showed sEH inhibitory activity in range of 0.65-1.56 μM . Omphalocarpin and kimcuongin showed potent sEH inhibitory activity with IC_{50} 21.9 and 35.6 μM , respectively. Omphalocarpin may thus represent a novel class of cardiovascular agent for enzyme soluble epoxide hydroxylase inhibition from natural source. [15]

In 2015, Rodanant and co-workers isolated four coumarins including murrangatin, murrangatin acetate, murranganone senecionate, micropubescin and one flavonoid, 3',4',5',7-tetramethoxyflavone from the EtOAc extract of *M. paniculata*. All compounds were tested for cytotoxicity on human gingival fibroblast and monocytes using MTT assay. In addition, five isolated compounds were evaluated for their antibacterial effect against *Porphyromonas gingivalis* (ATCC33277) and anti-inflammation on lipopolysaccharide-stimulated inflammation using monocyte cells. All isolated compounds exhibited antibacterial activity against *P. gingivalis* (ATCC 33277), and murranganone senecionate was highly potent anti-inflammation properties. [16]

In 2016, Qiang Xua and coworkers investigated anti-inflammatory property of isomeranzin isolating from *M. exotica* as well as potential molecular mechanisms. *In vivo* studies, isomeranzin inhibited LPS-induced sepsis for rising survival rate,

improving tissue damage and lessening inflammatory cytokines. *In vitro* study, the same compound significantly blocked expression of p-p65 and p-ERK in lung and liver tissues. Moreover, isomeranzin improved DSS and TNBS-induced colitis due to its anti-inflammatory effects. Therefore, isomeranzin suppressed inflammatory diseases by controlling M1 macrophage polarization through the NF- κ B and ERK pathway. [17]

In 2017, Wang and co-workers addressed twenty-two compounds from the leaves and stems of *M. alata*, including six new coumarins named muralatins L–Q. The repellent activity against *Tribolium castaneum* was tested for fourteen isolated compounds. A statistic model-grey relational analysis was introduced to evaluate repellent activity directly based on relative correlation degree. The testing compounds exhibited various repellent activities against *T. castaneum*. Among them, meranzin, phebalosin and muralatin K showed significant repellent activity against *T. castaneum* with RI (Repellency Index) values of 0.7047, 0.6990 and 0.6884, respectively, comparable to that of the positive control, *N,N*-diethyl-*meta*-toluamide (DEET). [18]

1.4 Insect bioassay

Many Insects are a problem throughout the world, because they reduce the quantity and quality of natural products such as cereals and grains. Insects destroyed harvest and kept grain and cereal products. Therefore, there are many methods to reduce this problem such as antifeedant, insecticidal and repellent activities.

1.4.1 Antifeedant activity

Insect antifeedants are determined as chemicals that control feeding activity of insect. Antifeedant agents do not directly kill insect but make it die after starvation. Insect antifeedants could be found from plants such as coumarins, flavones, isoflavonoids, limonoids, monoterpenes, diterpenes, sesquiterpenes, terpenoid, alkaloids.

1.4.2 Insecticidal activity

Insecticides are natural or synthetic chemicals used to control insects pests; they are important for disease control and providing food and fiber for a growing world population. Insect control with chemicals began about 2,000 years ago with the use of natural products, whereas the age of synthetic insecticides began with the introduction of dichlorodiphenyl trichloroethane (DDT) in the 1940s.

1.4.3 Repellent activity

Insect repellents are agents that used to protect the body from the bites of insects that can cause local or systemic effects. They currently fall into two categories: chemical and natural plant-derived repellents. The most well-known and

well-used chemical repellent is DEET,). Other chemical insect repellents include IR3535, MGK-326 and MGK-264. The latest chemical agent proving to be as effective as DEET is a piperidine-based repellent called picaridin. Plant-based insect repellents are becoming increasingly popular because of their low toxicity but to date have not shown to be as effective as DEET. These include citronella, soybean oil and eucalyptus products.

1.5 Antibacterial activity

Antibacterial agent is chemicals that can particular damage or inhibit bacteria. Most of antibacterial agents is produced from bacteria which can produce lactic acid because it is generally recognized as safe bacteria. Antibacterial agent exhibited against all bacteria with the inhibition zone.

1.6 Anti-inflammatory activity

Inflammation is the body's protective mechanism to ensure the removal of detrimental stimuli, but uncontrolled inflammatory response will lead to tissue damage and even more severe outcome, which must be tightly controlled. M1 macrophages, generally considering as the potent effector cells in response to microbial products or interferon- γ (IFN- γ), are characterized by high level pro-inflammatory cytokines such as tumor necrosis factors (TNF- α), nitric oxide (NO) and reactive oxygen intermediates, and consequently promote polarized type I immune response to mediate host defense against infections of bacteria, protozoa as well as

tumor cells. Targeting on macrophages seems feasible to control inflammation-associated diseases. In short, M1 inflammatory factors act significantly to inflammatory disease. Blocking M1 macrophage polarization emerges as a potential therapeutic approach for effective treatment. NF- κ B is clearly one of the most important regulators for M1 pro-inflammatory genes expression including TNF- α , IL- 1β and IL-6. NF- κ B signals can regulate M1 polarization and affect inflammatory diseases.

1.7 Antioxidant activity

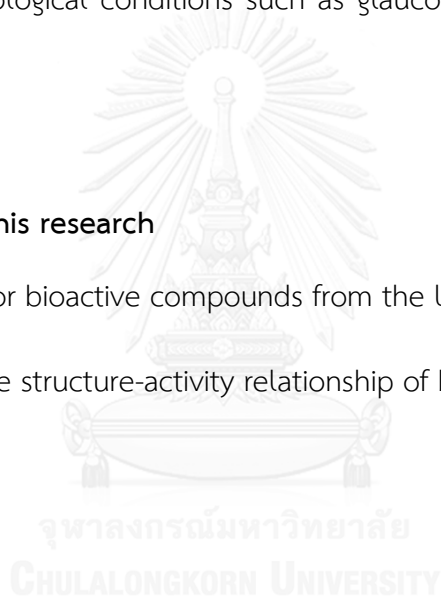
Antioxidants are molecules capable of inhibiting the oxidation of other molecules. Natural antioxidants can be phenolic compounds (flavonoids, tocopherols, and phenolic acids), nitrogen compounds (amines, alkaloids, chlorophyll derivatives, and amino acids), or carotenoids as well as ascorbic acid. Synthetic antioxidants are compounds with phenolic structures of various degrees of alkyl substitution, such as butylated hydroxyanisole (BHA) and butylated hydroxytoluene (BHT). Antioxidants are widely used as ingredients in dietary supplements with the hope of maintaining health and preventing diseases such as cancer, neurodegenerative disorders, cardiovascular diseases, cataracts, inflammation, even altitude sickness.

1.8 Anti-human carbonic anhydrase isozyme II activity

Carbonic anhydrase enzymes (CA, EC 4.2.1.1) are an enzyme that catalyzes the hydration of carbon dioxide to carbonic acid. It is involved in pathological and physiological processes such as pH and CO₂ homeostasis, transport of bicarbonate and CO₂, biosynthetic reactions, bone resorption, calcification, and tumorigenicity. Therefore, this enzyme is an important target for inhibitors that can be used for treating various pathological conditions such as glaucoma, epilepsy and Parkinson's disease.

1.9 The goal of this research

1. To search for bioactive compounds from the leaves of *Murraya paniculata*
2. To study the structure-activity relationship of bioactive compounds



CHAPTER II

MATERIAL AND METHODS

2.1 Plant materials

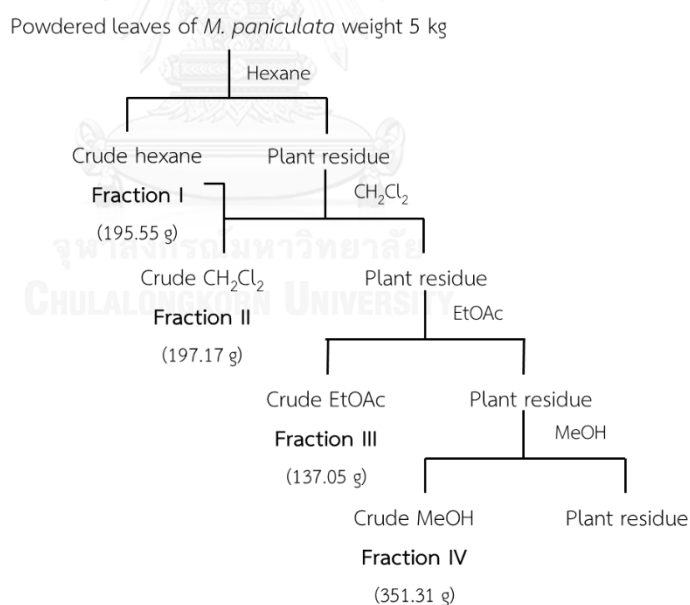
The leaves of *Murraya paniculata* were collected from Nakhonnayok, Thailand in May 2015. The fresh leaves were air-dried and roughly ground and kept until use.

2.2 Instrument and equipment

Thin layer chromatography (TLC) was performed on an aluminium sheet precoated with silica gel (Merck's Kieselgel 60 GF₂₅₄). Column chromatography was conducted on silica gel (70-230 mesh) (Merck's Kieselgel 60 G) 7734, silica gel (100-200 mesh) (Qingdao Mar. Chem. Ind. Co. Ltd.) and C18 reverse-phase silica gel (ODS-A-HG 12 nm, 50 mm, YMC, Japan) and quick column chromatography was performed on silica gel (Merck's Kieselgel 60 G) 7729. Semi-preparative HPLC was performed on a Waters 2535 pump equipped with a 2998 photodiode array detector and YMC C18 reverse-phase column (250 x 10 mm i.d., 5 mm). The ¹H and ¹³C spectra were obtained on a Varian model Mercury + 400 and a Bruker Advance 400 NMR spectrometer (¹H 400 MHz; ¹³C 100 MHz). Solvents for NMR spectra were deuterated chloroform (CDCl₃) and dimethyl sulfoxide (DMSO-d₆). HRESIMS were obtained on a Bruker maXis QTOF-MS in the positive-ion mode. [19]

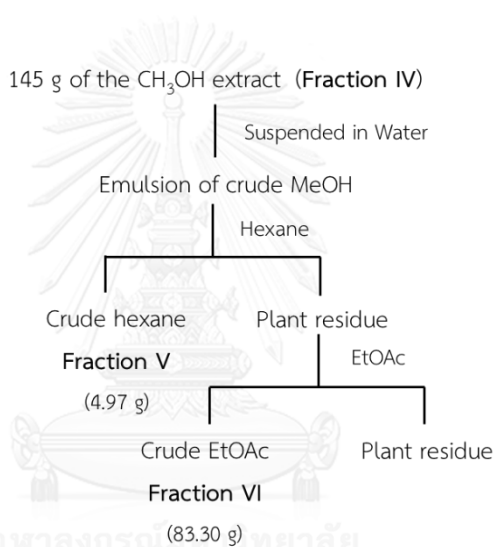
2.3 Extraction procedure

Procedure 1 5 kg of *M. paniculata* leaves were extracted in hexane (3 L) at RT for 7 days. After that, the extract was filtered through filter paper (No.1, Whatman, Maidstone, England) and then the residue was extracted in 3 L of CH_2Cl_2 , EtOAc and MeOH for 7 days, respectively. The extract was filtered through filter paper. The organic solvent was removed with a rotatory evaporator to give hexane (195.55 g, 3.91% base on leave weight), CH_2Cl_2 (197.17 g, 3.94% base on leave weight), EtOAc (137.05 g, 2.74% base on leave weight) and MeOH (351.31 g, 7.03% base on leave weight) crude extracts, designated as Fractions I–IV, respectively (Scheme 2.1).



Scheme 2.1 The extraction procedure for *M. paniculata* leaves

Procedure 2 145 g of the MeOH extract (Fraction IV) was suspended in water (1 L) and then added hexane (3 L) to extract 3 times, followed by the extraction with EtOAc (3 L) for 5 times. The organic solvent was removed with a rotatory evaporator to give hexane (4.97 g, 3.43 %yield base on 145 g of Fraction IV) and EtOAc (83.30 g, 57.45% yield base on 145 g of Fraction IV) crude extracts, named as Fractions V–VI, respectively (Scheme 2.2).

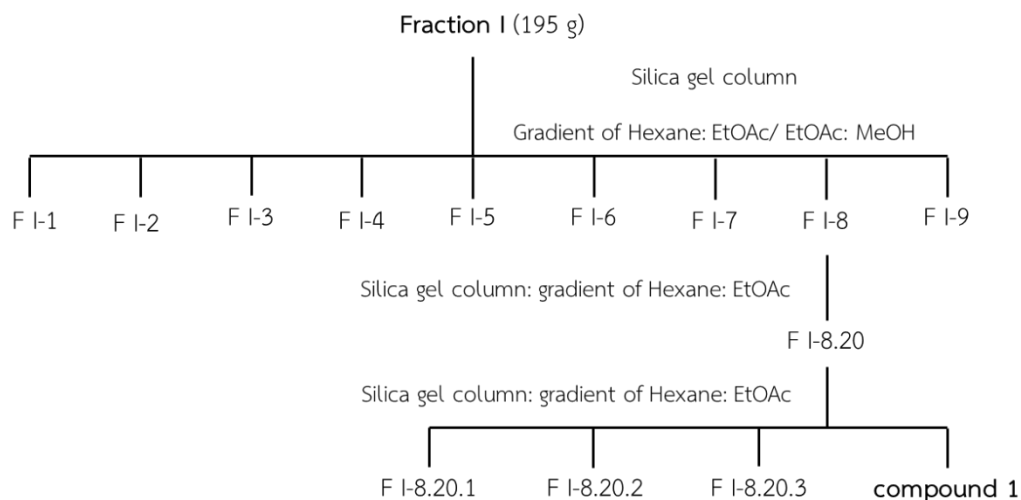


Scheme 2.2 The further extraction procedure for Fraction IV

2.4 Isolation and purification procedure

2.4.1 Separation of Fraction I

The crude hexane (Fraction I) as dark green oil (195 g) was subjected to silica gel quick column using gradient solvent starting from hexane and increased polarity by mixing with EtOAc and MeOH. Each subfraction was examined by TLC, and subfractions with similar TLC pattern were combined (Scheme 2.3).



Scheme 2.3 Fractionation of Fraction I

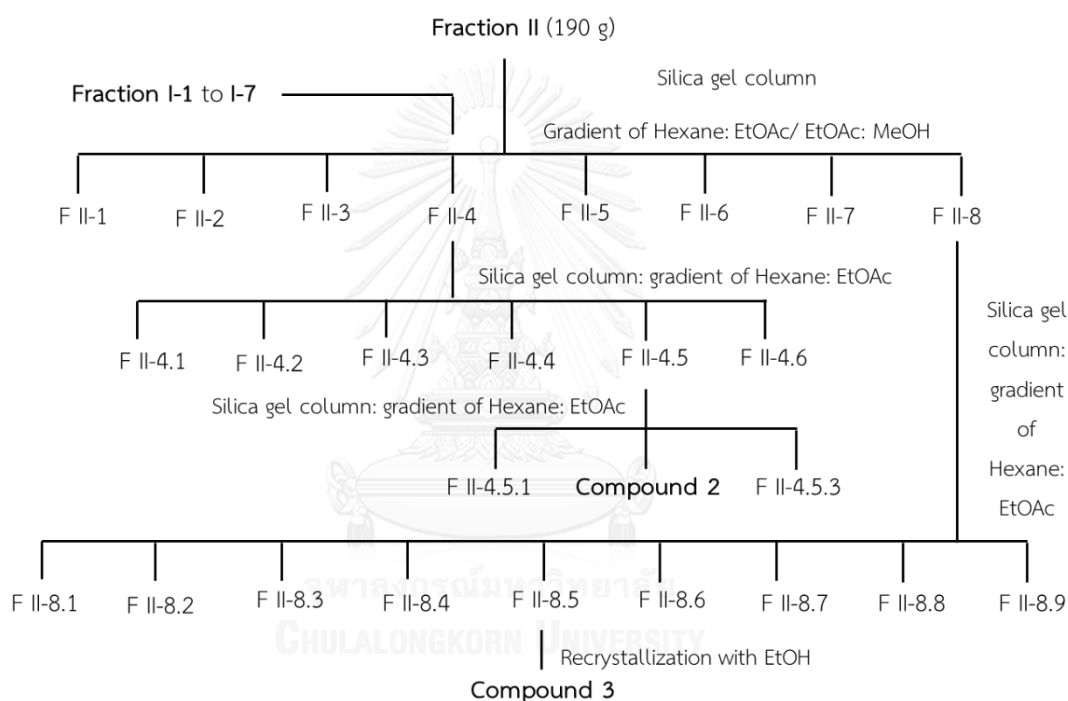
2.4.1.1 Separation of Fraction I-8

Fraction I-8 was fractionated by silica gel column. The column was eluted with hexane-EtOAc gradient in a stepwise fashion. The separation of Fraction I-8 gave compound 1.

Compound 1 was obtained as green plate (1 g, 0.51% yield based on Fraction I). $R_f = 0.21$ (60% EtOAc: hexane). $^1\text{H NMR}$ (400 MHz, CDCl_3): δ 7.62 (d, $J = 9.5$ Hz, 1H), 7.39 (d, $J = 8.6$ Hz, 1H), 6.87 (d, $J = 8.7$ Hz, 1H), 6.26 (d, $J = 9.5$ Hz, 1H), 5.29 (d, $J = 8.6$ Hz, 1H), 4.65 (m, 2H), 4.50 (d, $J = 8.5$ Hz, 1H), 3.96 (s, 3H), 3.72 (q, $J = 7.0$ Hz, 1H), 1.77 (s, 3H) and 1.24 (t, $J = 7.0$ Hz, 1H) ppm. $^{13}\text{C NMR}$ (100 MHz, CDCl_3): δ 160.1, 143.8, 143.6, 143.5, 129.2, 113.7, 113.6, 113.5, 113.1, 108.1, 81.6, 78.4, 72.7, 69.7, 56.3, 56.2, 30.9, 27.3, 27.0 and 17.4 ppm.

2.4.2 Separation of Fraction II

The crude CH_2Cl_2 (Fraction II) as dark green oil (190 g) was separated by silica gel quick column chromatography using gradient of hexane and EtOAc as solvent to afford many subfractions. Each subfraction was examined by TLC, and subfractions with similar TLC pattern were combined (Scheme 2.4).



Scheme 2.4 Fractionation of Fraction II

2.4.2.1 Separation of Fraction II-4

Fraction II-4 combined with Fractions I-1 to I-7 was subjected to silica gel column eluting with hexane-EtOAc gradient. The separation of Fraction II-4 yielded compound 2.

Compound **2** was obtained as orange oil (55 mg, 0.03%yield based on Fraction II). $R_f = 0.48$ (20% EtOAc: hexane). ^1H NMR (400 MHz, CDCl_3): δ 7.66 (d, $J = 9.5$ Hz, 1H), 7.38 (d, $J = 8.5$ Hz, 1H), 6.87(dd, $J = 8.5, 2.5$ Hz, 1H), 6.85 (s, 1H), 6.27 (d, $J = 9.5$ Hz, 1H), 5.49 (t, $J = 6.7$ Hz, 1H), 5.10 (d, $J = 7.2$ Hz, 1H), 4.63 (d, $J = 6.6$ Hz, 1H), 2.19 (d, $J = 1.1$ Hz, 1H), 2.14 (d, $J = 7.6$ Hz, 1H), 1.78 (s, 3H), 1.69 (s, 3H), 1.63 (s, 3H) ppm. ^{13}C NMR (100 MHz, CDCl_3): δ 143.4, 143.4, 123.6, 118.4, 113.2, 112.9, 101.6, 65.5, 39.5, 31.9, 26.2, 25.6 and 16.8 ppm

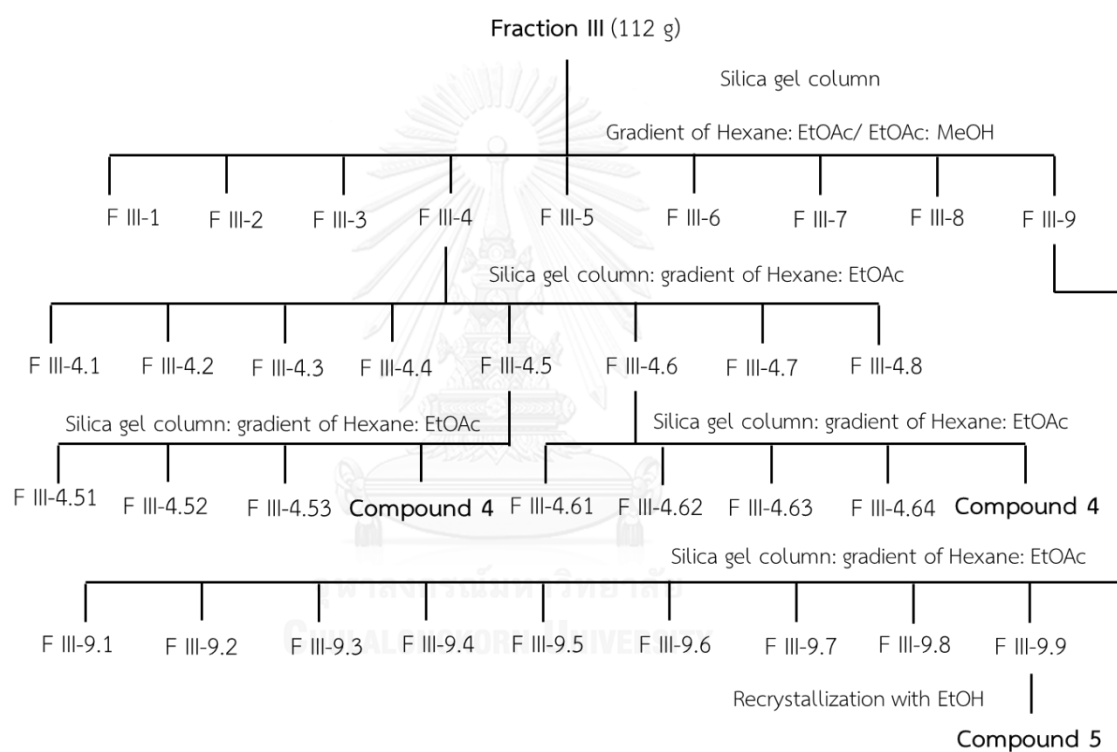
2.4.2.2 Separation of Fraction II-8

Fraction II-8 was separated by silica gel column eluting with hexane-EtOAc gradient in a stepwise fashion. The separation of Fraction II-8 furnished compound **3**.

Compound **3** was obtained as pale yellow solid (3 g, 1.58 %yield based on Fraction II). $R_f = 0.17$ (20% EtOAc: hexane). ^1H NMR (400 MHz, CDCl_3): δ 7.62 (d, $J = 9.5$ Hz, 1H), 7.42 (d, $J = 8.7$ Hz, 1H), 6.87 (d, $J = 8.7$ Hz, 1H), 6.26 (d, $J = 9.5$ Hz, 1H), 5.29 (s, 1H), 5.08 (s, 1H), 3.99 (d, $J = 2.4$ Hz, 2H), 3.96 (s, 3H), 3.91 (d, $J = 2.4$ Hz, 2H) and 1.60 (s, 3H) ppm. ^{13}C NMR (100 MHz, CDCl_3): δ 143.3, 128.9, 113.5, 113.4, 107.6, 107.6, 60.7, 56.3, 51.8 and 17.4 ppm

2.4.3 Separation of Fraction III

The crude EtOAc (Fraction III) as dark green oil (112 g) was subjected to silica gel quick column using gradient solvent starting from hexane and increased polarity by mixing with EtOAc and MeOH. Each subfraction was examined by TLC, and subfractions with similar TLC pattern were combined (Scheme 2.5).



Scheme 2.5 Fractionation of Fraction III

2.4.3.1 Separation of Fraction III-4

Fraction **III-4** was further separated by silica gel column. The column was eluted with hexane-EtOAc gradient in a stepwise fashion. The separation of Fraction **III-4** gave compound **4**.

Compound **4** was obtained as white crystal (10 mg, 0.01 %yield based on Fraction III). $R_f = 0.62$ (60% EtOAc: hexane). ^1H NMR (400 MHz, CDCl_3): δ 7.66 (d, $J = 9.5$ Hz, 1H), 7.38 (d, $J = 8.5$ Hz, 1H), 6.86 (m, 2H), 6.27 (d, $J = 9.5$ Hz, 1H), 4.63 (d, $J = 6.6$ Hz, 3H), 2.85 (d, $J = 6.3$ Hz, 1H), 2.13 (s, 1H), 1.28 (s, 3H) and 1.03 (s, 3H) ppm.

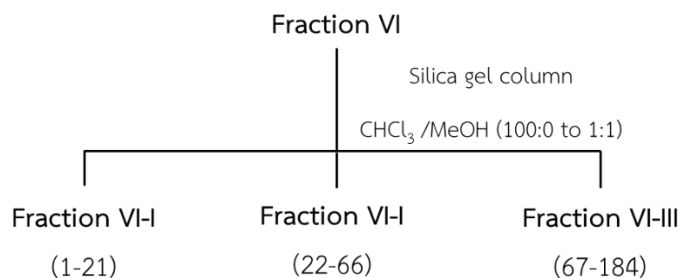
2.4.3.1 Separation of Fraction III-9

Fraction III-9 was fractionated by silica gel column which was eluted with hexane-EtOAc gradient in a stepwise fashion. The separation of Fraction III-9 afforded compound **5**.

Compound **5** was obtained as dark green solid (80 mg, 0.07 %yield based on Fraction III). $R_f = 0.33$ (60% EtOAc: hexane). ^1H NMR (400 MHz, CDCl_3): δ 7.62 (d, $J = 9.6$ Hz, 1H), 7.39 (d, $J = 8.8$ Hz, 1H), 6.87 (d, $J = 8.8$ Hz, 1H), 6.25 (d, $J = 9.6$ Hz, 1H), 5.73 (d, $J = 7.6$ Hz, 1H), 5.52 (d, $J = 8.0$ Hz, 1H), 4.76 (s, 1H), 4.73 (s, 1H), 4.00 (s, 3H), 2.13 (s, 1H) and 1.74 (s, 1H) ppm. ^{13}C NMR (100 MHz, CDCl_3): δ 171.1, 160.4, 160.2, 152.8, 143.8, 140.9, 128.9, 115.9, 114.9, 113.7, 113.2, 107.9, 79.7, 68.3, 56.5, 21.4 and 18.7 ppm.

2.4.4 Separation of Fraction VI

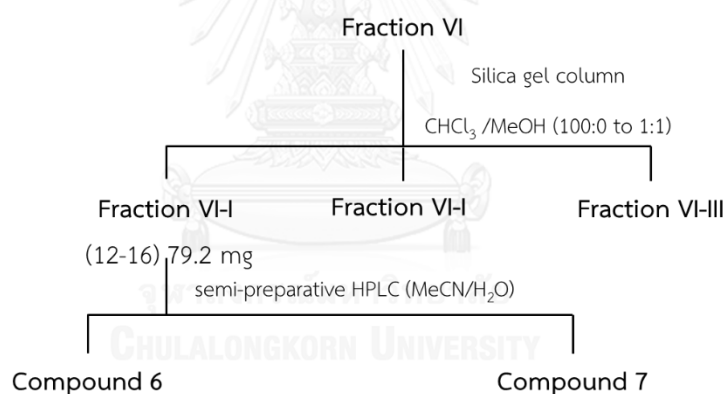
Fraction VI as dark green oil (83 g) was subjected to silica gel column using a gradient elution of CHCl_3 with increasing amount of MeOH up to 50% MeOH in CHCl_3 . yielded 184 fractions (Scheme 2.6).



Scheme 2.6 Fractionation of Fraction VI

2.4.4.1 Separation of Fraction VI-I

Subfractions **12-16** (79.2 mg) of Fraction **VI-I** was purified by semi-preparative HPLC (MeCN/H₂O) to afford compounds **6** and **7** (Scheme 2.7).



Scheme 2.7 Fractionation of Fraction VI-I

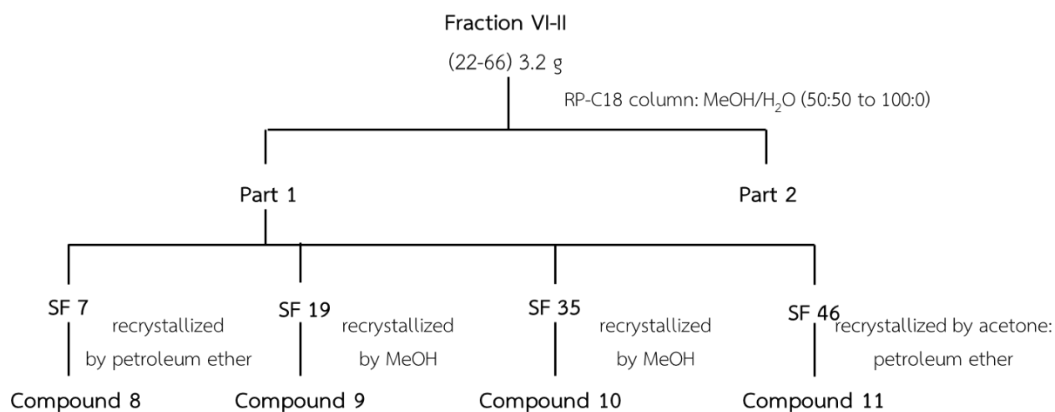
Compound **6** was obtained as brown oil (3 mg, 3.79 %yield based on Fraction **VI-I**). $R_f = 0.31$ (20% EtOAc: hexane). ^1H NMR (400 MHz, CDCl₃): δ 7.77 (s, 3H), 7.06 (dd, $J = 1.6, 2.0$ Hz, 1H), 7.01 (d, $J = 2.0$ Hz, 1H), 7.60 (d, $J = 16.0$ Hz, 1H), 6.88 (d, $J = 8.0$ Hz, 1H), 6.26 (d, $J = 15.6$ Hz, 1H) and 3.90 (s, 3H) ppm. ^{13}C NMR (100 MHz,

CDCl₃): δ 168.0, 148.3, 147.1, 145.2, 126.9, 123.1, 115.1, 115.0, 109.7, 56.0 and 51.7 ppm.

Compound **7** was obtained as brown oil (2 mg, 2.53 %yield based on Fraction **VI-I**). R_f = 0.43 (20% EtOAc: hexane). ¹H NMR (400 MHz, CDCl₃): δ 7.59 (d, J = 16.0 Hz, 1H), 7.12 (d, J = 2.0 Hz, 1H), 7.03 (dd, J = 2.0, 2.0 Hz, 1H), 6.84 (d, J = 8.4 Hz, 1H), 6.28 (d, J = 16.0 Hz, 1H), 3.92 (s, 3H), 3.78 (s, 3H) and 3.47 (s, 3H) ppm. ¹³C NMR (100 MHz, CDCl₃): δ 128.1, 110.7, 148.8, 146.0, 113.2, 121.9, 51.8, 50.9, 144.9, 115.9, 167.9 and 56.1 ppm.

2.4.4.2 Separation of Fraction **VI-II**

Fraction **VI-II** (3.2 g) was subjected to reverse phase column chromatography using a gradient elution of MeOH with decreasing amount of H₂O down to 100% MeOH (MeOH/H₂O ((50:50 to 100:0)), yielded 108 subfractions. Subfractions 7 (5.2 mg), 19 (39.0 mg), 35 (4.5 mg) and 46 (6.4 mg) were recrystallized by petroleum ether, MeOH, MeOH and acetone: petroleum ether, respectively to afford compounds **8**, **9**, **10** and **11** (Scheme 2.8).



Scheme 2.8 Fractionation of Fraction VI-II

Compound **8** was obtained as white solid (5.2 mg, 1.66 %yield based on Fraction VI-II). $R_f = 0.24$ (60% EtOAc: hexane). $^1\text{H NMR}$ (400 MHz, CDCl_3): δ 7.63 (d, $J = 9.6$ Hz, 1H), 7.41 (d, $J = 8.4$ Hz, 1H), 6.90 (d, $J = 8.8$ Hz, 1H), 6.27 (d, $J = 9.2$ Hz, 1H), 5.43 (d, $J = 7.2$ Hz, 1H), 4.99 (d, $J = 4.0, 1.6$ Hz, 2H), 4.53 (d, $J = 7.6$ Hz, 1H), 4.00 (s, 3H) and 1.90 (s, 3H) ppm. $^{13}\text{C NMR}$ (100 MHz, CDCl_3): δ 160.7, 160.3, 153.4, 113.7, 145.2, 144.0, 129.0, 116.6, 114.1, 113.4, 108.1, 78.6, 68.6, 56.6 and 18.1 ppm.

Compound **9** was obtained as white solid (39 mg, 12.48 %yield based on Fraction VI-II). $R_f = 0.36$ (60% EtOAc: hexane). $^1\text{H NMR}$ (400 MHz, CDCl_3): δ 7.61 (d, $J = 9.2$ Hz, 1H), 7.40 (d, $J = 8.8$ Hz, 1H), 6.86 (d, $J = 8.8$ Hz, 1H), 6.25 (d, $J = 9.6$ Hz, 1H), 5.05 (d, $J = 8.8$ Hz, 1H), 4.93 (d, $J = 8.8$ Hz, 1H), 4.69 (s, 1H), 4.63 (t, $J = 1.6$ Hz, 1H), 3.92 (s, 3H), 3.32 (s, 3H) and 1.68 (s, 3H) ppm. $^{13}\text{C NMR}$ (100 MHz, CDCl_3): δ 161.4, 160.5, 153.9, 143.7, 143.3, 129.1, 114.3, 113.5, 113.4, 112.9, 107.9, 77.9, 76.5, 57.6, 56.3 and 17.3 ppm.

Compound **10** was obtained as white solid (9.1 mg, 0.28 %yield based on Fraction **VI-II**). $R_f = 0.31$ (60% EtOAc: hexane). ^1H NMR (400 MHz, CDCl_3): δ 7.99 (d, $J = 9.6$ Hz, 1H), 6.34 (s, 1H), 6.14 (d, $J = 9.6$ Hz, 1H), 3.93 (d, $J = 2.8$ Hz, 3H), 3.93 (d, $J = 2.8$ Hz, 3H), 3.73 (dd, $J = 4.4$ Hz, 1H), 3.28 (s, 3H), 2.96 (s, 1H), 2.94 (t, $J = 1.6$ Hz, 1H), 1.28 (s, 1H) and 1.28 (s, 1H) ppm. ^{13}C NMR (100 MHz, CDCl_3): δ 161.6, 161.5, 154.3, 155.7, 138.9, 111.0, 108.2, 104.1, 90.5, 56.3, 56.0, 49.5, 24.7, 21.2 and 20.4 ppm.

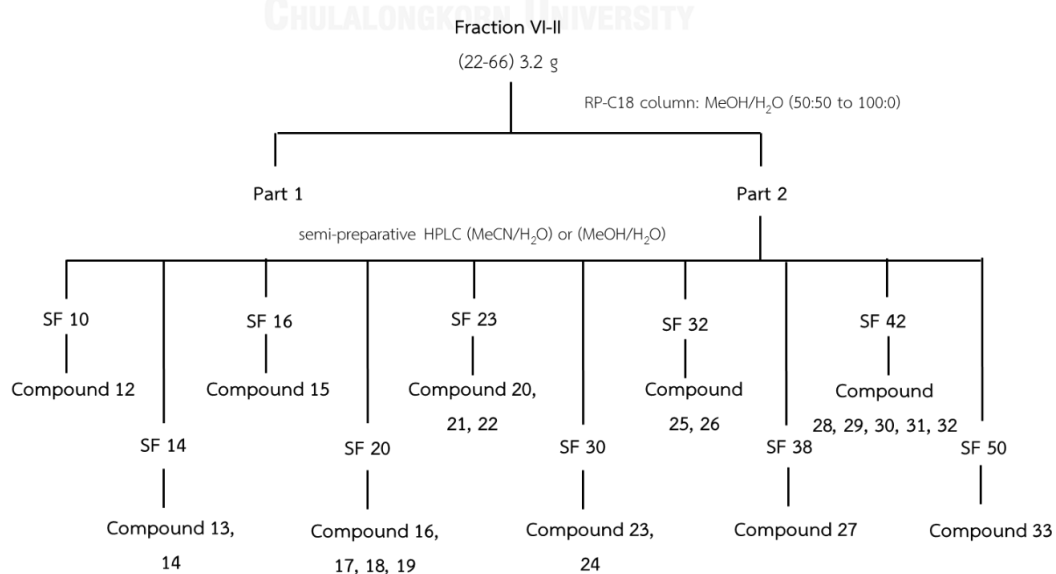
Compound **11** was obtained as white solid (6.4 mg, 0.20 %yield based on Fraction **VI-II**). $R_f = 0.17$ (60% EtOAc: hexane). ^1H NMR (400 MHz, CDCl_3): δ 7.37 (s, 1H), 6.50, 6.36 (dd, $J = 2.0, 2.4$ Hz, 1H), 3.97 (s, 1H), 3.94 (d, $J = 3.6$ Hz, 3H), 3.90 (d, $J = 10.8$ Hz, 3H) and 1.58 (s, 3H) ppm. ^{13}C NMR (100 MHz, CDCl_3): δ 174.0, 164.0, 161.1, 158.8, 152.4, 153.1, 153.1, 141.6, 140.0, 126.0, 109.5, 105.9, 105.9, 95.8, 92.5, 60.1, 61.0, 56.4, 56.5, 56.5 and 55.8 ppm.

2.4.4.3 Further Separation of Fraction **VI-II**

Twenty-two components (Compounds **12-33**) were collected successively corresponding to the HPLC peak, which were then dried by rotatory evaporator to give pure compounds.

Subfraction 10 (8.9 mg) of Fraction **VI-II** was purified by semi-preparative HPLC (MeCN/ H_2O , 15: 85) to afford compound **12** (4.6 mg) whereas subfraction 14 (10.3 mg) was purified by preparative HPLC to afford compounds **13** (3.0 mg) and **14** (2.6 mg).

Subfraction 16 (14.6 mg) was purified by preparative HPLC (MeOH/H₂O, 30: 70) to afford compound **15** (3.3 mg) while subfraction 20 (278.8 mg) was purified by preparative HPLC (MeCN/H₂O, 23:77) to afford compounds **16** (1.6 mg), **17** (20.1 mg), **18** (34.7 mg) and **19** (6.0 mg). The purification of subfraction 23 (33.9 mg) by preparative HPLC (MeCN/H₂O, 28:72) afforded compounds **20** (8.9 mg), **21** (2.9 mg) and **22** (3.2 mg). The preparative HPLC of subfraction 30 (165 mg) furnished compounds **23** (11.5 mg) and **24** (23.9 mg). Subfraction 32 (156.1 mg) was purified by preparative HPLC (MeCN/ H₂O, 30:70) to afford compounds **25** (49.7 mg) and **26** (6.7 mg). Subfraction 38 (25.5 mg) was purified by preparative HPLC to afford compound **27** (8.9 mg) whereas subfraction 42 (98.4 mg) was purified by preparative HPLC to gain compounds **28** (8.9 mg), **29** (2.9 mg), **30** (2.3 mg), **31** (3.2 mg) and **32** (1.2 mg). By the same fashion, subfraction 50 (14.9 mg) with the aids of preparative HPLC (MeCN /H₂O, 40: 60) afforded compound **33** (26.7 mg) (Scheme 2.9).



Scheme 2.9 Further fractionation of Fraction VI-II

Compound **12** was obtained as brown solid (4.6 mg, 0.14 %yield based on Fraction **VI-II**). $R_f = 0.48$ (60% EtOAc: hexane). ^1H NMR (400 MHz, CDCl_3): δ 7.60 (d, $J = 9.6$ Hz, 1H), 6.92 (s, 1H), 6.84 (s, 1H), 6.27 (d, $J = 9.6$ Hz, 1H) and 3.95 (s, 3H) ppm. ^{13}C NMR (100 MHz, CDCl_3): δ 161.6, 150.4, 149.8, 144.2, 143.5, 113.5, 111.6, 107.6, 103.3 and 56.6 ppm.

Compound **13** was obtained as white solid (3 mg, 0.09 %yield based on Fraction **VI-II**). $R_f = 0.75$ (70% EtOAc: hexane). ^1H NMR (400 MHz, CDCl_3): δ 7.63 (d, $J = 9.6$ Hz, 1H), 7.34(d, $J = 8.4$ Hz, 1H), 6.87 (d, $J = 8.4$ Hz, 1H), 6.23 (d, $J = 9.6$ Hz, 1H), 3.63 (dd, $J = 7.6$ Hz, 1H), 3.92 (s, 3H), 3.09 (d, $J = 2.4$ Hz, 1H), 2.99 (d, $J = 3.6$ Hz, 1H), 1.32 (s, 3H) and 1.31 (s, 3H) ppm. ^{13}C NMR (100 MHz, CDCl_3): δ 161.2, 160.5, 153.3, 143.9, 126.9, 115.7, 113.0, 113.0, 107.4, 78.3, 73.0, 56.2, 26.0, 25.5 and 24.0 ppm.

Compound **14** was obtained as white solid (2.6 mg, 0.08 %yield based on Fraction **VI-II**). $R_f = 0.62$ (70% EtOAc: hexane). ^1H NMR (400 MHz, CDCl_3): δ 7.39 (d, $J = 9.6$ Hz, 1H), 7.17 (d, $J = 8.4$ Hz, 1H), 6.63 (d, $J = 8.8$ Hz, 1H), 6.07 (d, $J = 9.6$ Hz, 1H), 4.82 (d, $J = 8.8$ Hz, 1H), 4.70 (d, $J = 8.8$ Hz, 1H), 4.47 (s, 1H), 4.40 (s, 1H), 3.70 (s, 3H), 3.10 (s, 3H), and 1.40 (s, 3H) ppm. ^{13}C NMR (100 MHz, CDCl_3): δ 161.4, 160.5, 154.0, 143.7, 143.4, 129.0, 114.3, 113.6, 113.4, 112.9, 107.9, 77.9, 76.5, 57.7, 56.2 and 17.3 ppm.

Compound **15** was obtained as brown oil (3.3 mg, 0.10 %yield based on Fraction **VI-II**). $R_f = 0.26$ (70% EtOAc: hexane). ^1H NMR (400 MHz, CDCl_3): δ 7.62 (d, $J = 9.6$ Hz, 1H), 7.39 (d, $J = 8.4$ Hz, 1H), 6.87 (d, $J = 8.8$ Hz, 1H), 6.26 (d, $J = 9.6$ Hz, 1H), 5.30 (d, $J = 8.4$ Hz, 1H), 4.65 (t, $J = 1.6$ Hz, 1H), 4.58 (t, $J = 0.8$ Hz, 1H), 4.50 (d, $J = 8.8$ Hz, 1H), 3.97 (s, 3H) and 1.77 (s, 3H) ppm. ^{13}C NMR (100 MHz, CDCl_3): δ 160.2, 160.2, 152.9, 143.8, 143.8, 128.7, 116.1, 113.9, 113.7, 113.2, 107.9, 78.6, 69.8, 56.4 and 17.5 ppm.

Compound **16** was obtained as pale yellow solid (1.6 mg, 0.05 %yield based on Fraction **VI-II**). $R_f = 0.43$ (70% EtOAc: hexane). ^1H NMR (400 MHz, CDCl_3): δ 7.63 (d, $J = 9.2$ Hz, 1H), 7.42 (d, $J = 8.8$ Hz, 1H), 6.91 (d, $J = 8.8$ Hz, 1H), 6.27 (d, $J = 9.6$ Hz, 1H), 5.19 (d, $J = 6.4$ Hz, 1H), 4.97 (s, 1H), 4.88 (t, $J = 1.2$ Hz, 1H), 4.79 (d, $J = 6.8$ Hz, 1H), 3.95 (s, 3H), 3.29 (s, 3H) and 1.87 (s, 3H) ppm. ^{13}C NMR (100 MHz, CDCl_3): δ 161.7, 160.7, 154.5, 145.0, 143.9, 129.0, 113.8, 113.6, 113.1, 113.1, 108.3, 76.4, 57.5, 56.6 and 18.7 ppm.

Compound **17** was obtained as yellow solid (20.1 mg, 0.63 %yield based on Fraction **VI-II**). $R_f = 0.40$ (70% EtOAc: hexane). ^1H NMR (400 MHz, CDCl_3): δ 7.65 (d, $J = 9.6$ Hz, 1H), 7.46 (d, $J = 8.4$ Hz, 1H), 6.86 (d, $J = 8.8$ Hz, 1H), 6.27 (d, $J = 9.6$ Hz, 1H), 5.88 (s, 1H), 3.86 (s, 3H), 2.59 (m, 1H), 1.11 (d, $J = 6.8$ Hz, 3H) and 0.96 (d, $J = 6.4$ Hz, 3H) ppm. ^{13}C NMR (100 MHz, CDCl_3): δ 160.6, 113.7, 143.7, 129.7, 107.9, 160.2, 114.6, 113.3, 153.5, 68.5, 212.6, 35.9, 56.3, 19.2 and 18.1 ppm.

Compound **18** was obtained as brown solid (34.7 mg, 1.08 %yield based on Fraction **VI-II**). $R_f = 0.50$ (70% EtOAc: hexane). ^1H NMR (400 MHz, CDCl_3): δ 10.20 (s, 1H), 7.63 (d, $J = 9.6$ Hz, 1H), 7.43 (d, $J = 8.8$ Hz, 1H), 6.88 (d, $J = 8.8$ Hz, 1H), 6.19 (d, $J = 9.6$ Hz, 1H), 3.81 (s, 3H), 2.41 (s, 1H) and 1.76 (s, 3H) ppm. ^{13}C NMR (100 MHz, CDCl_3): δ 188.9, 161.3, 160.1, 159.9, 152.6, 143.8, 128.7, 113.2, 107.7, 24.9, 56.3 and 19.93 ppm.

Compound **19** was obtained as brown solid (6 mg, 0.19 %yield based on Fraction **VI-II**). $R_f = 0.33$ (70% EtOAc: hexane). ^1H NMR (400 MHz, CDCl_3): δ 7.62 (d, $J = 9.6$ Hz, 1H), 7.39 (d, $J = 8.8$ Hz, 1H), 6.87 (d, $J = 8.8$ Hz, 1H), 6.25 (d, $J = 9.6$ Hz, 1H), 5.73 (d, $J = 7.6$ Hz, 1H), 5.52 (d, $J = 8.0$ Hz, 1H), 4.76 (s, 2H), 4.73 (t, $J = 7.6$ Hz, 2H), 4.00 (s, 3H), 2.13 (s, 1H) and 1.74 (s, 1H) ppm. ^{13}C NMR (100 MHz, CDCl_3): δ 171.1, 160.4, 160.2, 152.8, 143.8, 140.9, 128.9, 115.9, 114.9, 113.7, 113.2, 107.9, 79.7, 68.3, 56.5, 21.4 and 18.7 ppm.

Compound **20** was obtained as green oil (8.9 mg, 0.28 %yield based on Fraction **VI-II**). $R_f = 0.33$ (70% EtOAc: hexane). ^1H NMR (400 MHz, CDCl_3): δ 6.58 (s, 2H), 6.58 (s, 2H), 5.52 (brs, 2H), 4.73 (d, $J = 4.0$ Hz, 2H), 4.28 (m, 2H), 3.93 (m, 2H), 3.90 (s, 12H) and 3.10 (brs, 2H) ppm. ^{13}C NMR (100 MHz, CDCl_3): δ 147.1, 147.1, 134.3, 132.1, 102.6, 102.6, 86.1, 71.8, 56.4 and 54.3 ppm.

Compound **21** was obtained as brown oil (2.9 mg, 0.09 %yield based on Fraction **VI-II**). $R_f = 0.43$ (70% EtOAc: hexane). $^1\text{H NMR}$ (400 MHz, CDCl_3): δ 6.90-6.88 (m, 1H), 6.90-6.88 (m, 1H), 6.84-6.81 (m, 1H), 6.58 (s, 1H), 6.58 (s, 1H), 4.73 (dd, $J = 12.0, 4.4$ Hz, 1H), 4.26 (m, 1H), 3.91 (s, 3H), 3.90 (s, 3H), 3.90 (s, 3H), 3.88 (m, 1H), 3.10 (m, 1H) and 3.10 (m, 1H) ppm. $^{13}\text{C NMR}$ (100 MHz, CDCl_3): δ 147.2, 146.7, 146.7, 145.3, 134.3, 132.9, 118.9, 108.6, 132.1, 114.3, 102.7, 102.7, 86.2, 85.8, 71.9, 71.6, 56.4, 55.9, 55.9, 54.4, 54.1 ppm.

Compound **22** was obtained as white solid (3.2 mg, 0.10 %yield based on Fraction **VI-II**). $R_f = 0.43$ (70% EtOAc: hexane). $^1\text{H NMR}$ (400 MHz, CDCl_3): δ 7.62 (d, $J = 9.6$ Hz, 1H), 7.38 (d, $J = 8.8$ Hz, 1H), 6.88 (d, $J = 8.8$ Hz, 1H), 6.26 (d, $J = 9.6$ Hz, 1H), 5.37 (d, $J = 8.0$ Hz, 1H), 5.13 (s, 1H), 5.06 (s, 1H), 4.09 (d, $J = 8.4$ Hz, 1H), 3.95 (s, 3H), 3.91 (s, 1H), 3.09 (s, 3H), 1.84 (s, 3H) ppm. $^{13}\text{C NMR}$ (100 MHz, CDCl_3): δ 160.8, 160.4, 153.4, 143.8, 142.9, 128.2, 117.5, 116.5, 113.4, 113.2, 108.0, 88.0, 66.4, 56.6, 56.4 and 16.8 ppm.

Compound **23** was obtained as white solid (11.5 mg, 0.36 %yield based on Fraction **VI-II**). $R_f = 0.36$ (70% EtOAc: hexane). $^1\text{H NMR}$ (400 MHz, CDCl_3): δ 7.62 (d, $J = 9.2$ Hz, 1H), 7.35 (d, $J = 8.8$ Hz, 1H), 6.87 (d, $J = 8.8$ Hz, 1H), 6.24 (d, $J = 9.6$ Hz, 1H), 4.93 (d, $J = 1.2$ Hz, 1H), 4.90 (s, 1H), 4.37 (t, $J = 8.0$ Hz, 1H), 4.31 (dd, $J = 9.6$ Hz, 1H), 4.17 (dd, $J = 7.2, 7.2$ Hz, 1H), 3.89 (s, 3H) and 1.70 (s, 3H) ppm. $^{13}\text{C NMR}$

(100 MHz, CDCl₃): δ 161.2, 161.0, 153.9, 144.0, 143.2, 127.7, 116.8, 113.3, 111.74, 108.1, 62.9, 56.3 and 22.4 ppm.

Compound **24** was obtained as white solid (23.9 mg, 0.75 %yield based on Fraction **VI-II**). R_f = 0.40 (70% EtOAc: hexane). ¹H NMR (400 MHz, CDCl₃): δ 7.64 (d, *J* = 9.6 Hz, 1H), 7.49 (d, *J* = 8.8 Hz, 1H), 6.88 (d, *J* = 8.8 Hz, 1H), 6.95 (s, H-1'), 6.25 (d, *J* = 9.6 Hz, 1H), 3.89 (s, 3H), 2.82 (m, 1H), 2.14 (s, 1H), 1.15 (d, *J* = 6.8 Hz, 1H) and 1.01 (d, *J* = 6.8 Hz, 1H) ppm. ¹³C NMR (100 MHz, CDCl₃): δ 207.9, 169.6, 160.9, 159.9, 153.7, 143.4, 130.3, 113.8, 113.2, 111.9, 108.0, 69.4, 56.5, 36.3, 20.9, 19.2, 18.1 and 18.1 ppm.

Compound **25** was obtained as white solid (49.7 mg, 1.55 %yield based on Fraction **VI-II**). R_f = 0.36 (70% EtOAc: hexane). ¹H NMR (400 MHz, CDCl₃): δ 7.61 (d, *J* = 9.2 Hz, 1H), 7.31 (d, *J* = 8.4 Hz, 1H), 6.85 (d, *J* = 8.8 Hz, 1H), 6.21 (d, *J* = 9.6 Hz, 1H), 3.91 (s, 3H), 3.75 (dd, *J* = 3.3, 2.8 Hz, 1H), 3.28 (s, 3H), 3.04 (m, 1H), 2.99 (m, 1H), 2.28 (s, 1H), 1.27 (d, *J* = 1.6 Hz, 1H) and 1.27 (d, *J* = 1.6 Hz, 1H), ppm. ¹³C NMR (100 MHz, CDCl₃): δ 161.2, 160.7, 153.5, 143.8, 126.7, 116.1, 113.0, 113.0, 107.4, 77.2, 76.5, 56.2, 49.4, 25.0, 20.9 and 20.3 ppm.

Compound **26** was obtained as yellow solid (6.7 mg, 0.21 %yield based on Fraction **VI-II**). $R_f = 0.50$ (70% EtOAc: hexane). ^1H NMR (400 MHz, CDCl_3): δ 7.63 (d, $J = 9.2$ Hz, 1H), 7.34 (d, $J = 8.4$ Hz, 1H), 6.86 (d, $J = 8.8$ Hz, 1H), 6.25 (d, $J = 9.6$ Hz, 1H), 4.89 (s, 1H), 4.80 (s, 1H), 4.34 (dd, $J = 3.6$ Hz, 1H), 3.93 (s, 3H), 3.20 (dd, $J = 9.2$ Hz, 1H), 3.09 (d, $J = 5.2$ Hz, 1H) and 1.89 (s, 3H) ppm. ^{13}C NMR (100 MHz, CDCl_3): δ 161.1, 160.6, 153.5, 147.2, 143.8, 127.0, 115.0, 113.2, 113.0, 110.5, 107.3, 75.3, 56.2, 29.4 and 18.1 ppm.

Compound **27** was obtained as white solid (8.9 mg, 0.28 %yield based on Fraction **VI-II**). $R_f = 0.24$ (70% EtOAc: hexane). ^1H NMR (400 MHz, CDCl_3): δ 7.86 (s, 1H), 7.84 (s, 1H), 7.01 (d, $J = 8.40$ Hz, 1H), 6.41 (s, 1H), 4.00 (s, 6H), 3.97 (s, 6H), 3.94 (s, 3H) and 3.90 (s, 3H) ppm. ^{13}C NMR (100 MHz, CDCl_3): δ 174.4, 156.5, 156.3, 152.5, 151.0, 151.0, 148.8, 140.9, 130.6, 123.6, 121.9, 111.1, 111.0, 109.4, 92.4, 61.7, 60.1, 56.8, 56.5, 56.1 and 56.0 ppm.

Compound **28** was obtained as white solid (8.9 mg, 0.28 %yield based on Fraction **VI-II**). $R_f = 0.12$ (70% EtOAc: hexane). ^1H NMR (400 MHz, CDCl_3): δ 7.54 (s, 1H), 7.54 (s, 1H), 6.42 (s, 1H), 4.0 (d, $J = 3.2$ Hz, 6H), 3.94 (d, $J = 1.2$ Hz, 12H) and 3.91 (s, 3H) ppm. ^{13}C NMR (100 MHz, CDCl_3): δ 174.4, 156.6, 156.5, 153.0, 153.0, 152.1, 151.0, 141.5, 140.1, 130.5, 126.3, 109.4, 105.7, 105.7, 92.3, 61.6, 61.2, 60.1, 56.7, 56.5, 56.3 and 56.3 ppm.

Compound **29** was obtained as white solid (2.9 mg, 0.09 %yield based on Fraction **VI-II**). $R_f = 0.43$ (70% EtOAc: hexane). ^1H NMR (400 MHz, CDCl_3): δ 7.35 (s, 1H), 7.35 (s, 1H), 6.74 (s, 1H), 4.00 (d, $J = 12.4$ Hz, 3H), 3.94 (d, $J = 18.4$ Hz, 3H), 3.94 (d, $J = 18.4$ Hz, 3H), 3.94 (d d, $J = 18.4$ Hz, 3H), 3.90 (d, $J = 2.8$ Hz, 3H), 3.90 (d, $J = 2.8$ Hz, 3H) and 3.90 (d, $J = 2.8$ Hz, 3H) ppm. ^{13}C NMR (100 MHz, CDCl_3): δ 173.8, 157.9, 157.9, 153.7, 153.2, 153.2, 152.6, 141.3, 140.4, 140.3, 126.1, 113.3, 106.0, 106.0, 96.2, 62.4, 61.7, 61.2, 60.2, 56.5, 56.5 and 56.5 ppm.

Compound **30** was obtained as white solid (2.3 mg, 0.07 %yield based on Fraction **VI-II**). $R_f = 0.33$ (70% EtOAc: hexane). ^1H NMR (400 MHz, CDCl_3): δ 7.70 (s, 2H), 6.97 (d, $J = 9.2$ Hz, 1H), 6.74 (s, 1H), 4.01 (s, 3H), 3.97 (s, 3H), 3.96 (s, 6H), 3.92 (s, 3H) and 3.86 (s, 3H) ppm. ^{13}C NMR (100 MHz, CDCl_3): δ 173.8, 157.8, 153.7, 153.4, 152.6, 151.1, 148.8, 140.9, 140.2, 123.5, 121.9, 113.2, 111.4, 110.9, 96.2, 62.4, 61.7, 60.1, 56.5, 56.2 and 56.1 ppm.

Compound **31** was obtained as white solid (3.2 mg, 0.10 %yield based on Fraction **VI-II**). $R_f = 0.31$ (70% EtOAc: hexane). ^1H NMR (400 MHz, CDCl_3): δ 7.07 (s, 2H), 6.80 (s, 1H), 6.61 (s, 1H), 4.00 (s, 3H), 3.99 s, (3H), 3.95 (s, 6H) and 3.92 (s, 6H) ppm. ^{13}C NMR (100 MHz, CDCl_3): δ 177.3, 161.2, 157.9, 154.6, 153.7, 153.7, 152.7, 141.0, 140.6, 127.0, 113.0, 108.4, 103.6, 103.4, 96.4, 62.3, 61.7, 61.2, 56.5, 56.5 and 56.5 ppm.

Compound **32** was obtained as light brown solid (1.2 mg, 0.03 %yield based on Fraction **VI-II**). HRESIMS (m/z calcd for $[\text{M}+\text{H}]^+$: 366.3800, found: 366.1348) gave

the molecular formula $C_{21}H_{19}NO_5$. $R_f = 0.26$ (70% EtOAc: hexane). 1H NMR (400 MHz, $CDCl_3$): δ 8.87 (s, 1H), 8.79 (d, $J = 4.0$ Hz, 1H), 8.15 (dt, $J = 8.2, 2.0$ Hz, 1H), 8.0 (d, $J = 9.6$ Hz, 1H), 7.65 (d, $J = 8.4$ Hz, 1H), 7.55 (dd, $J = 8.0, 4.8$ Hz, 1H), 7.11 (d, $J = 8.4$ Hz, 1H), 6.28 (d, $J = 9.6$ Hz, 1H), 5.07 (dd, $J = 10.8, 7.2$ Hz, 1H), 4.92 (s, 1H), 4.89 (s, 1H), 4.78 (dd, $J = 10.8, 7.6$ Hz, 1H), 4.50 (t, $J = 7.2$ Hz, 1H), 3.86 (s, 3H) and 1.68 (s, 3H) ppm. ^{13}C NMR (100 MHz, $CDCl_3$): δ 164.2, 160.6, 159.8, 153.2, 153.0, 149.3, 144.9, 142.2, 137.2, 128.7, 128.8, 124.2, 114.4, 112.8, 112.3, 111.8, 108.6, 64.8, 56.4, 40.2, 21.8 ppm.

Compound **33** was obtained as light brown solid (26.7 mg, 2.29 %yield based on Fraction **VI-II**). $R_f = 0.40$ (70% EtOAc: hexane). 1H NMR (400 MHz, $CDCl_3$): δ 7.16 (s, 2H), 6.64 (s, 1H), 4.10 (s, 3H), 4.02 (s, 3H), 3.95 (s, 12H) and 3.92 (s, 3H) ppm. ^{13}C NMR (100 MHz, $CDCl_3$): δ 177.48, 160.96, 153.70, 151.71, 148.56, 147.87, 144.30, 141.14, 138.09, 126.81, 114.91, 107.75, 103.45, 62.41, 62.05, 61.96, 61.83, 61.18 and 56.36 ppm.

2.5 Synthesis of Coumarin Derivatives

2.5.1 General Esterification Procedure

The derivatization of 7-hydroxycoumarin into its ester analogue was performed into two steps. Firstly, PPh₃ (4 mmol) in CH₂Cl₂ (3 mL) was added into a mixture of carboxylic acid (2 mmol) and CCl₃CN (4 mmol) in CH₂Cl₂ (3 mL) at RT. Then, the mixture was stirred for 1 h. The second step, 7-hydroxycoumarin (2 mmol) in CH₂Cl₂ (10 mL) and 4-picoline (6 mmol) were added to the previous mixture (in step 1). The mixture was refluxed and stirred for 6 h or followed by TLC. After the reaction occurred completely, the organic layer was extracted with 10% HCl and NaHCO₃, respectively. Moreover, the organic layer was dried over anhydrous Na₂SO₄, filtered, and evaporated using rotary vacuum evaporator. The reaction mixture was purified by subjected into silica gel column and eluted with hexane: EtOAc yielding compounds **34** (2 mg, 5%yield), **35** (50 mg, 9%yield), **36** (260 mg, 38%yield), and **37** (580 mg, 73%yield). The synthesis of ester analogues of 7-hydroxycoumarin from carboxylic acids is concluded in Table 2.1.

Table 2.1 The synthesis of ester analogues of 7-hydroxycoumarin from carboxylic acids

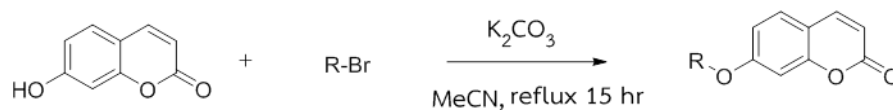
Entry	R	7-acylated products	
		compounds	% isolated yield
1		34	5
2		35	9
3		36	38
4		37	73

Compounds **34-37** were obtained as pale yellow solid, orange solid, brown solid and white solid, respectively. All structures of ester analogues were well-confirmed by ^1H NMR. The ^1H NMR spectrum of compound **34** showed signal at δ 7.62 (d, $J = 9.6$ Hz, 1H), 7.42 (d, $J = 8.4$ Hz, 1H), 7.04 (s, 1H), 6.98 (d, $J = 8.5$ Hz, 1H), 6.33 (d, $J = 9.5$ Hz, 1H), 2.51 (t, $J = 7.4$ Hz, 2H), 1.73 (sextet, $J = 7.3$ Hz, 2H) and 0.99 (t, $J = 7.4$ Hz, 3H) ppm. The ^1H NMR spectrum of compound **35** showed signal at δ 7.71 (d, $J = 9.6$ Hz, 1H), 7.51 (d, $J = 8.4$ Hz, 1H), 7.13 (s, 1H), 7.07 (d, $J = 8.4$ Hz, 1H), 6.42 (d, $J = 9.5$ Hz, 1H), 2.61 (t, $J = 7.5$ Hz, 2H), 1.79 (qui, $J = 7.4$ Hz, 2H), 1.37 (m, 8H)

and 0.91 (m, 3H) ppm. The ^1H NMR spectrum of compound **36** showed signal at δ 7.71 (d, $J = 9.5$ Hz, 1H), 7.51 (d, $J = 8.4$ Hz, 1H), 7.13 (s, 1H), 7.07 (d, $J = 8.4$ Hz, 1H), 6.42 (d, $J = 9.5$ Hz, 1H), 2.61 (t, $J = 7.5$ Hz, 2H), 1.79 (qui, $J = 7.5$ Hz, 2H), 1.30 (m, 16H) and 0.91 (t, $J = 6.6$ Hz, 3H) ppm. The ^1H NMR spectrum of compound **37** showed signal at δ 7.71 (d, $J = 9.6$ Hz, 1H), 7.51 (d, $J = 8.4$ Hz, 1H), 7.13 (s, 1H), 7.07 (d, $J = 8.5$ Hz, 1H), 6.42 (d, $J = 9.6$ Hz, 1H), 2.61 (t, $J = 7.5$ Hz, 2H), 1.78 (qui, $J = 7.5$ Hz, 2H), 1.29 (m, 24H) and 0.90 (t, $J = 6.6$ Hz, 3H) ppm.

2.5.2 General Alkylation Procedure

Alkylation of 7-hydroxycoumarin was accomplished in one step. A mixture of 7-hydroxycoumarin (3 mmol), K_2CO_3 (3.9 mmol), and alkyl halides (3.9 mmol) in anhydrous CH_3CN (20 mL) was stirred at reflux for 22-46 h, and monitored by TLC. The reaction was filtered and washed twice with EtOAc (10 mL). The organic layer was washed with H_2O (50 mL), dried over anhydrous Na_2SO_4 , and then evaporated in vacuum. The obtained residue was purified by column chromatography eluted with hexane: EtOAc to give the compounds **38** (0.55 g, 92%yield) and **39** (0.55 g, 80%yield). The synthesis of ether analogues of 7-hydroxycoumarin from alkyl halides is summarized in Table 2.2.

Table 2.2 Alkylation of 7-hydroxycoumarin from alkyl halides

Entry	R	7-acetylated products	
		compounds	% isolated yield
1		38	92
2		39	80

Compounds **38** and **39** were obtained as white solid and pale yellow solid, respectively. All structures of alkyl analogues were well-confirmed by ^1H NMR. The ^1H NMR spectrum of compound **38** showed signal at δ 7.64 (d, $J = 9.5$ Hz, 1H), 7.37 (d, $J = 8.6$ Hz, 1H), 6.86 (d, $J = 8.0$ Hz, 1H), 6.83 (s, 1H), 6.25 (d, $J = 9.5$ Hz, 1H), 6.04 (m, 1H), 5.44 (d, $J = 17.2$ Hz, 1H), 5.34 (d, $J = 10.4$ Hz, 1H) and 4.60 (d, $J = 5.3$ Hz, 2H) ppm. The ^1H NMR spectrum of compound **39** showed signal at δ 7.63 (d, $J = 9.5$ Hz, 1H), 7.36 (d, $J = 8.5$ Hz, 1H), 6.83 (d, $J = 8.0$ Hz, 1H), 6.82 (s, 1H), 6.23 (d, $J = 9.3$ Hz, 1H), 5.45 (m, 1H), 4.55 (d, $J = 7.0$ Hz, 2H), 1.79 (s, 3H) and 1.75 (s, 3H) ppm.

2.6 Bioassay

2.6.1 Exploration for insect control agent

2.6.1.1 Antifeedant activity

The antifeedant activity was evaluated through no-choice assay. Acetone which provided good solubility, high volatile rate and no toxicity was chosen. Crude extract and isolated compounds were weighed and diluted with 1 mL of acetone, then incorporated into artificial diet to final weight 10 g (0.25 %w/w for crude extracts and 2.5 mM for isolated compounds). For the control group, 1 mL of acetone was incorporated into 10 g of artificial diet. After each diet was kept at RT to release the solvent to evaporate, then divided into 30 pieces and weighed. After that put the piece of diet in 24-well plates at the number of 1 piece per well and second *Spodoptera litura* instar larvae were placed singly in each well after being starved for 6 h. The experiment was done under conditions of 27 ± 2 °C. After 24 h, the diet was weighed to record the weight loss from treatment and control. Each treatment was set up with 30 larvae.

Antifeedant activity was expressed as %antifeedant calculated according to the following the equation.

$$\% \text{ Antifeedant} = (1 - (T/C)) \times 100$$

Where: T is the weight loss of diet in treatment

C is the weight loss of diet in control

2.6.1.2 Insecticide activity

Pure compound was weighed, and diluted with 1 mL of acetone (2.5 mM final solutions) then sphere on surface of artificial diet. After that, put the second *S. litura* instar larvae in each well. Three repetitions with 20 larvae each were prepared, with a total of 60 larvae per treatment. The control procedure consisted of the application of sterile distilled water on larvae and also a control procedure with acetone. Mortality percentage of larvae that were being submitted to diet that treated with pure isolated compounds of *M. paniculata* for 15 days, under laboratory conditions ($27\pm 2^\circ\text{C}$).

$$\% \text{ Mortality} = (N/P) \times 100$$

Where: N = number of dead larvae

P = population of larvae

2.6.1.3 Repellent activity

- Petri dish choice bioassay

The repellent activity of isolated compounds from *M. paniculata* against *Ferrisia virgate* (Cockerell) adults was evaluated using the area preference method. The isolated compounds were diluted in acetone to prepare testing solutions of concentration $78.63 \mu\text{g}/\text{cm}^2$. The filter paper (9 cm in diameter) was cut into two equal pieces. One piece was uniformly dealt with 500 μL of testing solution as a testing part, and the other piece was treated with 500 μL of acetone as a control part. After that, the filter paper was air dried for 10 min to evaporate the solvent

completely, and full discs were accordingly reproduced by attaching testing part to control part with solid glue. Each remade filter paper was tightly fixed on the bottom of a 9 cm diameter Petri dish side by side. For each test, 20 insects were moved into the center of the filter paper disc which was then covered with lid. Each compound was replicated for five times. The number of insects present on the control and the testing parts of the filter paper was recorded after 2 and 4 h. Lemon glass oil was used as a positive control. The value of percent repellent (PR) was calculated as follows:

$$PR (\%) = [(N_c - N_t) / (N_c + N_t)] \times 100$$

Where: N_c = number of insects present on the control parts

N_t = number of insects present on the testing parts

2.6.2 Antibacterial activity

The compounds were tested against bacteria pathogens: *Propionibacterium acnes* (KCCM41747), *Staphylococcus aureus* (ATCC25923), *Streptococcus sobrinus* (KCCM11898), *Streptococcus mutans* (ATCC25175), and *Salmonella typhi* (ATCC442).

The antibacterial activity of *M. paniculata* was estimated by agar diffusion method. Muller Hinton agar medium was prepared and poured into Petri dishes. Then it was incubated with a swap of bacterial culture and spread throughout the medium uniformly with a sterile cotton swap. Using a sterile cork borer (10 mm diameter) wells were made in an agar medium. The test compound was introduced into the

well and all the plates were incubated at 37 °C for 24 h. The experiment was performed three times under clean conditions. Sensitivity of the organism was determined by measuring the diameter of the zone of inhibition. Each assay was replicated five times and the mean value was taken for analyses. The control experiment was carried out with chloramphenicol.

2.6.3 Anti-inflammatory activity

2.6.3.1 Cell culture

RAW 264.7 murine macrophages cells were maintained in DMEM medium supplemented with 10% FBS, penicillin (100 units/mL), streptomycin (100 µg/mL), and were incubated at 37 °C in a humidified atmosphere containing 5% CO₂. The medium was routinely changed every two days. RAW 264.7 cells were passaged by trypsinization until they attained confluence.

2.6.3.2 Cell viability assay

Cell viability was determined by MTT assay. RAW 264.7 macrophages were treated with different concentrations of test compounds (0.5, 1, 5, 10, 50 and 100 µM) in the presence of 1 µg/mL LPS for 24 h. The untreated group received an equal amount of DMSO, which resulted in a final concentration of 0.2% DMSO in the culture medium. After 24 h incubation, 0.5 mg/mL MTT was added to each well, and the cells were incubated for another 4 h at 37 °C with 5% CO₂. The supernatant was discarded and 100 mL of DMSO was added to the cells to dissolve the formazan.

The absorbance of each group was measured by using a microplate reader at 570 nm. The optical density of MTT-formazan formed in untreated cells was taken as 100% of viability.

2.6.3.3 Nitrite assay

Nitrite accumulation, an indicator of NO synthesis, was measured in culture media based on a diazotization reaction using the Griess reagent. Cells were seeded into a 96-well plate at the density of 5×10^4 cells/mL. After incubation, RAW 264.7 cells were pretreated with various concentrations of test compounds (3.125, 6.25, 12.5, 25, 50 and 100 μ M) with or without 1 μ g/mL of LPS for 24 h. An aliquot (100 μ L) of the supernatant was mixed with an equal volume of Griess reagent (1% (w/v) sulfanilamide in 5% (v/v) phosphoric acid and 0.1% (w/v) naphthylethylene diamine dihydrochloride), and incubated at room temperature for 10 min, and then the absorbance at 540 nm was measured in a microplate reader. Fresh culture media were used as blanks in all experiments. Nitrite concentration was determined by a sodium nitrite standard curve.

2.6.4 Antioxidant activity

Free radical-scavenging activities of test compounds were evaluated in comparison with ascorbic acid using DPPH assay. In brief, 0.05 mg/mL solution of DPPH in MeOH was prepared. This solution (100 μ L) was added to 50 μ L of different compounds in MeOH at different concentrations (62.5, 125, 250, 500, 1000 μ g/mL).

The mixture was shaken vigorously and allowed to stand at room temperature for 30 min. Then; absorbance was measured at 517 nm by using microplate reader (BioTek PowerWave XS2). A reference standard compound being used was ascorbic acid and the experiment was done in triplicate. The IC_{50} value of the sample, which is the concentration of sample required to inhibit 50% of DPPH free radical, was calculated using log dose inhibition curve. The percent DPPH scavenging effect was calculated by using the following equation:

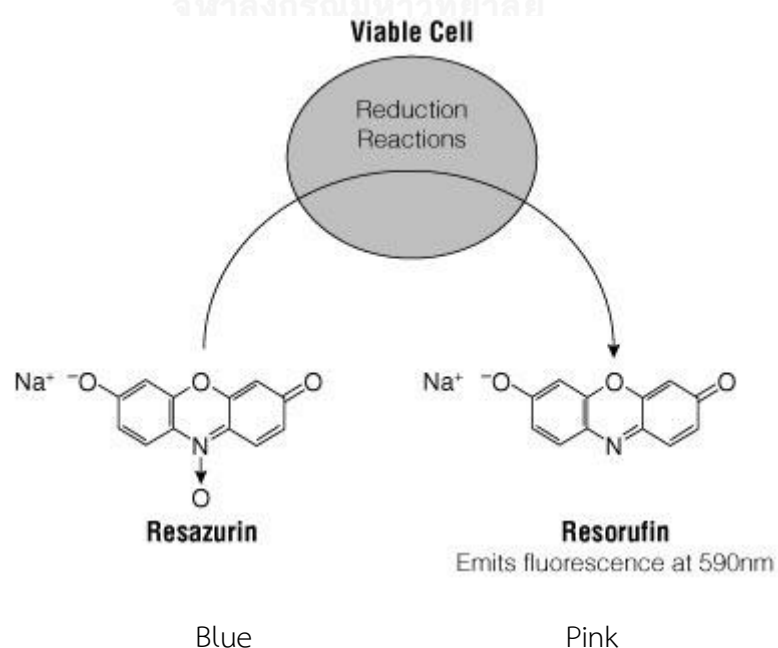
$$\text{Percent inhibition} = (A_0 - A_1) / A_0 \times 100$$

Where: A_0 = the absorbance of control reaction

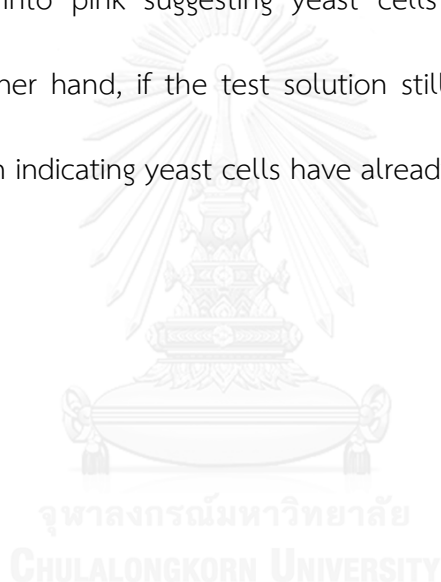
A_1 = the absorbance in the presence of test or standard sample

2.6.5 Anti-human carbonic anhydrase activity

- Resazurin Assay Protocol



Yeast cells and test compounds were prepared in opaque-walled 96-well plates containing a final volume of 100 μL /well. An optional set of wells could be prepared with medium containing tested compound. All test compounds were incubated for desired period of exposure. After that add resazurin solution (30 μL) to each well and incubated for 1 to 4 h at 37 $^{\circ}\text{C}$ to allow cells to convert resazurin to resorufin, and the result was noticed with naked eyes. If the test solution was changed from blue into pink suggesting yeast cells were still alive under that condition. On the other hand, if the test solution still has blue color after adding resazurin into solution indicating yeast cells have already died in that condition.



CHAPTER III

RESULTS AND DISCUSSION

Chemical constituents from the leaves of *M. paniculata* were investigated via the separation by column chromatography and semi-prep HPLC. In addition, some related compounds as ester and ether analogues of 7-hydroxycoumarin (umbelliferone) were synthesized. All compounds with sufficient amount were further evaluated for antifeedant, insecticidal, repellent, antibacterial, antioxidant, anti-inflammatory and antihuman carbonic anhydrase II activities.

3.1 Extraction of *M. paniculata* leaves

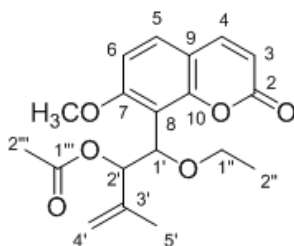
Two methods for leaf extraction were conducted. For the first method, dried powders of *M. paniculata* leaves were soaked into 3 L of hexane, CH₂Cl₂, EtOAc and MeOH for 7 days yielding Fractions I (3.91 %yield), II (3.94 %yield), III (2.74 %yield) and IV (7.03 %yield) all as dark green liquid. For the second method, parts of Fraction IV were suspended in water and then extracted with hexane and EtOAc for 3 and 5 times, respectively in order to keep high polar constituents remain in aqueous layer furnishing Fractions V (3.43 %yield) and VI (57.45 %yield) both as dark green.

3.2 Chemical constituents of *M. paniculata* leaves

3.2.1 Separation of Fraction I and structural elucidation of its constituents

The crude hexane extract (Fraction I) as dark green oil (190 g) was fractionated by silica gel column eluting with hexane-EtOAc gradient in a stepwise fashion yielding compound **1**.

Compound **1** was obtained as green plate (1.0 g, 0.51% yield based on Fraction I). According to the ^1H NMR spectrum (Figure A-1), compound **1** should contain 7-methoxy-8-substituted coumarin skeleton since the spectrum showed four high intensity doublet signals at δ_{H} 6.26 ($J = 9.5$ Hz), 7.62 ($J = 9.5$ Hz), 7.39 ($J = 8.6$ Hz) and 6.87 ($J = 8.7$ Hz) ppm. The methoxy group substituted on an aromatic ring exhibited a high intensity singlet signal at δ_{H} 3.96 ppm. A doublet signal of benzylic methine protons exhibited at δ_{H} 5.29 ppm ($J = 8.6$ Hz), a doublet signal of methine proton displayed at δ_{H} 4.50 ppm ($J = 8.5$ Hz), a singlet signal of allylic methyl protons showed at δ_{H} 1.77 ppm and a multiplet signal of methylene protons presented at δ_{H} 4.68 - 4.57 ppm. In addition, the ethoxy group showed a quartet signal at δ_{H} 3.72 ppm ($J = 7.0$ Hz) and a triplet signal at δ_{H} 1.24 ppm ($J = 7.0$ Hz). The methyl group adjacent to a carbonyl group exhibited a singlet signal at δ_{H} 1.77 ppm. The structure of compound **1** was clarified as murraxocin acetate ($\text{C}_{19}\text{H}_{22}\text{O}_6$). [20] The ^1H NMR spectral assignment of compound **1** and murraxocin acetate is collected in Table 3.1.



Compound 1

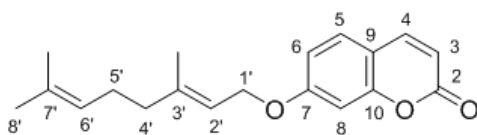
Table 3.1 The comparison of ^1H NMR spectral assignment of compound 1 and murraxocin acetate [20]

Positions	Chemical shift (ppm)	
	murraxocin acetate ²⁰	compound 1
3	6.24 (d, $J = 8.0$ Hz, 1H)	6.26 (d, $J = 9.5$ Hz, 1H)
4	7.58 (d, $J = 8.0$ Hz, 1H)	7.62 (d, $J = 9.5$ Hz, 1H)
5	7.38 (d, $J = 8.0$ Hz, 1H)	7.39 (d, $J = 8.6$ Hz, 1H)
6	6.84 (d, $J = 8.0$ Hz, 1H)	6.87 (d, $J = 8.7$ Hz, 1H)
1'	5.36 (d, $J = 8.0$ Hz, 1H)	5.29 (d, $J = 8.6$ Hz, 1H)
2'	6.06 (d, $J = 8.0$ Hz, 1H)	4.50 (d, $J = 8.5$ Hz, 1H)
4'	4.72 (m, 2H)	4.65 (m, 2H)
5'	1.52 (s, 3H)	1.77 (s, 3H)
1''	3.48 (m, 2H)	3.72 (q, $J = 7.0$ Hz, 2H)
2''	1.16 (t, $J = 6.0$ Hz, 3H)	1.24 (t, $J = 7.0$ Hz, 3H)
2'''	2.08 (s, 3H)	1.77 (s, 3H)
7-OMe	3.92 (s, 3H)	3.96 (s, 3H)

3.2.2 Separation of Fraction II and structural elucidation of its constituents

The CH₂Cl₂ extract (Fraction II) as dark green oil (190 g) was subjected to silica gel column using hexane-EtOAc gradient in a stepwise fashion. The separation of this extract furnished compounds **2** and **3**.

Compound **2** was obtained as orange oil (55 mg, 0.03% yield based on Fraction II). According to the ¹H NMR spectrum (Figure A-3), compound **2** should belong to 7-substituted coumarin group since three high intensity doublet signals at δ_{H} 6.27 ($J = 9.5$ Hz), 7.66 ($J = 9.5$ Hz) and 7.38 ppm ($J = 8.5$ Hz), double of doublet signal at 6.87 ppm ($J = 8.5, 2.5$ Hz) and a singlet signal at 6.85 ppm were visualized. At C-7, the methylene protons adjacent to oxygen atom revealed a doublet signal at δ_{H} 4.63 ppm ($J = 6.6$ Hz) together with three singlet signals of methyl groups at δ_{H} 1.63, 1.78 and 1.69 ppm, respectively. Corresponding to the ¹³C NMR spectrum (Figure A-4) of compound **2**, it characterized as 7-oxygenated coumarin that perceived carbon signals at δ_{C} 161.0 (C-2), 113.2 (C-3), 143.4 (C-4), 143.4 (C-5), 101.6 (C-6), 112.9 (C-9) ppm, together with methylene, methine, quaternary and methyl carbon signals being detected at δ_{C} 65.5 (C-1'), 118.4 (C-2'), 39.5 (C-4'), 26.2 (C-5'), 123.6 (C-6'), 25.6 (C-8'), and 16.8 (2C, C-3' and C-7'-OMe) ppm. The structure of compound **2** was elucidated as auraptene (C₁₉H₂₂O₃). [21] The NMR spectral assignment of compound **2** and auraptene is summarized in Table 3.2.



Compound 2

Table 3.2 The comparison of ^1H and ^{13}C NMR spectral assignment of compound 2 and auraptene [21]

Positions	Chemical shift (ppm)			
	auraptene ²¹		compound 2	
	^1H	^{13}C	^1H	^{13}C
2	-	161.4	-	161.0
3	6.23 (d, $J = 9.6$ Hz, 1H)	113.0	6.27 (d, $J = 9.5$ Hz, 1H)	113.2
4	7.61 (d, $J = 9.6$ Hz, 1H)	143.6	7.66 (d, $J = 9.5$ Hz, 1H)	143.4
5	7.34 (d, $J = 8.6$ Hz, 1H)	128.8	7.38 (d, $J = 8.5$ Hz, 1H)	143.4
6	6.83 (d, $J = 8.6$ Hz, 1H)	113.3	6.88 (m, 1H)	101.6
8	6.80 (d, $J = 2.4$ Hz, 1H)	101.7	6.85 (s, 1H)	-
9	-	155.9	-	112.9
1'	4.58 (d, $J = 6.5$ Hz, 2H)	65.6	4.63 (d, $J = 6.6$ Hz, 2H)	65.5
2'	5.45 (t, $J = 6.6$ Hz, 1H)	118.5	5.49 (t, $J = 6.7$ Hz, 1H)	118.4
4'	2.10 (m, 2H)	39.6	2.19 (d, $J = 1.1$ Hz, 2H)	39.5
5'	2.10 (m, 2H)	26.3	2.14 (d, $J = 7.6$ Hz, 2H)	26.2
6'	5.06 (t, $J = 6.6$ Hz, 1H)	123.7	5.10 (d, $J = 7.2$ Hz, 1H)	123.6
8'	1.65 (s, 3H)	17.8	1.63 (s, 3H)	25.6
3'-CH ₃	1.75 (s, 3H)	16.9	1.78 (s, 3H)	16.8
7'-CH ₃	1.59 (s, 3H)	25.8	1.69 (s, 3H)	16.8

Compound **3** was gained as yellow solid (3.0 g, 1.58 %yield based on Fraction II). According to the ^1H NMR spectrum (Figure A-5), 7-oxygenated coumarin moiety should be a core structure of this compound. To illustrate this, four doublet signals at δ_{H} 6.26 ($J = 9.5$ Hz), 7.62 ($J = 9.5$ Hz), 7.42 ($J = 8.7$ Hz) and 6.87 ppm ($J = 8.7$ Hz), and a methoxy group on aromatic ring with high intensity of 3H at δ_{H} 3.96 ppm were observed. A doublet signal at δ_{H} 5.29 ppm ($J = 1.9$ Hz) suggesting the presence of benzylic methine proton in this molecule. Moreover, methylene protons and allylic methyl group exhibited doublet and singlet signals at δ_{H} 3.99, 3.91 and 1.60 ppm, respectively. The ^{13}C NMR spectrum (Figure A-15) represented 7-methoxy-8-substituted coumarin carbons at δ_{C} 113.4 (C-3), 143.3 (C-4), 128.9 (C-5), 107.6 (C-6), 113.5 (C-8), 113.4 (C-9) ppm. Moreover, methylene, methine, quaternary and methyl carbon signals were detected. According to literature search, compound **3** was clearly fitted with phebalosin ($\text{C}_{15}\text{H}_{14}\text{O}_4$). [22] The NMR spectral assignments of compound **3** and phebalosin is presented in Table 3.3.

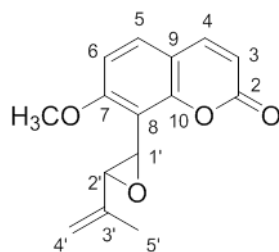
Compound **3**

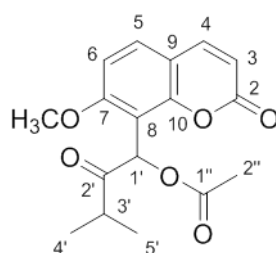
Table 3.3 The comparison of ^1H and ^{13}C NMR spectral assignment of compound **3** and phebalosin [22]

Positions	Chemical shift (ppm)			
	phebalosin ²²		compound 3	
	^1H	^{13}C	^1H	^{13}C
2	-	160.4	-	-
3	6.25 (d, $J = 9.5$ Hz, 1H)	113.2	6.26 (d, $J = 9.5$ Hz, 1H)	113.4
4	7.65 (d, $J = 9.5$ Hz, 1H)	143.7	7.62 (d, $J = 9.5$ Hz, 1H)	143.3
5	7.42 (d, $J = 8.5$ Hz, 1H)	127.6	7.42 (d, $J = 8.7$ Hz, 1H)	128.9
6	6.86 (d, $J = 8.5$ Hz, 1H)	108.7	6.87 (d, $J = 8.7$ Hz, 1H)	107.6
7	-	161.5	-	-
8	-	116.4	-	113.5
9	-	112.6	-	113.4
10	-	152.7	-	-
1'	5.28 (s, 1H)	53.2	5.29 (s, 1H)	51.8
2'	5.09 (s, 1H)	58.3	5.08 (s, 1H)	60.7
3'	-	142.6	-	-
4'	3.92(d, $J = 2.0$ Hz, 1H), 3.97(d, $J = 2.0$ Hz, 1H)	114.8	3.99 (d, $J = 2.4$ Hz, 1H), 3.91 (d, $J = 2.4$ Hz, 1H)	100.0
5'	1.87 (s, 3H)	18.9	1.60 (s, 3H)	17.4
7-OMe	3.96 (s, 3H)	56.3	3.96 (s, 3H)	56.3

3.2.3 Separation of Fraction III and structural elucidation of its constituents

The EtOAc extract (Fraction III) as dark green oil (112 g) was purified by silica gel column with hexane-EtOAc to achieve compounds **4** and **5**.

Compound **4** was obtained as white crystal (10 mg, 0.01 %yield based on Fraction III). According to the ^1H NMR spectrum (Figure A-7), coumarinic protons of this compound showed three high intensity doublet signals at δ_{H} 6.27 ($J = 9.5$ Hz), 7.66 ($J = 9.5$ Hz), 7.38 ($J = 8.5$ Hz) and a multiplet signal at δ_{H} 6.90 – 6.82 ppm. The aromatic $-\text{OCH}_3$ signal appeared at δ_{H} 4.63 ppm. The benzylic methine proton was detected as a singlet signal at δ_{H} 6.90 ppm, together with one multiplet signal of methine protons and two singlet signals of methyl groups at δ_{H} 2.85, 1.03 and 1.28 ppm, respectively. In addition, acetyl methyl protons were visualized as a singlet signal at δ_{H} 2.13 ppm. The structure of compound **4** was identified as hainanmurpanin ($\text{C}_{17}\text{H}_{18}\text{O}_6$) by comparing with those reported in literature. [8] The ^1H NMR spectral assignment of compound **4** and hainanmurpanin is illustrated in Table 3.4.



Compound **4**

Table 3.4 The comparison of ^1H NMR spectral assignment of compound **4** and hainanmurpanin [8]

Positions	Chemical shift (ppm)	
	hainanmurpanin ⁸	compound 4
	^1H	^1H
3	6.28 (d, $J = 9.5$ Hz, 1H)	6.27 (d, $J = 9.5$ Hz, 1H)
4	7.67 (d, $J = 9.5$ Hz, 1H)	7.66 (d, $J = 9.5$ Hz, 1H)
5	7.52 (d, $J = 8.5$ Hz, 1H)	7.38 (d, $J = 8.5$ Hz, 1H)
6	6.90 (d, $J = 8.5$ Hz, 1H)	6.86 (m, 1H)
1'	6.98 (s, 1H)	6.86 (m, 1H)
3'	2.85 (septet, $J = 7.0$ Hz, 1H)	2.85 (d, $J = 6.3$ Hz, 1H)
4'	1.03 (d, $J = 7.0$ Hz, 3H)	1.03 (s, 3H)
5'	1.18 (d, $J = 7.0$ Hz, 3H)	1.28 (s, 3H)
2''	2.12 (s, 3H)	2.13 (s, 3H)
7-OMe	3.91 (s, 3H)	4.63 (s, 3H)

Compound **5** was achieved as dark green solid (80 mg, 0.07 %yield based on Fraction III). The ^1H NMR spectrum (Figure A-8) of compound **5** exhibited four doublet signals at δ_{H} 6.25 ($J = 9.6$ Hz), 7.62 ($J = 9.6$ Hz), 7.39 ($J = 8.8$ Hz) and 6.87 ($J = 8.8$ Hz) ppm, together with a high intensity signal at δ_{H} 4.00 ppm of aromatic methoxy group, which readily indicated 7-methoxy-8-substituted coumarin system. The remaining part at 8-position was concluded according to the presence of doublet signal of benzylic methine and methine protons at δ_{H} 5.73 ($J = 7.6$ Hz) and 5.52

($J = 8.0$ Hz) ppm, respectively. The signals at δ_{H} 4.76 and 4.73 ppm were assignable to two exo-methylene protons. The singlet signals of acetyl methyl and allylic methyl protons were presented at δ_{H} 2.13 and 1.74 ppm, respectively. The ^{13}C NMR (Figure A-9) showed 17 carbon signals that were very similar to those of compound **3** except at the carbon side chain of C-8 position. Therefore, compound **5** was explicated as murrangatin acetate ($\text{C}_{17}\text{H}_{20}\text{O}_6$). [2][23] The NMR spectral assignment of compound **5** and murrangatin acetate is displayed in Table 3.5.

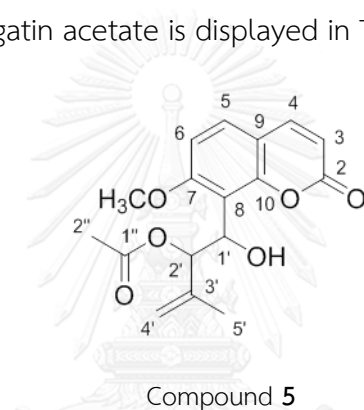


Table 3.5 The comparison of ^1H and ^{13}C NMR spectral assignment of compound **5** and murrangatin acetate [2][23]

Positions	Chemical shift (ppm)			
	murrangatin acetate ^{2,23}		compound 5	
	^1H	^{13}C	^1H	^{13}C
2	-	160.2	-	160.4
3	6.26 (d, $J = 9.4$ Hz, 1H)	113.5	6.25 (d, $J = 9.6$ Hz, 1H)	113.7
4	7.61 (d, $J = 9.4$ Hz, 1H)	143.7	7.62 (d, $J = 9.6$ Hz, 1H)	143.8
5	7.39 (d, $J = 8.7$ Hz, 1H)	128.8	7.39 (d, $J = 8.8$ Hz, 1H)	128.9

Table 3.5 The comparison of ^1H and ^{13}C NMR spectral assignment of compound **5** and murrangatin acetate [2][23] (cont)

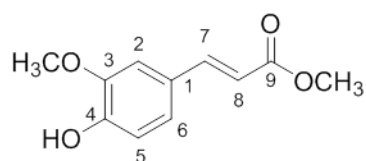
Positions	Chemical shift (ppm)			
	murrangatin acetate ^{2,23}		compound 5	
	^1H	^{13}C	^1H	^{13}C
6	6.87 (d, $J = 8.7$ Hz, 1H)	107.8	6.87 (d, $J = 8.8$ Hz, 1H)	107.9
7	-	160.0	-	160.2
8	-	115.8	-	115.9
9	-	113.1	-	113.2
10	-	152.7	-	152.8
1'	5.73 (d, $J = 7.7$ Hz, 1H)	68.2	5.73 (d, $J = 7.6$ Hz, 1H)	68.3
2'	5.53 (dd, $J = 11.1, 7.7$ Hz, 1H)	79.5	5.52 (d, $J = 8.0$ Hz, 1H)	79.7
3'	-	140.8	-	140.9
4'	4.77(s, 1H), 4.74(s, 1H)	114.9	4.76 (s, 1H), 4.73 (s, 1H)	114.9
5'	1.75 (s, 3H)	18.5	1.74 (s, 3H)	18.7
1''	-	170.9	-	171.1
2''	2.14 (s, 3H)	21.2	2.13 (s, 3H)	21.4
OH	3.56 (d, $J = 11.1$ Hz, OH)	-	-	-
7-OMe	4.00 (s, 3H)	56.3	4.00 (s, 3H)	56.5

3.2.4 Separation of Fraction VI and structural elucidation of its constituents

3.2.4.1 Separation of Fraction VI-I and structural elucidation of its constituents

Fraction **IV** was further partitioned with EtOAc and H₂O to afford the EtOAc portion (Fraction **VI**, 83.3 g). This fraction was further separated by silica gel column eluting with a gradient mixture of CHCl₃/MeOH (100:0 to 1:1), to yield 184 fractions. Subfractions 12-16 designated as Fraction **VI-I** (79.2 mg) was purified by semi-preparative HPLC (MeCN/H₂O) to afford compounds **6** and **7**.

Compound **6** was obtained as brown oil (3 mg, 3.79 %yield based on Fraction **VI-I**). Concerning with the ¹H-NMR spectrum (Figure A-10), it exhibited a high intensity signal at δ_{H} 7.01, 7.06 and 6.88 ppm suggesting the presence of aromatic protons in molecule. The doublet signals of two methine protons were detected at δ_{H} 7.60 ($J = 16.0$ Hz) and 6.26 ($J = 15.6$ Hz) ppm. The signal belonging to the methoxy group on aromatic ring and that adjacent to carbonyl group exhibited as a high intensity signal at δ_{H} 7.77 and 3.90 ppm, respectively. This phenolic compound presented eleven carbon signals such as six aromatic (C-1 to C-6), one carbonyl ketone (C-9), two methylene (C-7 and C-8) and two methoxy carbons. The structure of compound **6** was eventually explained as methyl ferulate (C₁₁H₁₂O₄) by comparing with the spectral data reported in previous literature. [24] The NMR spectral assignment of compound **6** and methyl ferulate is collected in Table 3.6.



Compound 6

Table 3.6 The comparison of ^1H and ^{13}C NMR spectral assignment of compound 6 and methyl ferulate [24]

Positions	Chemical shift (ppm)			
	methyl ferulate ²⁴		compound 6	
	^1H	^{13}C	^1H	^{13}C
1	-	127.2	-	126.9
2	7.05 (d, $J = 2.0$ Hz, 1H)	109.7	7.01 (d, $J = 2.0$ Hz, 1H)	109.7
3	-	147.0	-	147.1
4	-	148.2	-	148.3
5	7.09 (dd, $J = 8.0, 2.0$ Hz, 1H)	115.5	7.06 (dd, $J = 16.0, 2.0$ Hz, 1H)	115.1
6	6.94 (d, $J = 8.0$ Hz, 1H)	123.3	6.88 (d, $J = 8.0$ Hz, 1H)	123.1
7	7.64 (d, $J = 15.5$ Hz, 1H)	145.2	7.60 (d, $J = 16.0$ Hz, 1H)	145.2
8	6.31 (d, $J = 15.5$ Hz, 1H)	114.9	6.26 (d, $J = 15.6$ Hz, 1H)	115.0
9	-	167.9	-	168.0
7-OMe	3.81 (s, 3H)	51.8	3.77 (s, 3H)	51.7
-CO-OMe	3.95 (s, 3H)	56.2	3.90 (s, 3H)	56.0

Compound **7** was derived as brown oil (2 mg, 2.53 %yield based on Fraction VI-I). Its ^1H NMR spectrum (Figure A-12) presented a signal of aromatic protons at δ_{H} 7.03 (dd, $J = 2.0, 2.0$ Hz), 6.84 (d, $J = 8.4$ Hz) and 7.12 (d, $J = 2.0$ Hz) ppm. Two methine groups were detected at δ_{H} 7.59 (d, $J = 16.0$ Hz) and 6.28 (d, $J = 16.0$ Hz) ppm. The signal of a methoxy group on aromatic ring was presented at 3.92 ppm. Another methoxy group adjacent to carbonyl group exhibited a high intensity signal at δ_{H} 3.47 ppm. Compound **7** is a phenolic compound containing twelve carbon signals including six aromatic (C-1 to C-6), one carbonyl ketone (C-9), two methylene (C-7 and C-8) and three methoxy carbons. The structure of compound **7** was believed to be 3,4-*O*-dimethylcaffeic acid methyl ester ($\text{C}_{12}\text{H}_{14}\text{O}_4$). [25] The NMR spectral assignment of compound **7** and 3,4-*O*-dimethylcaffeic acid methyl ester is presented in Table 3.7.

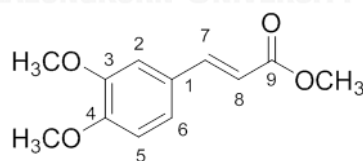
Compound **7**

Table 3.7 The comparison of ^1H NMR spectral assignment of compound **7** and 3,4-*O*-dimethylcaffeic acid methyl ester [25]

Positions	Chemical shift (ppm)	
	3,4- <i>O</i> -dimethylcaffeic acid methyl ester ²⁵	compound 7
2	7.05 (d, $J = 2.1$ Hz, 1H)	7.03 (dd, $J = 2.0, 2.0$ Hz, 1H)
5	6.87 (d, $J = 8.4$ Hz, 1H)	6.84 (d, $J = 8.4$ Hz, 1H)
6	7.11 (dd, $J = 8.4, 2.1$ Hz, 1H)	7.12 (d, $J = 2.0$ Hz, 1H)
3-OMe	3.92 (s, 3H)	3.92 (s, 3H)
4-OMe	3.92 (s, 3H)	3.78 (s, 3H)
1'	7.65 (d, $J = 15.9$ Hz, 1H)	7.59 (d, $J = 16.0$ Hz, 1H)
2'	6.33 (d, $J = 15.9$ Hz, 1H)	6.28 (d, $J = 16.0$ Hz, 1H)
3'-OMe	3.81 (s, 3H)	3.47 (s, 3H)

3.2.4.2 Separation of Fraction VI-II (Part 1) and structural elucidation of its constituents

The fractions 42-66 assigned as Fraction **VI-II** (3.2 g) were submitted for further separation on RP-18 column, eluted with a gradient mixture of MeOH/H₂O (50:50 to 100:0), yielding 108 subfractions. Subfraction 7 (5.2 mg), 19 (39.0 mg), 35 (4.5 mg) and 46 (6.4 mg) were recrystallized by petroleum ether, MeOH, MeOH and acetone: petroleum ether, respectively to afford compounds **8**, **9**, **10** and **11**.

Compound **8** was gained as white solid (5.2 mg, 1.66 %yield based on Fraction **VI-II**). The ^1H NMR spectrum (Figure A-14) shared the characteristic of 7-methoxy-8-substituted coumarin system which showed four doublet signals at δ_{H} 6.27 (d, $J = 9.2$ Hz), 7.63 (d, $J = 9.6$ Hz), 7.41 (d, $J = 8.4$ Hz) and 6.90 (d, $J = 8.8$ Hz) ppm. The methoxy group bearing on aromatic ring exhibited the signal at δ_{H} 4.00 ppm. The doublet signal of benzylic methine and methine protons presented at δ_{H} 5.43 (d, $J = 7.2$ Hz) and 4.53 (d, $J = 7.6$ Hz) ppm, respectively. The signal at δ_{H} 4.99 ppm was assignable to two exo-methylene protons. The singlet signal of allylic methyl protons was presented at δ_{H} 1.90 ppm. 7-Methoxy-8-substituted coumarin carbon signals were observed together with 2 methine, 1 quaternary, 1 methylene and 1 methyl carbon signals in the ^{13}C NMR spectrum (Figure A-15). The structure of compound **8** was compatible with minumicrolin ($\text{C}_{15}\text{H}_{16}\text{O}_5$) after making a comparison with previous report. [23][26] The NMR spectral assignment of compound **8** and minumicrolin is exhibited in Table 3.8.

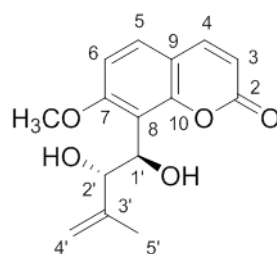
Compound **8**

Table 3.8 The comparison of ^1H and ^{13}C NMR spectra assignment of compound **8** and minumicrolin [23][26]

Positions	Chemical shift (ppm)			
	minumicrolin ^{23,26}		compound 8	
	^1H	^{13}C	^1H	^{13}C
2	-	160.2	-	160.3
3	6.25 (d, $J = 9.4$ Hz, 1H)	113.5	6.27 (d, $J = 9.2$ Hz, 1H)	113.7
4	7.63 (d, $J = 9.4$ Hz, 1H)	143.7	7.63 (d, $J = 9.6$ Hz, 1H)	144.0
5	7.40 (d, $J = 8.7$ Hz, 1H)	128.5	7.41 (d, $J = 8.4$ Hz, 1H)	129.0
6	6.89 (d, $J = 8.7$ Hz, 1H)	108.0	6.90 (d, $J = 8.8$ Hz, 1H)	108.1
7	-	160.6	-	160.7
8	-	116.5	-	116.6
9	-	153.3	-	153.4
10	-	113.3	-	113.4
1'	5.41 (dd, $J = 7.0$ Hz, 10.0, 1H)	68.6	5.43 (d, $J = 7.2$ Hz, 1H)	68.6
2'	4.51 (d, $J = 7.0$ Hz, 1H)	78.5	4.53 (d, $J = 7.6$ Hz, 1H)	78.6
3'	-	145.1	-	145.2
4'	4.97 (s, 1H), 4.98 (s, 1H)	113.8	4.99 (d, $J = 4.0, 1.6$ Hz, 2H)	114.1
5'	1.88 (s, 3H)	18.0	1.90 (s, 3H)	18.1
7-OMe	3.97 (s, 3H)	56.4	4.00 (s, 3H)	56.6

Compound **9** was furnished as white solid (39 mg, 12.48 %yield based on Fraction **VI-II**). The integration of the ^1H NMR spectrum (Figure A-16) of this compound indicated the presence of 17 protons. Four doublet signals at δ_{H} 6.25 (d, $J = 9.6$ Hz), 7.61 (d, $J = 9.2$ Hz), 7.40 (d, $J = 8.8$ Hz) and 6.86 (d, $J = 8.8$ Hz) ppm were the characteristics of H-3, H-4, H-5 and H-6 in a coumarin nucleus. The methoxy group on aromatic ring exhibited a high intensity singlet signal at δ_{H} 3.92 ppm. The doublet signal of benzylic methine and methine protons presented at δ_{H} 5.05 (d, $J = 8.8$ Hz) and 4.93 (d, $J = 8.8$ Hz) ppm, respectively, together with the singlet signal of methoxy group observed at δ_{H} 3.32 ppm. Exo-methylene protons were assignable by the signals at δ_{H} 4.63 and 4.69 ppm. The singlet signal of allylic methyl protons was visualized at δ_{H} 1.68 ppm. According to the ^{13}C NMR spectrum (Figure A-17), it showed a set of 7-methoxy-8-substituted coumarin carbon signals comprising carbon signals of side chain of C-8 position. Based on the spectral data and the comparison with chemical literature, the structure of compound **9** was elucidated as murracarpin ($\text{C}_{16}\text{H}_{18}\text{O}_5$) by comparing with those reported in literature. [3] The NMR spectral assignment of compound **9** and murracarpin is collected in Table 3.9.

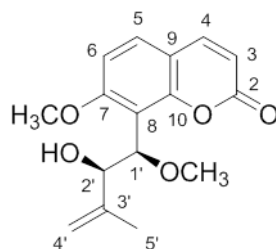
Compound **9**

Table 3.9 The comparison of ^1H and ^{13}C NMR spectra assignment of compound **9** and murracarpin [3]

Positions	Chemical shift (ppm)			
	murracarpin ³		compound 9	
	^1H	^{13}C	^1H	^{13}C
2	-	161.3	-	161.4
3	6.26 (d, $J = 9.4$ Hz, 1H)	113.4	6.25 (d, $J = 9.6$ Hz, 1H)	113.5
4	7.62 (d, $J = 9.4$ Hz, 1H)	143.3	7.61 (d, $J = 9.2$ Hz, 1H)	143.3
5	7.40 (d, $J = 8.7$ Hz, 1H)	129	7.40 (d, $J = 8.8$ Hz, 1H)	129.1
6	6.86 (d, $J = 8.7$ Hz, 1H)	107.9	6.86 (d, $J = 8.8$ Hz, 1H)	107.9
7	-	160.4	-	160.5
8	-	114.2	-	114.3
9	-	113.3	-	113.4
10	-	153.9	-	153.9
1'	5.04 (s, 1H)	76.4	5.05 (d, $J = 8.8$ Hz, 1H)	76.5
2'	4.92 (s, 1H)	77.8	4.93 (d, $J = 8.8$ Hz, 1H)	77.9
3'	-	143.6	-	143.6
4'	4.69 (s, 1H), 4.62(s, 1H)	112.8	4.63 (t, $J = 1.6$ Hz, 1H), 4.69 (s, 1H)	112.9
5'	1.67 (s, 3H)	17.3	1.68 (s, 3H)	17.3
7-OMe	3.92 (s, 3H)	56.2	3.92 (s, 3H)	56.3
1'-OMe	3.32 (s, 3H)	57.6	3.32 (s, 3H)	57.6

Compound **10** was derived as white solid (9.1 mg, 0.28 %yield based on Fraction **VI-II**). This compound possessed 5,7-dimethoxy-8-substituted coumarin system. To illustrate this, the ^1H NMR spectrum (Figure A-18) showed the characteristic coumarin signals as the singlet at δ_{H} 6.34 and doublets at δ_{H} 6.14 ($d, J = 9.6$ Hz) and δ_{H} 8.03 ($d, J = 9.6$ Hz) ppm. In addition, the signal of two aromatic methoxy groups was exhibited as a high intensity signal at δ_{H} 3.93 ppm. At C-8 position, the doublet signal of benzylic methylene protons at δ_{H} 2.94 and aliphatic methine proton at δ_{H} 3.73 ppm were observed. Furthermore, aliphatic methoxy group revealed the singlet signal at δ_{H} 3.29 ppm together with two singlet methyl signals at δ_{H} 1.28 ppm. Signals at δ_{C} 161.6 (C-2), 111.0 (C-3), 138.9 (C-4), 155.7 (C-5), 90.5 (C-6), 161.5 (C-7), 108.2 (C-8), 154.3 (C-9), 104.1 (C-10), 24.7 (C-1'), 20.4 (C-4'), 21.2 (C-5'), 56.3 (C-7-OMe), 56.0 (C-5-OMe) and 49.5 (C-3'-OMe) ppm were found in the ^{13}C NMR spectrum (Figure A-19). The structure of compound **10** was determined as omphalocarpin ($\text{C}_{17}\text{H}_{22}\text{O}_6$) by comparing the spectral data with those addressed in previous literature. [1] The NMR spectral assignment of compound **10** and omphalocarpin is summarized in Table 3.10.

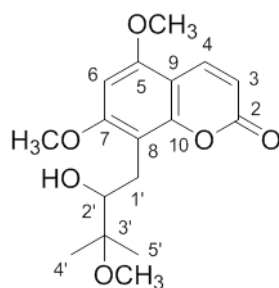
Compound **10**

Table 3.10 The comparison of ^1H and ^{13}C NMR spectral assignment of compound **10** and omphalocarpin [1]

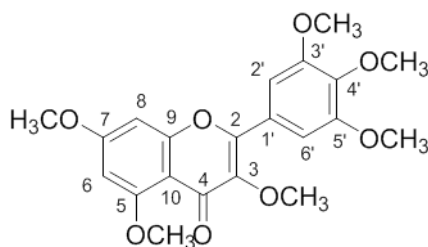
Positions	Chemical shift (ppm)			
	omphalocarpin ¹		compound 10	
	^1H	^{13}C	^1H	^{13}C
2	-	161.4	-	161.6
3	6.14 (d, $J = 9.4$ Hz, 1H)	110.8	6.14 (d, $J = 9.6$ Hz, 1H)	111.0
4	8.03 (d, $J = 9.4$ Hz, 1H)	138.8	7.99 (d, $J = 9.6$ Hz, 1H)	138.9
5	-	155.6	-	155.7
6	6.34 (s, 1H)	90.5	6.34 (s, 1H)	90.5
7	-	161.4	-	161.5
8	-	108.2	-	108.2
9	-	154.2	-	154.3
10	-	103.5	-	104.1
1'	2.94 (d, $J = 6.0$ Hz, 2H)	24.6	2.96 (s, 1H), 2.94 (t, $J = 1.6$ Hz, 1H)	24.7
2'	3.73 (q, $J = 6.0$ Hz, 1H)	76.6	3.73 (dd, $J = 4.0, 4.0$ Hz, 1H)	-

Table 3.10 The comparison of ^1H and ^{13}C NMR spectral assignment of compound **10** and omphalocarpin [1] (cont)

Positions	Chemical shift (ppm)			
	omphalocarpin ¹		compound 10	
	^1H	^{13}C	^1H	^{13}C
3'	-	77.3	-	-
4'	1.28(s, 3H)	20.3	1.28 (s, 3H)	20.4
5'	1.28(s, 3H)	21.0	1.28 (s, 3H)	21.2
7-OMe	3.93 (s, 3H)	56.2	3.93 (d, $J = 2.8$ Hz, 3H)	56.3
5-OMe	3.93(s, 3H)	55.9	3.93 (d, $J = 2.8$ Hz, 3H)	56.0
3'-OMe	3.29 (s, 3H)	49.4	3.28 (s, 3H)	49.5

Compound **11** was derived as white solid (6.4 mg, 0.20 %yield based on Fraction **VI-II**). According to the ^1H NMR spectrum (Figure A-20), the signals of 1,3,4,5-tretasubstituted phenyl protons at δ_{H} 7.52 and 7.37 ppm, and 2,3,5,7-tretasubstituted flavone protons at δ_{H} 6.50 and 6.36 ppm were detected. In addition, the signals of six methoxy protons were presented at δ_{H} 3.94 and 3.49 ppm. Concerning with the ^{13}C NMR spectrum, the signals at δ_{C} 60.11, 56.4, 55.8, 56.5, 61.0 and 56.5 ppm suggested the presence of six methoxy carbons. After making a comparison with the data reported previously, the structure of compound **11** was assigned as 3,5,7,3',4',5'-hexamethoxyflavone ($\text{C}_{21}\text{H}_{22}\text{O}_8$). [4] The NMR spectra

assignment of compound **11** and 3,5,7,3',4',5'-hexamethoxyflavone is collected in Table 3.11.



Compound **11**

Table 3.11 The comparison of ^{13}C NMR spectral assignment of compound **11** and 3,5,7,3',4',5'-hexamethoxyflavone [4]

Positions	Chemical shift (ppm)	
	3,5,7,3',4',5'-hexamethoxyflavone ⁴	Compound 11
2	152.3	152.4
3	140.1	140.0
4	174	174.0
5	161.1	161.1
6	95.8	95.8
7	164	164.0
8	92.5	92.5
9	158.8	158.8
10	109.5	126.0
1'	126	109.5
2'	105.9	105.9
3'	153.1	153.1

Table 3.11 The comparison of ^{13}C NMR spectral assignment of compound **11** and 3,5,7,3',4',5'-hexamethoxyflavone [4] (cont)

Positions	Chemical shift (ppm)	
	3,5,7,3',4',5'-hexamethoxyflavone ⁴	Compound 11
4'	141.6	141.6
5'	153.1	153.1
6'	105.9	105.9
3-OMe	60.1	60.1
5-OMe	56.4	56.4
7-OMe	55.8	55.8
3'-OMe	56.4	56.5
4'-OMe	61	61.0
5'-OMe	56.4	56.5

3.2.4.3 Separation of Fraction VI-II (Part 2) and structural elucidation of its constituents

Based on TLC patterns, several subfractions revealed interesting spots. Those subfractions were further purified by subjecting to HPLC as following described. The separation by preparative HPLC (MeCN/H₂O, 15: 85) of subfraction 10 (8.9 mg) afforded compound **12** (4.6 mg), whereas compounds **13** (3.0 mg) and **14** (2.6 mg) were obtained from subfraction 14 (10.3 mg). The separation of subfraction 16 (14.6 mg) by preparative HPLC (MeOH/H₂O, 30: 70) yielded compound **15** (3.3 mg) while that of subfraction 20 (278.8 mg) by preparative HPLC (MeCN/H₂O, 23: 77)

furnished four compounds as **16** (1.6 mg), **17** (20.1 mg), **18** (34.7 mg) and **19** (6.0 mg). Subfraction 23 (33.9 mg) was purified by preparative HPLC (MeCN/H₂O, 28:72) to afford compounds **20** (8.9 mg), **21** (2.9 mg) and **22** (3.2 mg). The purification of subfraction 30 (165 mg) was accomplished by preparative HPLC to gain compounds **23** (11.5 mg) and **24** (23.9 mg). Further separation of subfraction 32 (156.1 mg) by preparative HPLC (MeCN/ H₂O, 30:70) afforded compounds **25** (49.7 mg) and **26** (6.7 mg). Subfraction 38 (25.5 mg) was subjected to preparative HPLC to obtain compound **27** (8.9 mg), while compounds **28** (8.9 mg), **29** (2.9 mg), **30** (2.3 mg), **31** (3.2 mg) and **32** (1.2 mg) were derived from the separation of subfraction 42 (98.4 mg) by preparative HPLC. Subfraction 50 (14.9 mg) was also purified by preparative HPLC (MeCN /H₂O, 40: 60) to obtain compound **33** (26.7 mg).

Compound **12** was obtained as brown solid (4.6 mg, 0.14 %yield based on Fraction **VI-II**). The ¹H NMR spectrum (Figure A-22) revealed four aromatic protons at δ_{H} 6.27, 7.60, 6.92 and 6.84 ppm and one signal of methoxy group exhibited a high intensity singlet signal at δ_{H} 3.95 ppm. This is well-consistent with the observation of ten carbon signals from the ¹³C NMR spectrum (Figure A-23). Based on the spectral data and comparison with the data published earlier, the structure of compound **12** was recognized as scopoletin (C₁₀H₈O₄) by comparing with those reported in literature. [27] The NMR spectral assignments of compound **12** and scopoletin is presented in Table 3.12.

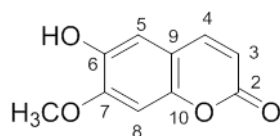
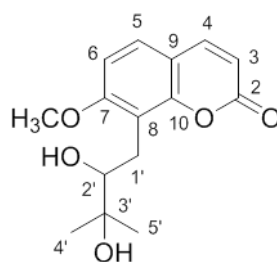
Compound **12**

Table 3.12 The comparison of ^1H and ^{13}C NMR spectral assignment of compound **12** and scopoletin [27]

Positions	Chemical shift (ppm)			
	scopoletin ²⁷		compound 12	
	^1H	^{13}C	^1H	^{13}C
2	-	160.8	-	161.6
3	6.25 (d, $J = 9.7$ Hz, 1H)	113.3	6.27 (d, $J = 9.6$ Hz, 1H)	113.5
4	7.84 (d, $J = 9.7$ Hz, 1H)	144.7	7.60 (d, $J = 9.6$ Hz, 1H)	143.4
5	7.19 (s, 1H)	112.1	6.92 (s, 1H)	111.6
6	-	109.9	-	107.6
7	-	146	-	144.2
8	6.79 (s, 1H)	151.9	6.84 (s, 1H)	149.8
9	-	103.7	-	103.3
10	-	151.2	-	150.4
7-OCH ₃	3.90 (s, 3H)	56.7	3.95 (s, 3H)	56.6

Compound **13** was gained as white solid (3 mg, 0.09 %yield based on Fraction VI-II). The $^1\text{H-NMR}$ spectrum of compound **13** (Figure A-24) revealed the characteristic signals assignable to 7-methoxy-8-substituted coumarin nucleus. To give more insight information, four doublet signals at δ_{H} 6.23 (d, $J = 9.6$ Hz), 7.63 (d, $J = 9.6$ Hz), 7.34 (d, $J = 8.4$ Hz) and 6.87 (d, $J = 8.4$ Hz) ppm, and the singlet signal at δ_{H} 3.92 ppm were observed. The presence of doublet signals at δ_{H} 3.09 (d, $J = 2.4$ Hz) and 2.99 (d, $J = 3.6$ Hz) ppm suggesting the presence of benzylic methylene protons in the molecule. Moreover, the methine proton and two methyl groups exhibited doublet and singlet signals at δ_{H} 3.63, 1.31 and 1.32 ppm, respectively. The ^{13}C NMR spectrum (Figure A-25) of this compound revealed 15 carbons containing a pair of methyl groups (δ_{C} 24.0 and 25.5 ppm). The structure of compound **13** was interpreted as meranzin hydrate ($\text{C}_{15}\text{H}_{18}\text{O}_5$). [28] The NMR spectral assignment of compound **13** and meranzin hydrate is gathered in Table 3.13.



Compound **13**

Table 3.13 The comparison of ^1H and ^{13}C NMR spectral assignment of compound **13** and meranzin hydrate [28]

Positions	Chemical shift (ppm)			
	meranzin hydrate ²⁸		compound 13	
	^1H	^{13}C	^1H	^{13}C
2	-	161.3	-	161.2
3	6.23 (d, $J = 9.5$ Hz, 1H)	113.0	6.23 (d, $J = 9.6$ Hz, 1H)	113.0
4	7.63 (d, $J = 9.5$ Hz, 1H)	144.0	7.63 (d, $J = 9.6$ Hz, 1H)	143.9
5	7.34 (d, $J = 8.5$ Hz, 1H)	127.0	7.34(d, $J = 8.4$ Hz, 1H)	126.9
6	6.87 (d, $J = 8.5$ Hz, 1H)	107.4	6.87 (d, $J = 8.4$ Hz, 1H)	107.4
7	-	160.5	-	160.5
8	-	115.7	-	115.7
9	-	113.1	-	113.0
10	-	153.4	-	153.3
1'	2.99 (dd, $J = 14, 10$ Hz, 1H) 3.08 (dd, $J = 14, 2.5$ Hz, 1H)	26.1	2.99 (d, $J = 3.6$ Hz, 1H), 3.09 (d, $J = 2.4$ Hz, 1H),	26.0
2'	3.62 (dd, $J = 10, 2.5$ Hz, 1H)	78.3	3.63(dd, $J = 7.6$ Hz, 1H)	78.3
3'	-	73.1	-	73.0
4'	1.32 (s, 3H)	24.0	1.31 (s, 3H)	24.0
5'	1.33 (s, 3H)	25.6	1.32 (s, 3H)	25.5
7-OCH ₃	3.92 (s, 3H)	56.2	3.92 (s, 3H)	56.2

Compound **14** was obtained as white solid (2.6 mg, 0.08 %yield based on Fraction **VI-II**). According to the ^1H NMR spectrum (Figure A-26), the detection of four doublet signals at δ_{H} 6.07 (d, $J = 9.6$ Hz), 7.17 (d, $J = 9.6$ Hz), 7.39 (d, $J = 8.4$ Hz) and 6.63 (d, $J = 8.8$ Hz) ppm, combined with a singlet signal at δ_{H} 3.70 ppm indicated the presence of 7-methoxy-8-substituted coumarin skeleton. Furthermore, the signals at δ_{H} 4.82, 4.70 and 3.10 ppm could be assignable to benzylic methine, methine and methoxy protons, respectively. The signals at δ_{H} 4.40 ppm was determined for two exo-methylene protons while the singlet signal of allylic methyl protons was presented at δ_{H} 1.40 ppm. The ^{13}C NMR spectrum (Figure A-27) showed nine coumarin carbons, one aromatic methoxy carbon and one methoxy carbon signals at δ_{C} 160.5, 113.4, 143.7, 129.0, 107.9, 161.4, 113.6, 112.9, 154.0, 56.2 and 57.7 ppm, respectively. The structure of compound **14** was taken to be albiflorin 3 ($\text{C}_{16}\text{H}_{17}\text{O}_5$) by comparing with data in literature. [29] The NMR spectral assignment of compound **14** and albiflorin 3 is reported in Table 3.14.

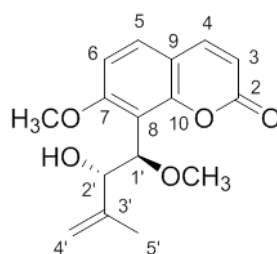
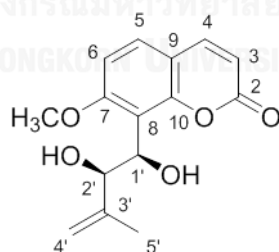
Compound **14**

Table 3.14 The comparison of ^1H and ^{13}C NMR spectral assignment of compound **14** and albiflorin **3** [29]

Positions	Chemical shift (ppm)			
	albiflorin 3 ²⁹		compound 14	
	^1H	^{13}C	^1H	^{13}C
2	-	160.4	-	160.5
3	6.26 (d, $J = 9.0$ Hz, 1H)	113.1	6.07 (d, $J = 9.6$ Hz, 1H)	113.4
4	7.43 (d, $J = 9.0$ Hz, 1H)	143.3	7.39 (d, $J = 9.6$ Hz, 1H)	143.7
5	7.65 (d, $J = 9.0$ Hz, 1H)	129.0	7.17 (d, $J = 8.4$ Hz, 1H)	129.0
6	6.88 (d, $J = 9.0$ Hz, 1H)	107.6	6.63 (d, $J = 8.8$ Hz, 1H)	107.9
7	-	161.3	-	161.4
8	-	113.4	-	113.6
9	-	112.8	-	112.9
10	-	153.8	-	154.0
1'	5.05 (d, $J = 9.0$ Hz, 1H)	76.4	4.82 (d, $J = 8.8$ Hz, 1H)	76.5
2'	4.94 (d, $J = 9.0$ Hz, 1H)	77.6	4.70 (d, $J = 8.8$ Hz, 1H)	77.9
3'	-	143.3	-	143.4
4'	4.70 (s, 1H), 4.63 (s, 1H)	114.0	4.47 (s, 1H), 4.40 (s, 1H)	114.3
5'	1.69	17.2	1.40 (s, 3H)	17.3
7-OMe	3.94	56.1	3.70 (s, 3H)	56.2
1'-OMe	3.33	57.5	3.10 (s, 3H)	57.7

Compound **15** was found as brown oil (3.3 mg, 0.10 %yield based on Fraction VI-II). The ^1H NMR signals (Figure A-28) at δ_{H} 6.26, 7.62, 7.39, 6.87 and 3.97 (OCH₃) ppm were consistent with 7-methoxy-8-substituted coumarin system. Moreover, the doublet signal at δ_{H} 5.30 (d, $J = 8.4$ Hz) and 4.50 (d, $J = 8.8$ Hz) ppm were attributable to the presence of benzylic methine and methine protons, respectively. The signals at δ_{H} 4.65 and 4.58 ppm were assignable to two exo-methylene protons whereas the singlet signal of allylic methyl protons was presented at δ_{H} 1.77 ppm. Carbon signals at δ_{C} 160.2, 113.7, 143.8, 128.7, 107.9, 160.2, 116.1, 113.2 and 152.9 ppm suggesting the presence of 7-oxygenated coumarin. Furthermore, two methylene carbons displayed the signals at δ_{C} 143.8 and 113.9 ppm. The structure of compound **15** was exposed to be (-)-murrangatin (C₁₅H₁₆O₅). [3] The NMR spectral assignment of compound **15** and (-)-murrangatin is gathered in Table 3.15.



Compound **15**

Table 3.15 The comparison of ^1H and ^{13}C NMR spectral assignment of compound **15** and (-)-murrangatin [3]

Positions	Chemical shift (ppm)			
	(-)-murrangatin ³		compound 15	
	^1H	^{13}C	^1H	^{13}C
2	-	160.2	-	160.2
3	6.25 (d, $J = 9.4$ Hz, 1H)	113.4	6.26 (d, $J = 9.6$ Hz, 1H)	113.7
4	7.62 (d, $J = 9.4$ Hz, 1H)	143.8	7.62 (d, $J = 9.6$ Hz, 1H)	143.8
5	7.39 (d, $J = 8.7$ Hz, 1H)	128.6	7.39 (d, $J = 8.4$ Hz, 1H)	128.7
6	6.87 (d, $J = 8.7$ Hz, 1H)	107.9	6.87 (d, $J = 8.8$ Hz, 1H)	107.9
7	-	160.2	-	160.2
8	-	116.1	-	116.1
9	-	113.1	-	113.2
10	-	152.9	-	152.9
1'	5.30 (t, $J = 8.7$ Hz, 1H)	69.6	5.30 (d, $J = 8.4$ Hz, 1H)	69.7
2'	4.51 (d, $J = 8.7$ Hz, 1H)	78.4	4.50 (d, $J = 8.8$ Hz, 1H)	78.6
3'	-	143.9	-	143.8
4'	4.65 (s, 1H), 4.58 (s, 1H)	113.7	4.65 (t, $J = 1.6$ Hz, 1H), 4.58 (t, $J = 0.8$ Hz, 1H)	113.9
5'	1.78 (s, 3H)	17.4	1.77 (s, 3H)	17.5
7-OMe	3.97 (s, 3H)	56.3	3.97 (s, 3H)	56.4

Compound **16** was discovered as pale yellow solid (1.6 mg, 0.05 %yield based on Fraction **VI-II**). Its ^1H NMR data (Figure A-30) presented the signals at δ_{H} 6.27, 7.63, 7.42, 6.91 and 3.95 ppm, suggesting the sharing of 7-methoxy-8-substituted coumarin skeleton. In addition, the presence of benzylic methine and methine protons at δ_{H} 5.19 and 4.97 ppm, respectively, together with ethoxy group that showed the signal at 3.29 and 1.17 ppm. The coupling constant between H-1' and H-2' ($J = 6.4$ Hz) indicated that **16** is the *erythro* isomer. The signals at δ_{H} 4.88 and 4.79 ppm were assignable to two exo-methylene protons whereas the singlet signals of allylic methyl protons were presented at δ_{H} 1.87 ppm. The ^{13}C NMR spectrum displayed the chemical shift at δ_{C} 160.7 (C-2), 113.6 (C-3), 143.9 (C-4), 129.0 (C-5), 108.3 (C-6), 161.7 (C-7), 113.8 (C-8), 154.5 (C-9), 113.1 (C-10), 76.4 (C-1'), 76.4 (C-2'), 145.0 (C-3'), 113.1 (C-4'), 18.7 (C-5'), 57.5 (C-1'') and 56.6 (C-7-OMe) ppm. The structure of compound **16** was revealed as muralatin K ($\text{C}_{17}\text{H}_{20}\text{O}_5$). [30] The NMR spectral assignments of compound **16** and muralatin K are assembled in Table 3.16.

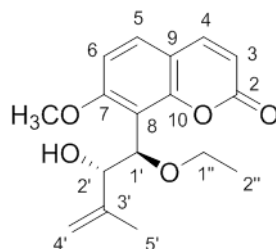
Compound **16**

Table 3.16 The comparison of ^1H and ^{13}C NMR spectral assignment of compound **16** and muralatin K [30]

Positions	Chemical shift (ppm)			
	muralatin K ³⁰		compound 16	
	^1H	^{13}C	^1H	^{13}C
2	-	160.5	-	160.7
3	6.26 (d, $J = 9.5$ Hz, 1H)	113.4	6.27 (d, $J = 9.6$ Hz, 1H)	113.6
4	7.63 (d, $J = 9.5$ Hz, 1H)	143.6	7.63 (d, $J = 9.2$ Hz, 1H)	143.9
5	7.40 (d, $J = 8.6$ Hz, 1H)	128.6	7.42 (d, $J = 8.8$ Hz, 1H)	129.0
6	6.90 (d, $J = 8.6$ Hz, 1H)	108.2	6.91 (d, $J = 8.8$ Hz, 1H)	108.3
7	-	161.5	-	161.7
8	-	114.4	-	113.8
9	-	154.2	-	154.5
10	-	113	-	113.1
1'	5.30 (d, $J = 6.0$ Hz, 1H)	75.3	5.19 (d, $J = 6.4$ Hz, 1H)	76.4
2'	4.76 (d, $J = 6.0$ Hz, 1H)	76.5	4.97 (s, 1H)	76.4
3'	-	144.8	-	145.0
4'	4.83 (s, 1H), 4.92 (s, 1H)	112.4	4.88 (t, $J = 1.2$ Hz, 1H), 4.79 (d, $J = 6.8$ Hz, 1H)	113.1
5'	1.87 (s, 3H)	18.9	1.87 (s, 3H)	18.7
1''	3.43 (m, 3H)	64.9	3.29 (s, 3H)	57.5
2''	-	15.2	1.17 (s, 3H)	-
7-OMe	3.94, s	56.5	3.95 (s, 3H)	56.6

Compound **17** was received as yellow solid (20.1 mg, 0.63 %yield based on Fraction **VI-II**). According to the ^1H NMR spectrum (Figure A-32), compound **17** showed a collection of 7-methoxy-8-substituted coumarin exhibiting doublet signals at δ_{H} 6.27 (d, $J = 9.6$ Hz), 7.65 (d, $J = 9.6$ Hz), 7.46 (d, $J = 8.4$ Hz), 6.86 (d, $J = 8.8$ Hz) and a singlet signal of OCH_3 at δ_{H} 3.86 ppm. The presence of benzylic methine, methine and allylic methyl protons could be detected from the appearance of singlet signal at δ_{H} 5.88 ppm, multiplet signal at δ_{H} 2.59 ppm and doublet signal at δ_{H} 1.11 (d, $J = 6.8$ Hz) and 0.96 (d, $J = 6.4$ Hz) ppm, respectively. Concerning the ^{13}C NMR spectrum (Figure A-33), there were 15 carbons containing a set of coumarin carbons (δ_{C} 160.6, 113.7, 143.6, 129.7, 107.9, 160.2, 114.6, 113.3 and 153.5 ppm), another carbonyl carbon (δ_{C} 212.6 ppm) and a pair of methyl groups (δ_{C} 24.0 and 25.5 ppm). The structure of compound **17** was recognized as murpaniculol ($\text{C}_{15}\text{H}_{16}\text{O}_5$). [8] The NMR spectral assignment of compound **17** and murpaniculol is accumulated in Table 3.17.

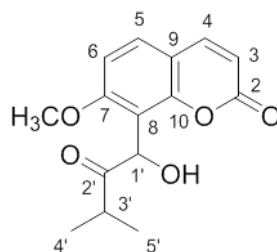
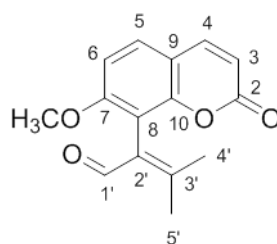
Compound **17**

Table 3.17 The comparison of ^1H and ^{13}C NMR spectral assignment of compound **17** and murpaniculol [8]

Positions	Chemical shift (ppm)			
	murpaniculol ⁸		compound 17	
	^1H	^{13}C	^1H	^{13}C
2	-	160.4	-	160.6
3	6.27 (d, $J = 9.5$ Hz, 1H)	113.3	6.27 (d, $J = 9.6$ Hz, 1H)	113.7
4	7.69 (d, $J = 9.5$ Hz, 1H)	143.5	7.65 (d, $J = 9.6$ Hz, 1H)	143.6
5	7.50 (d, $J = 8.4$ Hz, 1H)	129.5	7.46 (d, $J = 8.4$ Hz, 1H)	129.7
6	6.90 (d, $J = 8.4$ Hz, 1H)	107.8	6.86 (d, $J = 8.8$ Hz, 1H)	107.9
7	-	159.9	-	160.2
8	-	114.3	-	114.6
9	-	113.1	-	113.3
10	-	153.2	-	153.5
1'	5.89 (s, 1H)	68.3	5.88 (s, 1H)	68.5
2'	-	212.4	-	212.6
3'	2.62 (m, 1H)	35.7	2.59 (m, 1H)	35.9
4'	1.13 (d, $J = 6.9$ Hz, 3H)	19.4	1.11(d, $J = 6.8$ Hz, 3H)	19.2
5'	0.99 (d, $J = 6.9$ Hz, 3H)	17.8	0.96 (d, $J = 6.4$ Hz, 3H)	18.1
7-OMe	3.88 (s, 1H)	56.1	3.86 (s, 1H)	56.3

Compound **18** was harvested as brown solid (34.7 mg, 1.08 %yield based on Fraction **VI-II**). According to the ^1H NMR spectrum (Figure A-34), compound **18** should belong to 7-methoxy-8-substituted coumarin group. To illustrate this, four high intensity doublet signals at δ_{H} 6.19 (d, $J = 9.6$ Hz), 7.63 (d, $J = 9.6$ Hz), 7.43 (d, $J = 8.8$ Hz) and 6.88 (d, $J = 8.8$ Hz) ppm, the methoxy group on aromatic ring with high intensity signal at δ_{H} 3.81 ppm were visualized. The singlet signal at δ_{H} 10.20 ppm demonstrated the signal of the aldehydic proton. Two allylic methyl groups exhibited at δ_{H} 2.41 and 1.76 ppm. The ^{13}C NMR spectrum exposed fifteen carbon signals containing an aldehydic carbonyl carbon and the coumarin moiety signal at δ_{C} 188.9 and 161.2 ppm, respectively. A pair of methyl carbons was found at δ_{C} 24.9 and 19.9 ppm. The structure of compound **18** was accepted as murralongin ($\text{C}_{15}\text{H}_{14}\text{O}_4$). [23][26] The NMR spectral assignment of compound **18** and murralongin is listed in Table 3.18.



Compound **18**

Table 3.18 The comparison of ^1H and ^{13}C NMR spectral assignment of compound **18** and murralongin [23][26]

Positions	Chemical shift (ppm)			
	murralongin ^{23,26}		compound 18	
	^1H	^{13}C	^1H	^{13}C
2	-	160.9	-	161.2
3	6.23 (d, $J = 9.4$ Hz, 1H)	113.1	6.19 (d, $J = 9.6$ Hz, 1H)	113.2
4	7.65 (d, $J = 9.4$ Hz, 1H)	143.5	7.63 (d, $J = 9.6$ Hz, 1H)	143.8
5	7.45 (d, $J = 8.7$ Hz, 1H)	128.5	7.43 (d, $J = 8.8$ Hz, 1H)	128.7
6	6.90 (d, $J = 8.7$ Hz, 1H)	107.5	6.88 (d, $J = 8.8$ Hz, 1H)	107.7
7	-	159.4	-	159.9
8	-	113.0	-	-
9	-	112.9	-	-
10	-	160.0	-	160.1
1'	10.22 (s, 1H)	188.6	10.20 (s, 1H)	188.9
2'	-	129.1	-	-
3'	-	152.5	-	152.6
4'	2.43 (s, 3H)	24.7	2.41 (s, 3H)	24.9
5'	1.79 (s, 3H)	19.7	1.76 (s, 3H)	19.9
7-OMe	3.83 (s, 3H)	56.1	3.81 (s, 3H)	56.3

Compound **19** was earned as dark green solid (6 mg, 0.19 %yield based on Fraction **VI-II**). The ^1H NMR spectrum of compound **19** exhibited the signals attributable to 7-methoxy-8-substituted coumarin system. Four doublet signals at δ_{H} 6.25 (d, $J = 9.6$ Hz), 7.62 (d, $J = 9.6$ Hz), 7.39 (d, $J = 8.8$ Hz) and 6.87 (d, $J = 8.8$ Hz) ppm, combined with a singlet signal at δ_{H} 4.00 ppm were observed. Moreover, one benzylic methine, one methine, two exo-methylene and two allyl methyl protons presented at δ_{H} 5.73, 5.52, 4.76, 4.73, 2.13 and 1.74 ppm were detected, respectively. The ^{13}C NMR spectrum (Figure A-9) showed 17 carbon signals very similar to that of compound **5**. The structure of compound **19** was clarified as murrangatin acetate ($\text{C}_{17}\text{H}_{18}\text{O}_6$). [2][23] The NMR spectral assignment of compound **19** and murrangatin acetate is collected in Table 3.19.

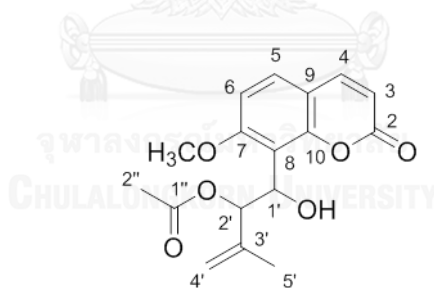
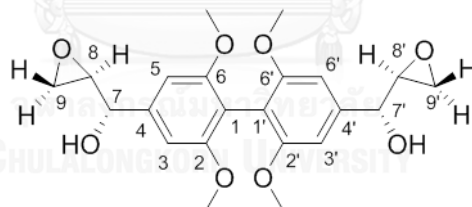
Compound **19**

Table 3.19 The comparison of ^1H and ^{13}C NMR spectral assignment of compound **19** and murrangatin acetate [2][23]

Position	Chemical shift (ppm)			
	murrangatin acetate ^{2,23}		compound 19	
	^1H	^{13}C	^1H	^{13}C
2	-	160.2	-	160.4
3	6.26 (d, $J = 9.4$ Hz, 1H)	113.5	6.25 (d, $J = 9.6$ Hz, 1H)	113.7
4	7.61 (d, $J = 9.4$ Hz, 1H)	143.7	7.62 (d, $J = 9.6$ Hz, 1H)	143.8
5	7.39 (d, $J = 8.7$ Hz, 1H)	128.8	7.39 (d, $J = 8.8$ Hz, 1H)	128.9
6	6.87 (d, $J = 8.7$ Hz, 1H)	107.8	6.87 (d, $J = 8.8$ Hz, 1H)	107.9
7	-	160.0	-	160.2
8	-	115.8	-	115.9
9	-	113.1	-	113.2
10	-	152.7	-	152.8
1'	5.73 (d, $J = 7.7$ Hz, 1H)	68.2	5.73 (d, $J = 7.6$ Hz, 1H)	68.3
2'	5.53 (dd, $J = 11.1, 7.7$ Hz, 1H)	79.5	5.52 (d, $J = 8.0$ Hz, 1H)	79.7
3'	-	140.8	-	140.9
4'	4.77 (s, 1H), 4.74 (s, 1H)	114.9	4.76 (s, 1H), 4.73 (t, $J = 1.6$ Hz, 1H)	114.9
5'	1.75 (s, 3H)	18.5	1.74 (s, 3H)	18.7
1''	-	170.9	-	171.1
2''	2.14 (s, 3H)	21.2	2.13 (s, 3H)	21.4
7-OMe	4.00 (s, 3H)	56.3	4.00 (s, 3H)	56.5

Compound **20** was found as green oil (8.9 mg, 0.28 %yield based on Fraction VI-II). Concerning with the ^1H NMR spectrum (Figure A-38), it showed the signals of 1,2,4,5-tetrasubstituted phenyl protons at δ_{H} 6.58 ppm. The signals of benzylic methine, methine and methylene protons were presented at δ_{H} 4.73, 3.10, 4.28 and 3.93 ppm, respectively. In addition, the signals of four methoxy protons were detected at δ_{H} 3.90 ppm. The ^{13}C NMR spectrum revealed two collections of carbon signals which showed the same set of chemical shift. Compound **20** was suggested as 2,6,2',6'-tetramethoxy-4,4'-bis(1,2-*trans*-2,3-epoxy-1-hydroxypropyl)bi phenyl ($\text{C}_{22}\text{H}_{26}\text{O}_8$) by comparing with literature. [31] The NMR spectral assignment of compound **20** and 2,6,2',6'-tetramethoxy-4,4'-bis(1,2-*trans*-2,3-epoxy-1-hydroxypropyl) biphenyl is gathered in Table 3.20.



Compound **20**

Table 3.20 The comparison of ^1H and ^{13}C NMR spectral assignment of compound **20** and 2,6,2',6'-tetramethoxy-4,4'-bis(1,2-*trans*-2,3-epoxy-1-hydroxypropyl)biphenyl [31]

Positions	Chemical shift (ppm)			
	2,6,2',6'-tetramethoxy-4,4'-bis(1,2- <i>trans</i> -2,3-epoxy-1-hydroxypropyl)biphenyl ³¹		compound 20	
	^1H	^{13}C	^1H	^{13}C
1, 1'	-	132.1	-	132.1
2, 2'	-	147.2	-	147.1
3, 3'	6.59 (s, 2H)	102.8	6.58 (s, 2H)	102.6
4, 4'	-	134.3	-	134.3
5, 5'	6.59 (s, 2H)	102.8	6.58 (s, 2H)	102.6
6, 6'	-	147.2	-	147.1
7, 7'	4.74 (d, $J = 4.0$ Hz, 2H)	86.1	4.73 (d, $J =$ Hz, 2H)	86.1
8, 8'	3.10 (m, 2H)	54.4	3.10 (brs, 2H)	54.3
9a, 9a'	4.28 (m, 2H)	71.8	4.28 (m, 2H)	71.8
9b, 9b'	3.93 (m, 2H)	-	3.93 (m, 2H)	-
2, 2', 6, 6'- OMe	3.90 (s, 12H)	56.4	3.90 (s, 12H)	56.4
7, 7' OH	5.52 (brs, 2H)	-	5.52 (brs, 2H)	-

Compound **21** was received as brown oil (2.9 mg, 0.09 %yield based on Fraction **VI-II**). According to the ^1H NMR (Figure A-40), it showed the signals of 1,3,4,5-tetrasubstituted phenyl protons at δ_{H} 6.58 and 6.84-6.81 ppm, and 1,3,4-trisubstituted phenyl protons at δ_{H} 6.90-6.88, 6.90-6.88 and 6.58 ppm. In addition, the signals of three methoxy protons presented at δ_{H} 3.91, 3.90, and 3.90 ppm. Comparison of the ^1H and ^{13}C NMR data with the reported literature indicated that compound **21** was medioresinol ($\text{C}_{21}\text{H}_{22}\text{O}_7$). [32] The NMR spectral assignments of compound **21** and medioresinol is collected in Table 3.21.

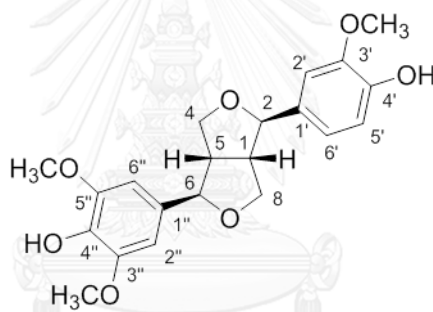
Compound **21**

Table 3.21 The comparison of ^1H and ^{13}C NMR spectral assignment of compound **21** and medioresinol [32]

Positions	Chemical shifts (ppm)			
	medioresinol ³²		compound 21	
	^1H	^{13}C	^1H	^{13}C
1	2.92-3.16 (m, 1H)	53.6	3.10 (m, 1H)	54.1
2	4.61(d, $J = \text{Hz}$, 1H)	85.3	4.73 (dd, $J = \text{Hz}$, 1H)	86.2
3	-	-	-	-

Table 3.21 The comparison of ^1H and ^{13}C NMR spectral assignment of compound **21** and medioresinol [32] (cont)

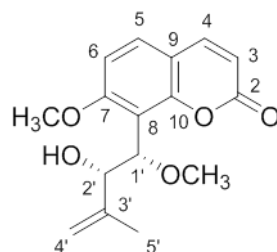
Positions	Chemical shifts (ppm)			
	medioresinol ³²		compound 21	
	^1H	^{13}C	^1H	^{13}C
4	3.80-4.40 (m, 2H)	71.0	4.26 (m, 2H)	71.89
5	2.92-3.16 (m, 1H)	53.7	3.10 (m, 1H)	54.4
6	4.61(d, $J = 4$ Hz, 1H)	85.3	4.73 (dd, $J =$ Hz, 1H)	85.8
7	-	-	-	-
8	3.80-4.40 (m, 2H)	71.0	3.88 (m, 2H)	71.6
1'	-	132.3	-	132.9
2'	6.60 (s, 1H)	118.6	6.90-6.88 (m, 1H)	118.9
3'	-	115.2	-	114.3
4'	-	148.0	-	145.3
5'	6.60 (s, 1H)	148.0	6.90-6.88 (m, 1H)	147.2
6'	6.60 (s, 1H)	110.6	6.58 (s, 1H)	108.6
1''	-	131.6	-	132.1
2''	6.60 (s, 1H)	104.0	6.58 (s, 1H)	102.7
3''	-	148.0	-	146.7
4''	-	132.3	-	134.3
5''	-	148.0	-	146.7
6''	6.60 (s, 1H)	104.0	6.84-6.81 (m, 1H)	102.7

Table 3.21 The comparison of ^1H and ^{13}C NMR spectral assignment of compound **21** and medioresinol [32] (cont)

Positions	Chemical shifts (ppm)			
	medioresinol ³²		compound 21	
	^1H	^{13}C	^1H	^{13}C
3'-OMe	3.87(s, 3H)	56.1	3.91 (s, 3H)	56.4
3''-OMe	3.76 (s, 3H)	55.8	3.90 (s, 3H)	55.9
5''-OMe	3.76 (s, 3H)	55.8	3.90 (s, 3H)	55.9

Compound **22** was obtained as white solid (3.2 mg, 0.10 %yield based on Fraction VI-II). The ^1H NMR signals belonging to coumarin and aromatic methyl protons at δ_{H} 6.26, 7.38, 7.62, 6.88 and 3.95 ppm indicated the presence of 7-methoxy-8-substituted coumarin skeleton. The doublet signals of benzylic methine and methine protons were presented at δ_{H} 5.37 (d, $J = 8.0$ Hz and 5.13 ppm, respectively, together with the singlet signal of methoxy group at δ_{H} 3.09 ppm. The signals at δ_{H} 5.06 and 4.09 ppm were assignable to two exo-methylene protons. The singlet signals of allylic methyl protons were presented at δ_{H} 1.84 ppm. Its ^{13}C NMR spectroscopic data were similar to those of compounds **9** and **14**. The marked differences were due to the optical rotation of methyl and hydroxyl groups at C-1' and C-2'. The structure of compound **22** was identical to albiflorin 2 ($\text{C}_{16}\text{H}_{18}\text{O}_5$). [29]

The NMR spectral assignment of compound **22** and albiflorin 2 is accumulated in Table 3.22.



Compound **22**

Table 3.22 The comparison of ^1H and ^{13}C NMR spectral assignment of compound **22** and albiflorin 2 [29]

Positions	Chemical shift (ppm)			
	albiflorin 2 ²⁹		compound 22	
	^1H	^{13}C	^1H	^{13}C
2	-	160.1	-	160.4
3	6.08 (d, $J = 9.0$ Hz, 1H)	113.1	6.26 (d, $J = 9.6$ Hz, 1H)	113.4
4	7.32 (d, $J = 9.0$ Hz, 1H)	143.7	7.38 (d, $J = 8.8$ Hz, 1H)	143.8
5	7.54 (d, $J = 9.0$ Hz, 1H)	128.9	7.62 (d, $J = 9.6$ Hz, 1H)	128.2
6	6.77 (d, $J = 9.0$ Hz, 1H)	107.7	6.88 (d, $J = 8.8$ Hz, 1H)	108.0
7	-	161.0	-	160.8
8	-	113.3	-	116.5
9	-	112.6	-	113.2
10	-	153.4	-	153.4
1'	4.90 (d, $J = 9.0$ Hz, 1H)	76.1	5.37 (d, $J = 8.0$ Hz, 1H)	66.4

Table 3.22 The comparison of ^1H and ^{13}C NMR spectral assignment of compound **22** and albiflorin **2** [29] (cont)

Positions	Chemical shift (ppm)			
	albiflorin 2 ²⁹		compound 22	
	^1H	^{13}C	^1H	^{13}C
2'	4.81 (d, $J = 9.0$ Hz, 1H)	77.4	4.09 (d, $J = 8.4$ Hz, 1H)	88.0
3'		143.2		142.9
4'	4.54 (brs, 1H), 4.43(brs, 1H)	113.4	5.06 (s, 1H), 5.13 (s, 1H)	117.5
5'	1.51 (s, 3H)	16.9	1.84 (s, 3H)	16.8
7-OMe	3.78 (s, 3H)	55.9	3.95 (s, 3H),	56.4
1'-OMe	3.15 (s, 3H)	57.0	3.09 (s, 3H),	56.6

Compound **23** was received as white solid (11.5 mg, 0.36 %yield based on Fraction VI-II). The ^1H NMR spectrum of compound **23** confirmed the presence of 7-methoxy-8-substituted coumarin skeleton, showing the characteristic coumarin doublets at δ_{H} 6.24 (d, $J = 9.6$ Hz), 7.62 (d, $J = 9.2$ Hz), 7.35 (d, $J = 8.8$ Hz) and 6.87 (d, $J = 8.8$ Hz) ppm, combined with the methoxy group on aromatic ring at δ_{H} 3.89 ppm. At C-8 position, a doublet signal of benzylic methine proton at δ_{H} 4.37 ($J = 8.0$ Hz) ppm and aliphatic methine proton at δ_{H} 4.31 (dd, $J = 9.6$ Hz ppm) ppm, combined with two exo-methylene and allylic methyl protons at δ_{H} 4.90 and 1.70 ppm were detected. The ^{13}C NMR spectroscopic data of this compound was

comparable to those of compounds **8** and **15**. The differences were due to the optical rotation of a methyl and hydroxyl groups at C-1' and C-2'. The structure of compound **23** was elucidated as (+)murrangatin (C₁₅H₁₆O₆). [3] The NMR spectral assignment of compound **23** and (+)murrangatin is assembled in Table 3.23.

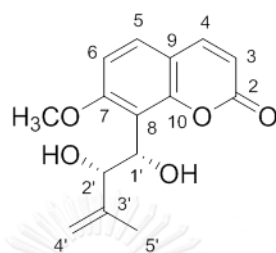
Compound **23**

Table 3.23 The comparison of ¹H and ¹³C NMR spectral assignment of compound **23** and (+)murrangatin [3]

Positions	Chemical shifts (ppm)			
	+(+)murrangatin ³		compound 23	
	¹ H	¹³ C	¹ H	¹³ C
2	-	160.2	-	161.2
3	6.25 (d, <i>J</i> = 9.4 Hz, 1H)	113.4	6.24 (d, <i>J</i> = 9.6 Hz, 1H)	113.3
4	7.62 (d, <i>J</i> = 9.4 Hz, 1H)	143.8	7.62 (d, <i>J</i> = 9.2 Hz, 1H)	144.0
5	7.39 (d, <i>J</i> = 8.7 Hz, 1H)	128.6	7.35 (d, <i>J</i> = 8.8 Hz, 1H)	127.7
6	6.87 (d, <i>J</i> = 8.7 Hz, 1H)	107.9	6.87 (d, <i>J</i> = 8.8 Hz, 1H)	108.1
7	-	160.2	-	161.0
8	-	116.1	-	116.8
9	-	113.1	-	111.7

Table 3.23 The comparison of ^1H and ^{13}C NMR spectral assignment of compound **23** and (+)-murrangatin [3] (cont)

Positions	Chemical shifts (ppm)			
	(+)-murrangatin ³		compound 23	
	^1H	^{13}C	^1H	^{13}C
10	-	152.9	-	153.9
1'	5.30 (t, $J = 8.7$ Hz, 1H)	69.6	4.37 (t, $J = 8.0$ Hz, 1H)	62.9
2'	4.51 (d, $J = 8.7$ Hz, 1H)	78.4	4.31 (dd, $J = 9.6$ Hz, 1H)	-
3'	-	143.9	-	143.2
4'	4.65 (s, 1H), 4.58 (s, 1H)	113.7	4.90 (s, 1H)	-
5'	1.78 (s, 3H)	17.4	1.70 (s, 3H)	22.4
7-OMe	3.97 (s, 3H)	56.3	3.89 (s, 3H)	56.3

Compound **24** was gained as white solid (23.9 mg, 0.75 %yield based on Fraction VI-II). According to the ^1H NMR spectrum (four doublet signals at δ_{H} 6.25 (d, $J = 9.6$ Hz), 7.64 (d, $J = 9.6$ Hz), 7.49 (d, $J = 8.8$ Hz) and 6.88 (d, $J = 8.8$ Hz) ppm, and one singlet signal at δ_{H} 3.89 ppm) (Figure A-46), compound **24** displayed the characteristic signals for 7-methoxy-8-substituted coumarin skeleton. The substituents at C-8 should contain the singlet signal of benzylic methine protons at δ_{H} 6.95 ppm, a multiplet signal of methine proton at δ_{H} 2.82 ppm and the doublet signal of methyl groups at δ_{H} 1.01 (d, $J = 6.8$ Hz) and 1.15 (d, $J = 6.8$ Hz) ppm. Furthermore, two methoxy groups were detected as the singlet signal at δ_{H} 2.14 ppm.

The ^{13}C NMR spectrum exposed twenty carbon signals comprising three signals at δ_c 207.9, 169.6, and 159.9 ppm assignable to the carbonyl carbons of ketone, ester, and the coumarin nucleus, respectively. The structure of compound **24** was assigned as murpaninulol senecioate ($\text{C}_{21}\text{H}_{26}\text{O}_7$). [33] The NMR spectral assignments of compound **24** and murpaninulol senecioate is included in Table 3.24.

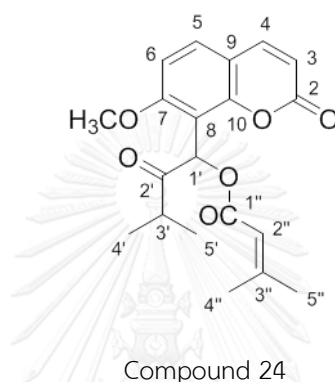


Table 3.24 The comparison of ^1H and ^{13}C NMR spectral assignment of compound **24** and murpaninulol senecioate [33]

Positions	Chemical shift (ppm)			
	murpaninulol senecioate ³³		Compound 24	
	^1H	^{13}C	^1H	^{13}C
2	-	159.8	-	159.9
3	6.26 (d, $J = 9.5$ Hz, 1H)	113.7	6.25 (d, $J = 9.6$ Hz, 1H)	113.8
4	7.62 (d, $J = 9.5$ Hz, 1H)	143.2	7.64 (d, $J = 9.6$ Hz, 1H)	143.4
5	7.47 (d, $J = 8.7$ Hz, 1H)	129.8	7.49 (d, $J = 8.8$ Hz, 1H)	130.3
6	6.88 (d, $J = 8.7$ Hz, 1H)	107.9	6.88 (d, $J = 8.8$ Hz, 1H)	108.0
7	-	160.9	-	160.9
8	-	112.8	-	111.8

Table 3.24 The comparison of ^1H and ^{13}C NMR spectral assignment of compound **24** and murpaninulol senecioate [33] (cont)

Positions	Chemical shift (ppm)			
	murpaninulol senecioate ³³		Compound 24	
	^1H	^{13}C	^1H	^{13}C
9	-	153.6	-	153.7
10	-	113.1	-	113.2
1'	7.03 (s, 1H)	68.6	6.95 (s 1H)	69.4
2'	-	209.1	-	207.9
3'	2.97 (septet, $J = 6.7$ Hz, 1H)	36.2	2.82 (m, 1H)	36.3
4'	1.04 (d, $J = 6.7$ Hz, 3H)	18.2	1.01 (d, $J = 6.8$ Hz, 3H)	18.1
5'	1.20 (d, $J = 6.7$ Hz, 3H)	18.9	1.15 (d, $J = 6.8$ Hz, 3H)	18.1
1''	-	165	-	169.6
2''	5.79 (m, 1H)	115.4	-	-
3''	-	158.4	-	-
4''	1.89 (d, $J = 1.4$ Hz, 3H)	27.5	2.14 (s, 3H)	19.2
5''	2.19 (d, $J = 1.2$ Hz, 3H)	20.4	2.14 (s, 3H)	20.9
7-OMe	3.91 (s, 3H)	56.4	3.89 (s, 3H)	56.5

Compound **25** was obtained as white solid (49.7 mg, 1.55 %yield based on Fraction **VI-II**). The 7-methoxy-8-substituted coumarin system for this compound was indicated by the ^1H NMR spectrum (Figure A-48) comprising the doublet at δ_{H} 6.21 (d, $J = 9.6$ Hz), 7.61 (d, $J = 9.2$ Hz), 7.31 (d, $J = 8.4$ Hz), 6.85 (d, $J = 8.8$ Hz) ppm, and the singlet signal at δ_{H} 3.91 ppm. The substituents at C-8 should contain the multiplet signal of benzylic methylene protons at δ_{H} 3.04 and 2.99, the double of doublet of aliphatic methine proton at δ_{H} 3.75 (dd, $J = 3.3, 2.8$ Hz) ppm. Furthermore, an aliphatic methoxy group showed the singlet signal at δ_{H} 3.28 together with two doublet signals of methyl group at δ_{H} 1.27 (d, $J = 1.6$ Hz). According to the ^{13}C NMR spectrum (Figure A-49), compound **25** showed sixteen carbons which could be assigned for a pair of methyl groups (δ_{C} 20.3 and 20.9 ppm) and two methoxy carbons (δ_{C} 56.2 and 49.4 ppm). The structure of compound **25** was proposed as 7-methoxy-8-(2'-methoxy-3'-hydroxy-3'-methylbutyl)coumarin ($\text{C}_{16}\text{H}_{20}\text{O}_5$). The NMR spectral assignment of compound **25** is collected in Table 3.25.

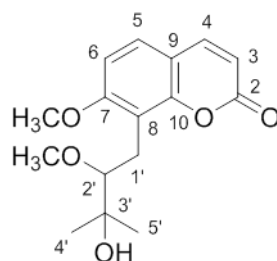
Compound **25**

Table 3.25 ^1H and ^{13}C NMR spectral assignment of compound **25**

Positions	Chemical shifts (ppm)	
	^1H	^{13}C
2	-	161.2
3	6.21 (d, $J = 9.6$ Hz, 1H)	113.0
4	7.61 (d, $J = 9.2$ Hz, 1H)	143.8
5	7.31 (d, $J = 8.4$ Hz, 1H)	126.7
6	6.85 (d, $J = 8.8$ Hz, 1H)	107.4
7	-	160.7
8	-	116.1
9	-	153.5
10	-	113.0
1'	3.04 (m, 1H), 2.99 (m, 1H)	25.0
2'	3.75 (dd, $J = 3.3, 2.8$ Hz, 1H)	77.2
3'	-	76.5
4'	1.27 (d, $J = 1.6$ Hz, 3H)	20.3
5'	1.27 (d, $J = 1.6$ Hz, 3H)	20.9
7-OMe	3.91 (s, 3H)	56.2
2'-OMe	3.28 (s, 3H)	49.4
3'-OH	2.28 (s, 1H)	-

Compound **26** was found as yellow solid (6.7 mg, 0.21 %yield based on Fraction **VI-II**). The ^1H NMR spectrum (Figure A-50) displayed the characteristic signals for the methyl group at δ_{H} 1.89 ppm, a $\text{CH}_2\text{-CH}$ -system at δ_{H} 3.09 and 4.34 ppm, methoxy group at δ_{H} 3.93 ppm, exo-methylene group at δ_{H} 4.89 and 4.80 ppm, two aromatic *ortho* protons at δ_{H} 6.86 and 7.34 ppm, and the C-3 and C-4 protons of the coumarin nucleus at δ_{H} 6.26 and 7.63 ppm. The ^{13}C NMR spectrum (Figure A-51) performed a set of 7-methoxy-8-substituted coumarin carbon signals covering carbon signals of side chain of C-8 position. The structure of compound **26** was labeled as auraptenol ($\text{C}_{15}\text{H}_{16}\text{O}_4$) by analyses and comparisons ^1H and ^{13}C NMR data with relevant literature reports. [5] The NMR spectral assignment of compound **26** and auraptenol is combined in Table 3.26.

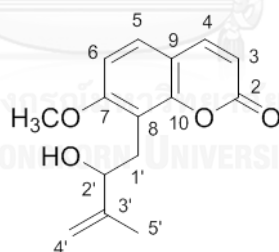
Compound **26**

Table 3.26 The comparison of ^1H and ^{13}C NMR spectral assignment of compound **26** and auraptinol [5]

Positions	Chemical shift (ppm)			
	auraptinol ⁵		compound 26	
	^1H	^{13}C	^1H	^{13}C
2	-	161.1	-	161.1
3	6.10 (d, $J = 9.5$ Hz, 1H)	113.0	6.25 (d, $J = 9.6$ Hz, 1H)	113.0
4	7.56, (d, $J = 9.5$ Hz, 1H)	143.8	7.63 (d, $J = 9.2$ Hz, 1H)	143.8
5	6.78 (d, $J = 8.6$ Hz, 1H)	127.0	6.86 (d, $J = 8.8$ Hz, 1H)	127.0
6	7.27 (d, $J = 8.6$ Hz, 1H)	107.3	7.34 (d, $J = 8.4$ Hz, 1H)	107.3
7	-	160.7	-	160.6
8	-	115.1	-	115.0
9	-	153.5	-	153.5
10	-	113.1	-	113.2
1'	3.05 (m, 2H)	29.4	3.09 (d, $J = 5.2$ Hz, 1H), 3.20 (dd, $J = 9.2$ Hz, 1H)	29.4
2'	4.27 (m, 1H)	75.2	4.34 (dd, $J = 3.6$ Hz, 1H)	75.3
3'	4.76 (m, 1H)	147.2	4.89 (s, 1H)	147.2
4'	4.76 (m, 1H)	110.5	4.80 (s, 1H)	110.5
5'	1.82 (s, 3H)	18.1	1.89 (s, 3H)	18.1
7-OMe	3.86 (s, 3H)	56.2	3.93 (s, 3H)	56.2

Compound **27** was taken as white solid (8.9 mg, 0.28 %yield based on Fraction **VI-II**). According to the ^1H NMR spectrum (Figure A-52), it showed the signals of 1,3,4-trisubstituted phenyl protons at δ_{H} 7.84, 7.01 and 7.86 ppm, and 2,3,5,7,8-pentasubstituted flavone protons at δ_{H} 6.41 ppm. In addition, the signals of six methoxy protons were presented at δ_{H} 3.94, 3.97, 4.00, 4.00, 3.90 and 3.97 ppm. Concerning with the ^{13}C NMR spectrum (Figure A-53), the signals at δ_{C} 61.7, 60.1, 56.8, 56.5, 56.1 and 56.0 ppm suggested the presence of six methoxy carbons in the molecule. The structure of compound **27** was identified as 3,5,7,8,3',4'-hexamethoxyflavone ($\text{C}_{21}\text{H}_{22}\text{O}_8$). [34, 35]The NMR spectral assignment of compound **27** and 3,5,7,8,3',4'-hexamethoxyflavone is collected in Table 3.27.

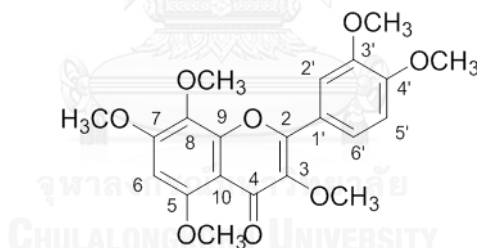
Compound **27**

Table 3.27 The comparison of ^{13}C NMR spectral assignment of compound **27** and 3,5,7,8,3',4'-hexamethoxyflavone [34, 35]

Positions	Chemical shift (ppm)	
	3,5,7,8,3',4'-hexamethoxyflavone ^{34,35}	compound 27
2	150.8	151.0
3	140.8	140.9
4	174.2	174.4
5	152.2	152.5
6	92.4	92.4
7	156.4	156.5
8	130.4	130.6
9	156.3	156.3
10	109.4	109.4
1'	123.6	123.6
2'	110.9	111.0
3'	148.7	148.8
4'	150.9	151.0
5'	111.0	111.1
6'	121.8	121.9
3-OMe	61.4	61.7
5-OMe	59.9	60.1
7-OMe	56.5	56.8
8-OMe	56.4	56.5
3'-OMe	56.0	56.1
4'-OMe	55.9	56.0

Compound **28** was gained as white solid (8.9 mg, 0.28 %yield based on Fraction **VI-II**). Concerning with the ^1H NMR spectrum (Figure A-54), it exhibited the signals of $\text{H}_{2'}$ and $\text{H}_{6'}$ at δ_{H} 7.54 and 7.54 ppm, and H_6 at δ_{H} 6.42 ppm. In addition, the signal of seven methoxy protons could be detected at δ_{H} 4.0, 3.94 and 3.91 ppm. The structure of compound **28** was mentioned as 3,5,7,8,3',4',5'-heptamethoxyflavone ($\text{C}_{22}\text{H}_{24}\text{O}_9$). [36] The NMR spectral assignment of compound **28** and 3,5,7,8,3',4',5'-heptamethoxyflavone is summarized in Table 3.28.

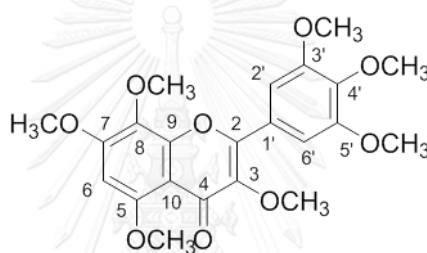
Compound **28**

Table 3.28 The comparison of ^1H and ^{13}C NMR spectral assignment of compound **28** and 3,5,7,8,3',4',5'-heptamethoxyflavone [36]

Positions	Chemical shifts (ppm)			
	3,5,7,8,3',4',5'-heptamethoxyflavone ³⁶		compound 28	
	^1H	^{13}C	^1H	^{13}C
2	-	156.1	-	156.5
3	-	139.6	-	140.1
4	-	174.0	-	174.4
5	-	151.6	-	152.1
6	6.45 (s, 1H)	91.9	6.42 (s, 1H)	92.3

Table 3.28 The comparison of ^1H and ^{13}C NMR spectral assignment of compound **28** and 3,5,7,8,3',4',5'-heptamethoxyflavone [36] (cont)

Positions	Chemical shifts (ppm)			
	3,5,7,8,3',4',5'-heptamethoxyflavone ³⁶		compound 28	
	^1H	^{13}C	^1H	^{13}C
7	-	156.2	-	156.6
8	-	130.0	-	130.5
9	-	150.5	-	151.0
10	-	108.8	-	109.4
1'	-	125.9	-	126.3
2'	7.57 (s, 1H)	105.2	7.54 (s, 1H)	105.7
3'	-	152.8	-	153.0
4'	-	141.0	-	141.5
5'	-	152.8	-	153.0
6'	7.57 (s, 1H)	105.2	7.54 (s, 1H)	105.7
3-OMe	4.00 (m, 3H)	55.8	3.94 (m, 3H)	56.3
5-OMe	4.00 (m, 3H)	55.8	3.94 (m, 3H)	56.3
7-OMe	4.00 (m, 3H)	56.1	3.94 (m, 3H)	56.5
8-OMe	4.00 (m, 3H)	56.2	3.94 (m, 3H)	56.7
3'-OMe	4.00 (m, 3H)	59.7	4.00 (m, 3H)	60.1
4'-OMe	4.00(m, 3H)	62.0	4.00 (m, 3H)	61.2
5'-OMe	4.00 (m, 3H)	62.4	3.91 (m, 3H)	61.6

Compound **29** was received as white solid (2.9 mg, 0.09 %yield based on Fraction **VI-II**). The $^1\text{H-NMR}$ spectrum (Figure A-56) of compound **29** presented three singlet signals of $\text{H}_{2'}$, $\text{H}_{6'}$ and H_8 at δ_{H} at 7.35 and 6.74 ppm. The signals of seven methoxy protons appeared at δ_{H} 4.00, 3.90, 3.90, 3.90, 3.94, 3.94 and 3.94 ppm. The structure of compound **29** was suggested to be 3,5,6,7,3',4',5'-heptamethoxyflavone ($\text{C}_{22}\text{H}_{24}\text{O}_9$). [36] The NMR spectral assignment of compound **29** and 3,5,6,7,3',4',5'-heptamethoxyflavone is gathered in Table 3.29.

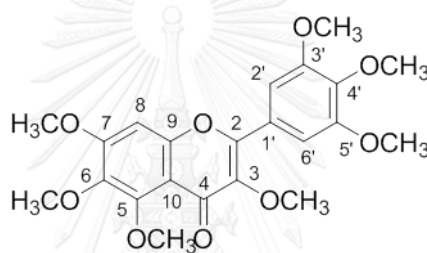
Compound **29**

Table 3.29 The comparison of ^1H NMR spectral assignment of compound **29** and 3,5,6,7,3',4',5'-heptamethoxyflavone [36]

Positions	Chemical shift (ppm)	
	3,5,6,7,3',4',5'-heptamethoxyflavone ³⁶	compound 29
2	157.7	157.9
3	140.1	140.3
4	173.7	173.8
5	153.5	153.7
6	140.2	140.4

Table 3.29 The comparison of ^1H NMR spectral assignment of compound **29** and 3,5,6,7,3',4',5'-heptamethoxyflavone [36] (cont)

Positions	Chemical shift (ppm)	
	3,5,6,7,3',4',5'-heptamethoxyflavone ³⁶	compound 29
7	157.7	157.9
8	96.0	96.2
9	152.4	152.6
10	113.1	113.3
1'	125.1	126.1
2'	105.8	106.0
3'	153.1	153.2
4'	141.1	141.3
5'	153.1	153.2
6'	105.8	106.0
3-OMe	62.3	62.4
5-OMe	61.6	61.7
6-OMe	61	61.2
7-OMe	60.1	60.2
3'-OMe	56.4	56.5
4'-OMe	56.4	56.5
5'-OMe	56.4	56.5

Compound **30** was obtained as white solid (2.3 mg, 0.07 %yield based on Fraction VI-II). According to the ^1H NMR spectrum (Figure A-58), it showed the signals of 1,2,5-trisubstituted phenyl protons at δ_{H} 7.00, 7.71 and 7.70 ppm, and 2,3,6,7,8-tretasubstituted flavone protons at δ_{H} 6.74 ppm. In addition, the signals at δ_{H} 3.86, 3.97, 3.92, 4.01, 3.96 and 3.96 ppm were occupied for six methoxy protons (3-OMe, 6-OMe, 7-OMe, 8-OMe, 2'-OMe and 5'-OMe). Concerning with the ^{13}C NMR (Figure A-59), the signals at δ_{C} 62.4, 61.7, 56.5, 60.1, 56.2 and 56.1 ppm suggested the presence of six methoxy carbons in molecule. The structure of compound **30** was identified as 3,6,7,8,2',5'-hexamethoxyflavone ($\text{C}_{21}\text{H}_{22}\text{O}_8$). [37] The NMR spectral assignment of compound **30** and 3,6,7,8,2',5'-hexamethoxyflavone is counted in Table 3.30.

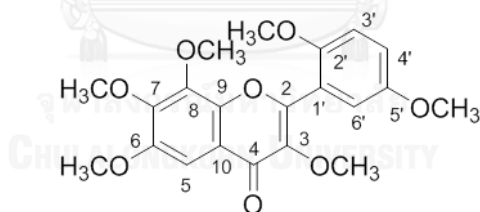
Compound **30**

Table 3.30 The comparison of ^1H NMR spectral assignment of compound **30** and 3,6,7,8,2',5'-hexamethoxyflavone [37]

Positions	Chemical shift (ppm)	
	3,6,7,8,2',5'-hexamethoxyflavone ³⁷	compound 30
2	153.5	153.4
3	140.8	140.9
4	173.7	173.8
5	96.0	96.2
6	157.7	157.8
7	140.2	140.2
8	152.4	152.6
9	153.6	153.7
10	113.1	113.2
1'	123.4	123.5
2'	151.0	151.1
3'	110.9	110.9
4'	121.7	121.9
5'	148.7	148.8
6'	111.4	111.4
3-OMe	62.2	62.4
6-OMe	61.6	61.7
7-OMe	56.3	56.5
8-OMe	60.0	60.1
2'-OMe	56.1	56.2
5'-OMe	56.0	56.1

Compound **31** was received as white solid (3.2 mg, 0.10 %yield based on Fraction **VI-II**). Concerning with the ^1H NMR spectrum (Figure A-60), two protons of 1,3,4,5-tetrasubstituted phenyl showed signals at δ_{H} 7.07 ppm, and two protons of 2,5,6,7-tretasubstituted flavone presented the signal at δ_{H} 6.61 and 6.80 ppm. In addition, the signals of 5-OMe, 6-OMe, 7-OMe, 3'-OMe, 4'-OMe and 5'-OMe presented at δ_{H} 3.92, 3.92, 3.95, 3.95, 3.99 and 4.00 ppm, together with the ^{13}C NMR spectrum (Figure A-61) that showed the signal at δ_{C} 56.5, 56.5, 56.5, 61.2, 61.7 and 62.3 ppm. The structure of compound **31** was known as 5,6,7,3',4',5'-hexamethoxyflavone ($\text{C}_{21}\text{H}_{22}\text{O}_8$). [38] The NMR spectral assignment of compound **31** and 5,6,7,3',4',5'-hexamethoxyflavone is concluded in Table 3.31.

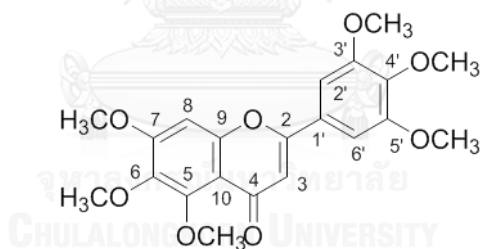
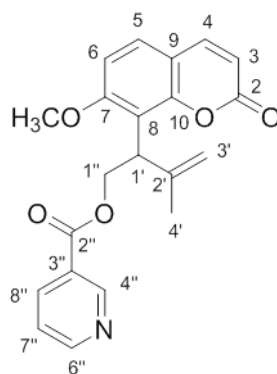
Compound **31**

Table 3.31 The comparison of ^{13}C NMR spectral assignment of compound **31** and 5,6,7,3',4',5'-hexamethoxyflavone [38]

Positions	Chemical shift (ppm)	
	5,6,7,3',4',5'-hexamethoxyflavone ³⁸	compound 31
2	161.0	161.2
3	108.3	108.4
4	177.2	177.3
5	154.5	154.6
6	140.4	140.6
7	157.8	157.9
8	96.3	96.4
9	152.6	152.7
10	112.9	113.0
1'	126.9	127.0
2'	103.4	103.6
3'	153.6	153.7
4'	140.9	141.0
5'	153.6	153.7
6'	103.4	103.4
5-OMe	56.4	56.5
6-OMe	56.4	56.5
7-OMe	61.1	61.2
3'-OMe	61.6	61.7
4'-OMe	62.2	62.3
5'-OMe	56.4	56.5

Compound **32** was earned as light brown solid (1.2 mg, 0.03 %yield based on Fraction **VI-II**). According to the ^1H NMR spectrum (Figure A-62), the 7-methoxy-8-substituted coumarin skeleton of compound **32** could be indicated by four doublet signals at δ_{H} 6.28 (J), 8.0, 7.65, 7.11 and one singlet aromatic methoxy signal at δ_{H} 3.86 ppm. The side chain at C-8 comprised a triplet signal of benzylic methine protons at δ_{H} 4.50 (J) ppm, the double of doublet signal of methine proton at δ_{H} 5.07 ($J = 10.8, 7.2$ Hz) and 4.78 ($J = 10.8, 7.6$ Hz) ppm, the singlet signal of allylic methyl protons at δ_{H} 1.68 ppm and the broad singlet signal of methylene protons at δ_{H} 4.89 and 4.92 ppm. Furthermore, pyridine ring protons revealed the signals at δ_{H} 8.87, 8.15, 7.55 and 8.79 ppm. There are twenty-one carbon signals in the ^{13}C NMR spectrum of compound **32**. It significantly presented five signals at δ_{C} 125.8, 149.8, 153.2, 124.2 and 137.2 ppm assignable to pyridine carbons. In addition, the carbonyl carbon signals of ester and coumarin nucleus exhibited at δ_{C} 164.2 and 159.8 ppm, respectively. The structure of compound **32** was clarified as isomurralonginol nicotinate ($\text{C}_{21}\text{H}_{19}\text{NO}_5$) [39] by interpretation of NMR data.⁴⁵ The NMR spectral assignment of compound **32** is collected in Table 3.32.



Compound 32

Table 3.32 The ^1H and ^{13}C NMR spectral assignment of compound **32**

Positions	Chemical shift (ppm)	
	^1H	^{13}C
2	-	159.8
3	6.28 (d, $J = 9.6$ Hz, 1H)	112.3
4	8.0 (d, $J = 9.6$ Hz, 1H)	144.9
5	7.65 (d, $J = 8.4$ Hz, 1H)	128.7
6	7.11 (d, $J = 8.4$ Hz, 1H)	108.6
7	-	160.6
8	-	112.8
9	-	114.4
10	-	153.0
1'	4.50 (t, $J = 7.2$ Hz, 1H)	40.2
2'	-	142.2
3'	4.92 (s, 1H), 4.89 (s, 1H)	111.8
4'	1.68 (s, 3H)	21.8

Table 3.32 The ^1H and ^{13}C NMR spectral assignment of compound **32** (cont)

Positions	Chemical shift (ppm)	
	^1H	^{13}C
1''	5.07 (dd, $J = 10.8, 7.2$ Hz, 1H), 4.78 (dd, $J = 10.8, 7.6$ Hz, 1H)	64.8
2''	-	164.2
3''	-	125.8
4''	8.87 (s, 1H)	149.8
6''	8.79 (d, $J = 4.0$ Hz, 1H)	153.2
7''	7.55 (dd, $J = 8.0, 4.8$ Hz, 1H)	124.2
8''	8.15 (dt, $J = 8.2, 2.0$ Hz, 1H)	137.2

Compound **33** was obtained as brown solid (26.7 mg, 2.29 %yield based on Fraction VI-II). The ^1H NMR spectrum (Figure A-64) of compound **33** showed signals of 1,3,4,5-tetrasubstituted phenyl protons at δ_{H} 7.16 ppm, and 2,5,6,7,8-pentasubstituted flavone protons at 6.64 ppm. In addition, seven signals presented at δ_{H} 4.1, 4.02, 3.95 and 3.92 ppm. Signal at δ_{C} 62.4, 62.1, 61.9, 61.8, 56.4, 61.2 and 56.4 ppm suggesting the presence of seven methoxy carbons in the molecule. The structure of compound **33** was revealed as 5,6,7,8,3',4',5'-heptamethoxyflavone ($\text{C}_{22}\text{H}_{24}\text{O}_9$). [40] The NMR spectral assignment of compound **33** and 5,6,7,8,3',4',5'-heptamethoxyflavone is summarized in Table 3.33.

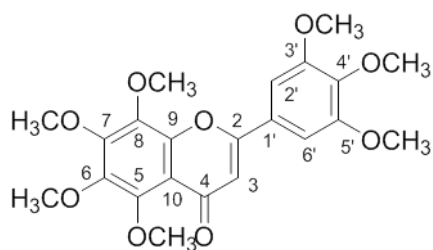
Compound **33**

Table 3.33 The comparison of ^{13}C NMR spectral assignment of compound **33** and 5,6,7,8,3',4',5'-heptamethoxyflavone [40]

Positions	Chemical shift (ppm)	
	5,6,7,8,3',4',5'-heptamethoxyflavone ⁴⁰	Compound 33
2	160.7	160.9
3	107.6	107.8
4	177.3	177.5
5	148.4	148.6
6	144.1	144.3
7	151.5	151.7
8	137.9	138.1
9	147.6	147.9
10	114.8	114.9
1'	126.6	126.8
2'	103.2	103.5
3'	153.5	153.7
4'	140.9	141.1
5'	153.5	153.7
6'	103.2	103.5

Table 3.33 The comparison of ^{13}C NMR spectral assignment of compound **33** and 5,6,7,8,3',4',5'-heptamethoxyflavone [40] (cont)

Positions	Chemical shift (ppm)	
	5,6,7,8,3',4',5'-heptamethoxyflavone ⁴⁰	Compound 33
5-OMe	62.2	62.4
6-OMe	61.8	62.1
7-OMe	61.6	61.9
8-OMe	61.8	61.8
3'-OMe	56.2,	56.4
4'-OMe	61.0	61.2
5'-OMe	56.2	56.4

3.3 Synthesis of coumarin derivatives

Certain derivatives of coumarin have been reported to possess biological activities such as anti-tumor-promoting activity, [41] and antifungal activity. [42] Umbelliferone containing a hydroxyl group at C-7 provided a good possibility for further modification to furnish target analogues. In this research, two types as ester and ether derivatives of coumarins were selected.

3.3.1 Ester derivatives

Four esters of umbelliferone with different in carbon side chains (compounds **34-37**) were synthesized using carboxylic acid as a starting material through

generated acid chloride react with umbelliferone. All compounds were well-characterized by ^1H NMR.

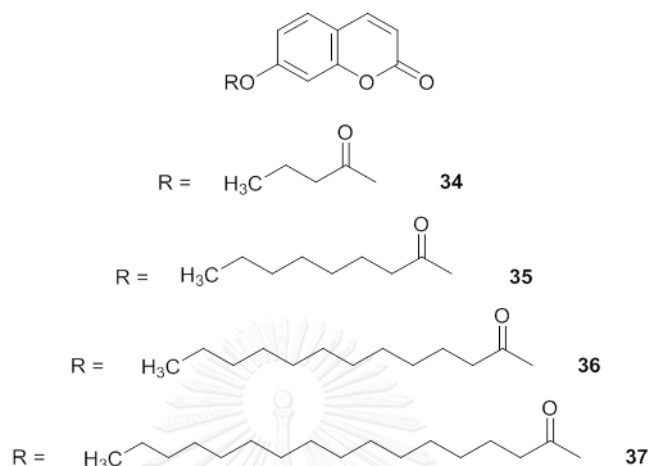


Figure 3.1 The structures of compounds **34**, **35**, **36** and **37**

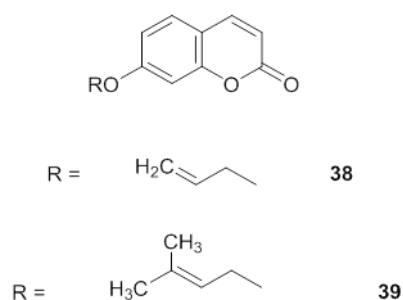
The ^1H NMR spectra of compounds **34-37** showed the signal of 7-substituted coumarin group containing four high intensity doublet signals and a singlet signal in the range of δ_{H} 7.62-6.33 ppm together with triplet signals of methyl group and methylene protons adjacent to a carbonyl carbon, and a multiplet signal of methylene group. The ^1H NMR spectral assignment of compounds **34-37** is assembled in Table 3.34.

Table 3.34 The ^1H NMR spectral assignment of compounds **34-37**

Positions	Chemical shift (ppm)			
	compound 34	compound 35	compound 36	compound 37
3	6.33 (d, $J = 9.5$ Hz, 1H)	6.42 (d, $J = 9.5$ Hz, 1H)	6.42 (d, $J = 9.5$ Hz, 1H)	6.42 (d, $J = 9.6$ Hz, 1H)
4	7.62 (d, $J = 9.6$ Hz, 1H)	7.71 (d, $J = 9.6$ Hz, 1H)	7.71 (d, $J = 9.5$ Hz, 1H)	7.71 (d, $J = 9.6$ Hz, 1H)
5	7.42 (d, $J = 8.4$ Hz, 1H)	7.51 (d, $J = 8.4$ Hz, 1H)	7.51 (d, $J = 8.4$ Hz, 1H)	7.51 (d, $J = 8.4$ Hz, 1H)
6	6.98 (d, $J = 8.5$ Hz, 1H)	7.07 (d, $J = 8.4$ Hz, 1H)	7.07 (d, $J = 8.4$ Hz, 1H)	7.07 (d, $J = 8.5$ Hz, 1H)
8	7.04 (s, 1H)	7.13 (s, 1H)	7.13 (s, 1H)	7.13 (s, 1H)
2'	2.51 (t, $J = 7.4$ Hz, 2H)	2.61 (t, $J = 7.5$ Hz, 2H)	2.61 (t, $J = 7.5$ Hz, 2H)	2.61 (t, $J = 7.5$ Hz, 2H)
CH ₂	1.73 (sextet, $J = 7.3$ Hz, 2H)	1.79 (qui, $J = 7.4$ Hz, 2H), 1.37 (m, 8H)	1.79 (qui, $J = 7.5$ Hz, 2H), 1.30 (m, 16H)	1.78 (qui, $J = 7.5$ Hz, 2H), 1.29 (m, 24H)
CH ₃	0.99 (t, $J = 7.4$ Hz, 3H)	0.91 (m, 3H)	0.91 (t, $J = 6.6$ Hz, 3H)	0.90 (t, $J = 6.6$ Hz, 3H)

3.3.2 Ether derivatives

Two ethers of umbelliferone were synthesized by reacting the starting coumarin with selected alkyl halides in the presence of K_2CO_3 . All compounds were characterized by ^1H NMR.

**Figure 3.2** The structures of compounds **38** and **39**

According to the ^1H NMR spectra of compounds **38** and **39**, they should contain 7-substituted coumarin skeleton since the spectrum exhibited four doublet signals and one singlet signal in the range of δ_{H} 7.64-6.25 ppm. In addition, compound **38** displayed three double signals of methylene proton at δ_{H} 5.44 ($J = 17.2$ Hz), 5.34 ($J = 10.4$ Hz) and 4.60 ($J = 5.3$ Hz) ppm and multiplet signal of methine proton at δ_{H} 6.04. At C-7 of compound **39**, one multiplet signal of methine proton at δ_{H} 5.45 ppm, one doublet signal of methylene protons at δ_{H} 4.55 ($J = 7.0$ Hz) and two singlet signals of methyl group at δ_{H} 1.79 and 1.75 ppm were detected. The ^1H NMR spectral assignment of compounds **38** and **39** is assembled in Table 3.35.

Table 3.35 The ^1H NMR spectral assignment of compounds **38** and **39**

Positions	Chemical shift (ppm)	
	compound 38	compound 39
3	6.25 (d, $J = 9.5$ Hz, 1H)	6.23 (d, $J = 9.3$ Hz, 1H)
4	7.64 (d, $J = 9.5$ Hz, 1H)	7.63 (d, $J = 9.5$ Hz, 1H)
5	7.37 (d, $J = 8.6$ Hz, 1H)	7.36 (d, $J = 8.5$ Hz, 1H)
6	6.86 (d, $J = 8.0$ Hz, 1H)	6.83 (d, $J = 8.0$ Hz, 1H)
8	6.83 (s, 1H)	6.82 (s, 1H)
1'	5.44 (d, $J = 17.2$ Hz, 1H), 5.34 (d, $J = 10.4$ Hz, 1H)	4.55 (d, $J = 7.0$ Hz, 2H)
2'	6.04 (m, 1H)	5.45 (m, 1H)
3'	4.60 (d, $J = 5.3$ Hz, 2H)	-
4'	-	1.79 (s, 3H)
3'-OMe	-	1.75 (s, 3H)

3.4 Biological activities of isolated compounds from *M. paniculata* leaves and related compounds

3.4.1 Exploration for insect control agent

3.4.1.1 Antifeedant activity

Four crude extracts (Fractions I-IV) and three pure compounds (**2**, **3** and **5**) were evaluated for antifeedant activity against the 2nd instars *Spodoptera litura* larvae at concentration of 0.25%w/w for the extract and 2.5 mM for pure compound for 6 h, respectively. The results are presented in Figure 3.3.

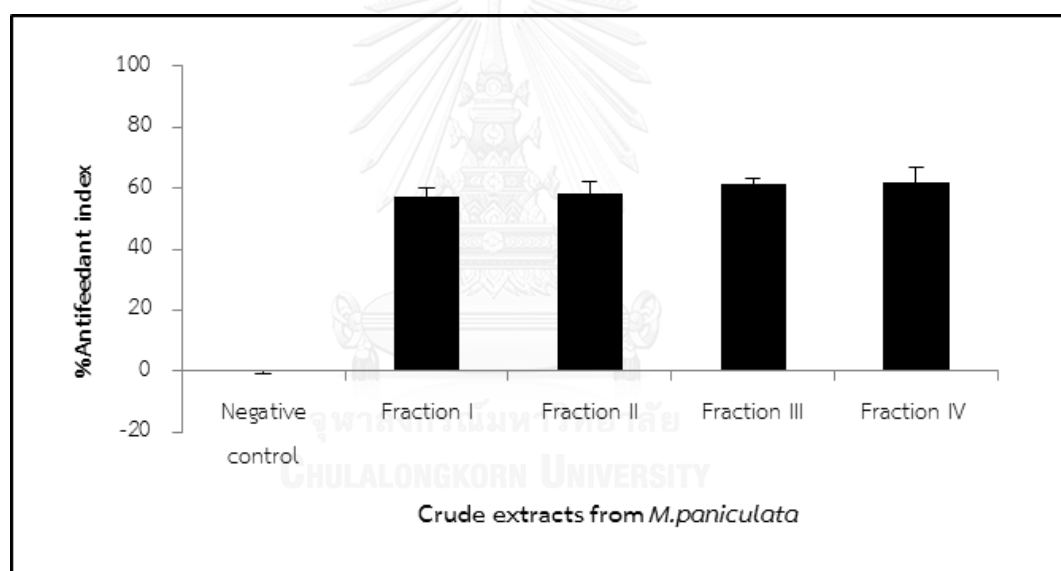


Figure 3.3 Antifeedant index (%) of the crude extracts from *M. paniculata* leaves

The four crude extracts studied were crudes hexane (Fraction I), CH₂Cl₂ (Fraction II), EtOAc (Fraction III) and MeOH (Fraction IV) extracts. The obtained values were derived from the means of thirty independent replicates. Figure 3.3 reveals that Fraction IV showed the highest percentage of larval antifeedant with 62% antifeedant index, whereas the EtOAc, CH₂Cl₂ and hexane extracts exhibited 61, 58 and 57 % at

the same concentration (0.25%w/w), respectively, suggesting all four crude extracts did not present different ability as antifeedant agent.

The antifeedant activity of plant extracts has been reviewed by many authors. [43-46] The antifeedant activity against *S. litura* of these crude extracts was compared with the information of Arivoli [47], the food feeding of the 3rd instars larvae of *S. litura* treatment was highly decreased by the extracts of *Murraya koeingii* (same genus with *M. paniculata*).

According to the above results, all crude extracts exhibited significant antifeedant activity. Therefore, some isolated compounds were selected to continue testing on antifeedant activity. Three compounds (**2**, **3** and **5**) were selected at concentration of 2.5 mM. The results are summarized in Figure 3.4.

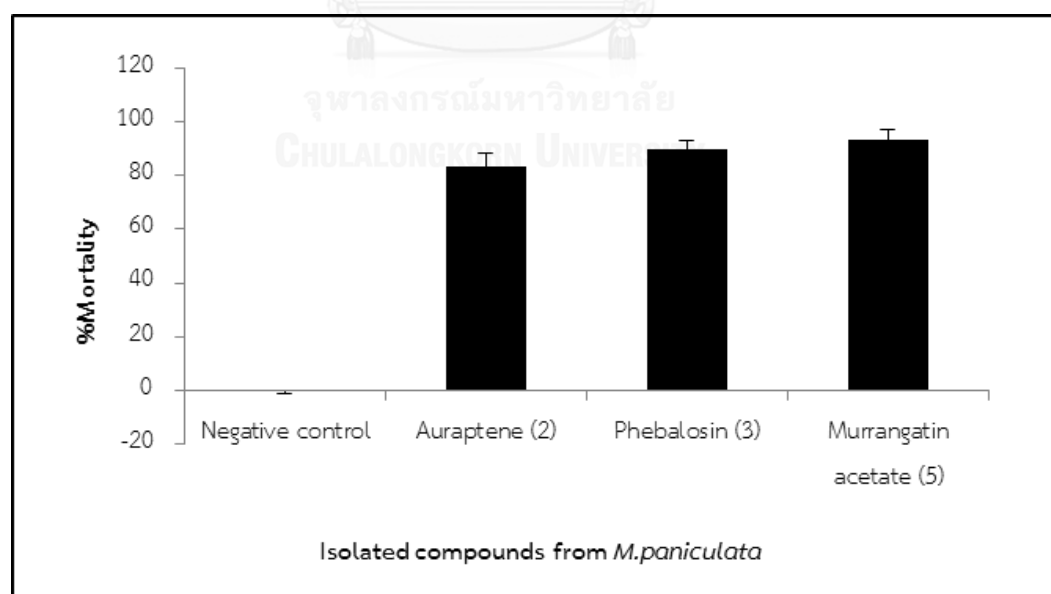


Figure 3.4 Antifeedant index (%) of compounds **2**, **3** and **5**

Three pure compounds studied were auraptene (2), phebalosin (3) and murrangatin acetate (5). Values are the means of thirty independent replicates. The antifeedant activity results of three major compounds revealed that auraptene (2) possessed the highest feeding deterrence activity of 61 % against the 2nd instars of *S. litura*, whereas phebalosin (3) and murrangatin acetate (5) showed 54 and 55%, respectively. Therefore, all three main coumarins from *M. paniculata* showed antifeedant activity against the 2nd instars of *S. litura*.

Plant ingredients acting as antifeedants are found in all the compound groups of secondary plant metabolism. However, the most effective insect feeding inhibitors come from terpenoids, alkaloids, saponins and polyphenols [44] The active compounds occupying antifeedant activity were often oxygenated compounds comparable to that reported by Papachristos *et al.* (2004) [48] that oxygenated monoterpenoids showed the inhibitory activity higher than hydrocarbons. All selected compounds (2, 3 and 5) contained oxygen atom in their structures, accordingly they exposed good antifeedant activity. Carpinella addressed that certain compounds possessed antifeedant activity could demonstrate insecticidal activity when the concentration increased. [49]

3.4.1.2 Insecticidal activity

Insecticidal activity against *S. litura* larvae of three major compounds (**2**, **3** and **5**) were thus evaluated at concentrations of 2.5 mM for 15 days. The result is demonstrated in Figure 3.5.

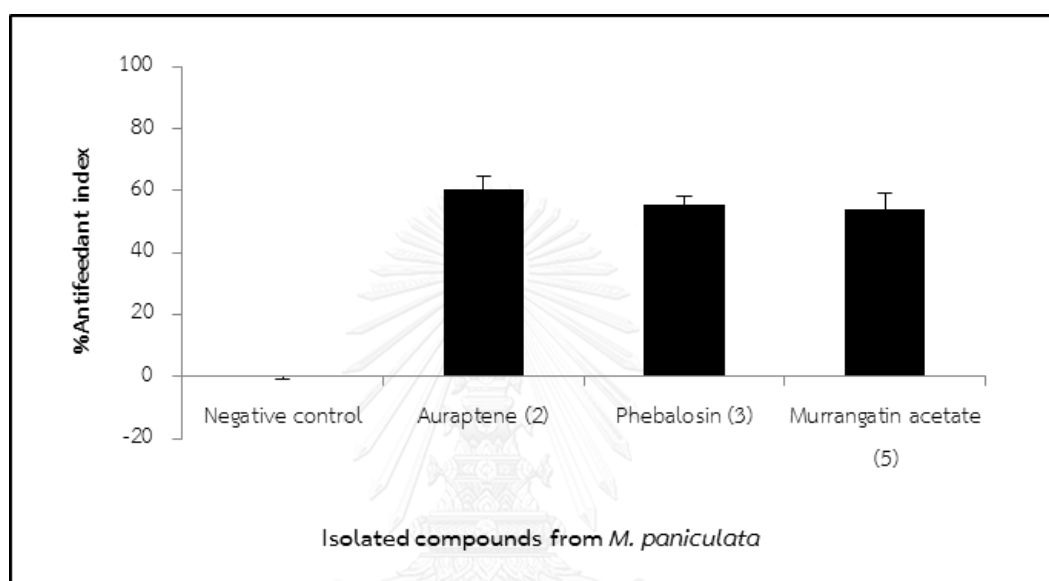


Figure 3.5 Insecticidal activity of compounds from *M. paniculata* on larvae of *S. litura*

From Figure 3.5, murrangatin acetate (**5**) exhibited the highest percentage of larval mortality (93%), whereas auraptene (**2**) and phebalosin (**3**) exhibited 83 and 90% at the same concentration, respectively. It suggests that all three compounds have potential as an insect-control agent.

This research is the first report of the insecticidal activity of these coumarins. Although, murraxocin, a coumarin separated from the leaves of *Boenninghausenia albiflora* afforded an insecticidal property against *Plecoptera reflexa* and *Clostera cupreata* with 80 and 85% mortality, respectively. [50] Interestingly, the petroleum ether and EtOAc fractions of *M. paniculata* were evaluated the toxicity by a residual film bioassay against male and female adults of *Callosobruchus maculatus* (F.). The results showed that the petroleum ether fraction was more toxic than EtOAc fraction and insect males were more susceptible than females. [51]

3.4.1.3 Repellent activity

The repellent activity of isolated compounds (**2**, **3** and **5**) against *Ferrisia virgate* (Cockerell) adults was evaluated using the area preference method. All compounds were diluted in acetone to prepare testing solutions of concentrations $78.63 \mu\text{g}/\text{cm}^2$ (Table 3.36), and then the best activated compounds were selected to test at various concentrations (78.63 , 15.73 , 3.15 , 0.63 and $0.13 \mu\text{g}/\text{cm}^2$) for 2, 4 and 6 h. The repellent activity results of phebalosin (**3**) at various concentrations are collected in Table 3.37.

Table 3.36 The PR values of isolated compounds on *Ferrisia virgate* adults

compounds	percent repellency (% PR)	
	2h	4h
auraptene (2)	33 ± 11	26 ± 11
phebalosin (3)	70 ± 14	60 ± 0
murrangatin acetate (5)	53 ± 23	40 ± 40
lemon glass	50 ± 42	30 ± 14

In previous screening database of seven *Murraya* species, some species expressed significant repellent activity. Thus, chemical constituents of *M. paniculata* were further studied as repellent inhibitor. According to Table 3.34, percent repellency of all compounds was evaluated at 2 and 4 h. At 2 h, phebalosin (3) showed the best percent repellency on *F. virgate* adults with 70%, whereas auraptene (2) and murrangatin acetate (5) exhibited 33 and 53% at the same concentration, respectively. At 4 h, phebalosin (3) also exhibited the highest percent repellency with 60%, whereas auraptene (2) and murrangatin acetate (5) exhibited 26 and 40% at the same concentration, respectively. Interestingly, phebalosin (3) and murrangatin acetate (5) showed higher activity than the positive control (lemon glass conc. 78.63 $\mu\text{g}/\text{cm}^2$) at both 2 and 4 h. The results designated that coumarins with similar structures displayed various capacities of repellent activities. Recent literature revealed that phebalosin (3) expressed strong laticidal activity against *Tribolium castaneum*, but no information on antifeedant activity against *S. litura*. [18]

Table 3.37 The PR values of phebalosin (**3**) on *F. virgate* adults

time	concentrations ($\mu\text{g}/\text{cm}^2$)				
	78.63	15.73	3.15	0.63	0.13
2h	73.0 \pm 7	55.3 \pm 5	36.7 \pm 7	26.7 \pm 3	17.5 \pm 4
4h	71.7 \pm 8	55.0 \pm 9	32.5 \pm 11	23.3 \pm 7	10.0 \pm 8
6h	66.0 \pm 4	53.3 \pm 3	32.5 \pm 5	16.0 \pm 5	7.5 \pm 9

According to the highest percent repellency of phebalosin (**3**), further evaluation of the repellent activity at various concentrations (78.63, 15.73, 3.15, 0.63 and 0.13 $\mu\text{g}/\text{cm}^2$) for 2, 4 and 6 h was carried out. The results showed that percent repellency decreased when the compound was diluted together with increasing time of testing. This suggests that, when solution had high concentration, the amount of active ingredient in testing solution was also high, so insects could move to the area that was sprayed with negative control more than testing solution during testing as in Figure 3.6. Figure 3.6 reveals the amount of insect at testing part (left side) increased when conc. of phebalosin (**3**) was decreased. In addition, phebalosin (**3**) might evaporate or decompose at 4 and 6 h after testing.

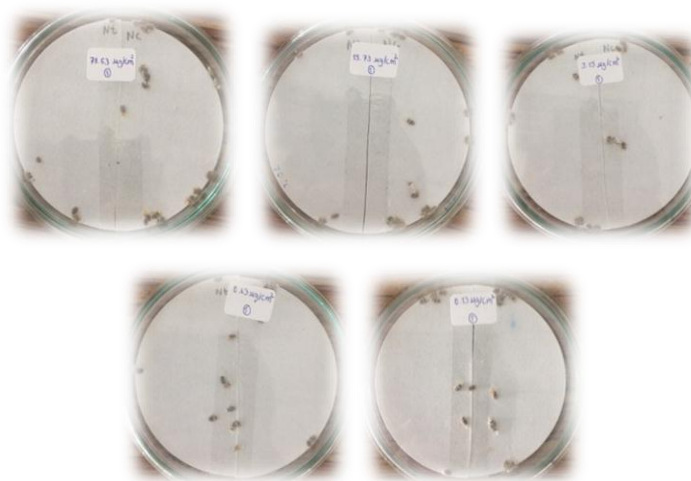


Figure 3.6 Repellent activity of phebalosin (**3**) on adults of *Ferrisia virgate* (Cockerell)

3.4.2 Antibacterial activity

Three major compounds (**2**, **3** and **5**) were selected to perform antibacterial activity due to the availability of sample. The antibacterial activities were tested *in vitro* against *Propionibacterium acnes* (KCCM41747), *Staphylococcus aureus* (ATCC25923), *Streptococcus sobrinus* (KCCM11898), *Streptococcus mutans* (ATCC25175), and *Salmonella typhi* (ATCC442). Chloramphenicol was used as a positive control. The results are exhibited in Table 3.38.

Table 3.38 Antibacterial activity of compounds **2**, **3** and **5**

compound	Inhibition zone average (mm) \pm SD				
	<i>P. acnes</i>	<i>S. aureus</i>	<i>S. sobrinus</i>	<i>S. mutans</i>	<i>S. typhi</i>
auraptene (2)	7.00 \pm 0.00	7.33 \pm 0.47	7.00 \pm 0.00	7.67 \pm 0.47	8.00 \pm 0.82
phebalosin (3)	7.33 \pm 0.47	8.67 \pm 0.00	8.00 \pm 0.00	7.67 \pm 0.47	7.67 \pm 0.47
murrangatin acetate (5)	7.00 \pm 0.00	7.33 \pm 0.47	9.00 \pm 0.00	7.67 \pm 0.47	7.67 \pm 0.47
chloramphenicol	23.00 \pm 0.00	21.00 \pm 0.00	18.00 \pm 0.00	19.00 \pm 0.00	20.00 \pm 0.00

All three compounds at 100 µg/mL were evaluated for antibacterial activity against four gram-negative bacteria. The inhibitory activity of these compounds was expressed by inhibition zone as shown in Table 3.36. All three compounds (**2**, **3** and **5**) presented narrow inhibition zone with the range of 7.00-9.00 mm indicating weak activity against all bacteria. This might describe as the coumarin did not diffuse well on the prepared nutrient agar [52] and owing to the pattern of the substitution on C-7 and C-8 positions of coumarin. [53]

3.4.3 Anti-inflammatory activity

This experiment was kindly performed by Associate Professor Dr. Tanapat Palaga and co-worker at Department of Microbiology, Faculty of Science, Chulalongkorn University. Eighteen constituents of *M. paniculata* leaves (compounds **1**, **2**, **3**, **5**, **6**, **8**, **9**, **10**, **11**, **12**, **15**, **17**, **18**, **25**, **26**, **28**, **29** and **33**) were screened for cell viability by MTT assay and further tested on NO production. The result is presented in Figure 3.7.

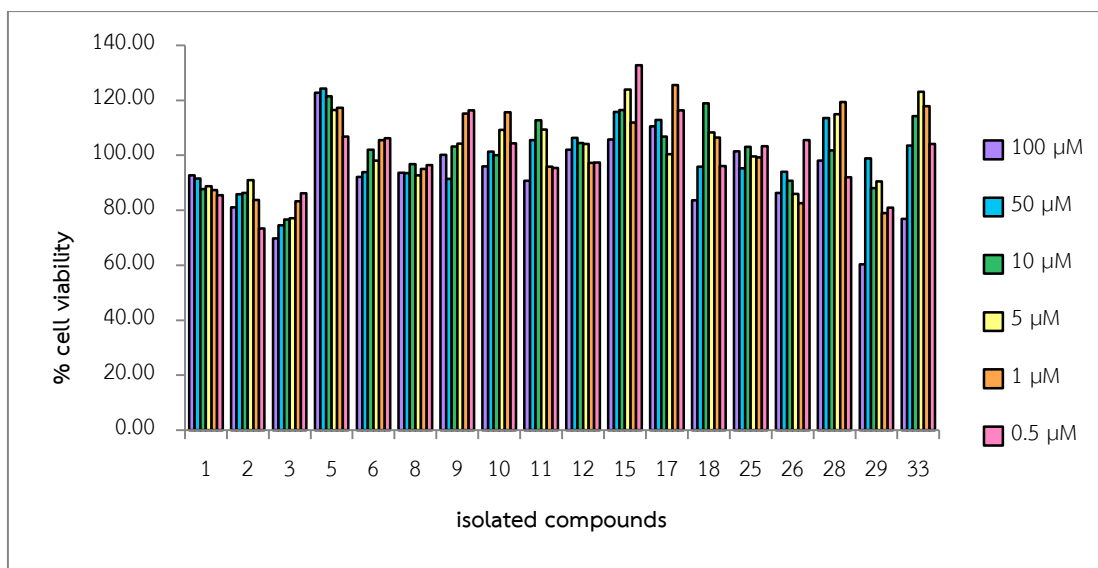


Figure 3.7 Effect of compounds **1, 2, 3, 5, 6, 8, 9, 10, 11, 12, 15, 17, 18, 25, 26, 28, 29** and **33** on the viability of RAW 264.7 cells by the MTT assay

The percentage of cell viability of the systems incubated with selected compounds (**1, 2, 3, 5, 6, 8, 9, 10, 11, 12, 15, 17, 18, 25, 26, 28, 29** and **33**) was about 60-120. Within the range of 0.5-100 μM , all compounds revealed no cytotoxicity with RAW 264.7 cells. Since, all compounds did not show cytotoxicity with cells so it is interesting to further test on any biological activities. Therefore, all compounds were selected for next study on the inhibition of NO production. The result is summarized in Figure 3.8.

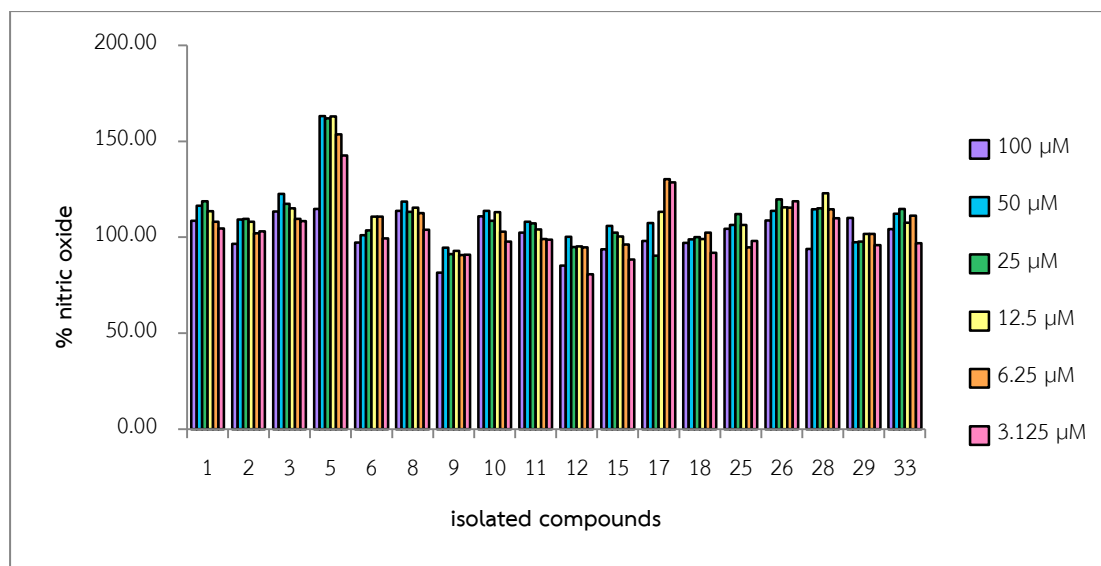


Figure 3.8 The inhibitory activity on NO production when treated with compounds **1**, **2**, **3**, **5**, **6**, **8**, **9**, **10**, **11**, **12**, **15**, **17**, **18**, **25**, **26**, **28**, **29** and **33**

According to Figure 3.8, all compounds did not inhibit NO production with 80-140 % NO. Even though, the highest concentration (100 μM) of these compounds still did not exhibit NO production. These results supported the previous report on the structural requirements of flavonoids: the methoxy in ring A enhanced anti-inflammatory activity, while the methoxy substitution in ring B abolished inhibitory activity. [54] Therefore, compounds **11**, **28**, **29** and **33** displayed a weak anti-inflammatory activity. From the result, compound **9** could be estimated as the best inflammatory inhibitor in this group because it is presented lowest %NO in every concentration followed by compound **12**.

Various coumarin derivatives isolated from plants have been reported to possess anti-inflammatory activities. [55] These acted by reducing tissue edema, altering the functions of enzymatic systems, such as cyclooxygenase and lipoxygenase, and preventing the generation of free radicals. Hadjipavlou-Litina has studied various hydroxyaryl-substituted coumarin derivatives to develop a SAR and found a polar group at 5-/ 6-/7-position incurs LOX inhibitory activity on coumarin. [56]

3.4.4 Antioxidant activity

Free radical-scavenging activities of eleven selected compounds (**1**, **2**, **3**, **5**, **8**, **9**, **10**, **11**, **12**, **17** and **18**) were evaluated in comparison with ascorbic acid using DPPH assay. Based on this protocol, DPPH radicals react with proton donated substances leading to the change of purple of DPPH radicals to yellow. The change of the strong absorption band of DPPH detected at 517 nm would directly relate to antioxidant activity. The results are summarized in Table 3.39.

Table 3.39 Antioxidant activity of selected isolated compounds from the leaves of *M. paniculata*

compound	% antioxidant at concentrations					IC ₅₀ (µg/mL)
	62.5 µg/mL	125 µg/mL	250 µg/mL	500 µg/mL	1000 µg/mL	
1	13.09 ± 2.90	10.59 ± 2.05	11.05 ± 1.89	12.75 ± 2.23	12.24 ± 4.57	-
2	12.18 ± 4.49	13.99 ± 0.39	17.39 ± 1.04	20.34 ± 0.98	24.42 ± 2.46	-
3	14.22 ± 2.26	12.52 ± 2.05	13.99 ± 1.93	16.37 ± 1.37	17.96 ± 3.41	-
5	9.46 ± 5.73	12.07 ± 0.59	10.48 ± 2.39	13.43 ± 0.68	13.99 ± 0.71	-
8	12.86 ± 3.97	13.31 ± 1.42	10.37 ± 2.90	35.75 ± 1.74	16.15 ± 1.92	-
9	10.93 ± 1.71	11.16 ± 1.09	10.71 ± 1.56	11.27 ± 1.99	11.50 ± 1.74	-
10	12.98 ± 1.68	13.20 ± 2.46	9.58 ± 1.29	33.60 ± 2.73	14.22 ± 0.52	-
11	14.22 ± 1.09	11.95 ± 1.71	12.86 ± 1.04	13.54 ± 5.79	14.67 ± 0.52	-
12	26.69 ± 1.48	37.45 ± 2.05	45.72 ± 1.02	69.63 ± 1.53	74.39 ± 0.71	289
17	13.99 ± 1.09	16.03 ± 2.08	14.33 ± 1.53	38.02 ± 0.86	27.14 ± 1.29	-
18	13.88 ± 1.53	9.69 ± 0.34	11.61 ± 1.87	17.51 ± 0.59	17.17 ± 0.34	-
Ascorbic acid	97	97	97	97	97	45

The percentage of DPPH radical scavenging activity of selected compounds as presented in Table 3.39 demonstrated that most of them were not free radical inhibitor except for scopoletin (**12**) which exhibited significant antioxidant activities with IC₅₀ 289 µg/mL. Compound **12** showed moderate potential on antioxidant activity because it comprised of free benzylic hydroxyl group suggesting that this hydroxyl group could generate free radical reacting with another free radical, so this molecule could inhibit oxidation reaction of other molecules. In previous research,

the EtOH extract of the seeds of *M. paniculata* was tested on antioxidant activity with DPPH free radical and H₂O₂ scavenging activity. The extract exhibited potent antioxidant activity with IC₅₀ 23 and 20 µg/mL for DPPH free radical and H₂O₂, respectively. Moreover, flavone derivatives were separated from the crude extract implying that this compound may have potential in antioxidant activity. [57]

3.4.5 Anti-Human carbonic anhydrase II activity

This experiment was kindly performed by Associate Professor Dr. Chulee Yompakdee and her team at Department of Microbiology, Faculty of Science, Chulalongkorn University. Fourteen selected compounds including nine natural (**1**, **2**, **3**, **5**, **8**, **9**, **10**, **17** and **18**) and five synthesized (**35-39**) compounds were tested on antihuman carbonic anhydrase II activity at various concentrations. The concentrations of all compounds were diluted from 100 to 0.032 µM and treated with yeast cells. Each concentration of test compounds was incubated for desired period of exposure (24 h). After that resazurin solution (30 µL) was added to each well and incubated for 1 to 4 h at 37 °C to allow cells convert blue solution of resazurin into pink which was noticeable by naked eyes. This activity was evaluated in both high and low CO₂ conditions. The results are presented in Table 3.40.

Table 3.40 Minimal effective dose of coumarins on *in vivo* inhibitory activity against human carbonic anhydrase isozyme II

compound	Minimal effective dose (μM)	Non-toxic dose (μM)
1	100.00	100.00
2	100.00	100.00
3	20.00	100.00
5	20.00	20.00
8	0.80	100.00
9	0.80	0.80
10	0.80	0.80
17	<0.032	20.00
18	0.16	4.00
35	<0.032	20.00
36	N/A	>500.00
37	100.00	100.00
38	4.00	100.00
39	100.00	100.00
acetazolamide	0.78	25.00

N/A = No Activity

Inhibitory activity of isolated compounds on carbonic anhydrase enzyme activities was tested under *in vivo* conditions. Anti hCA II activity of testing compounds was assessed in both high and low CO₂ conditions for investigating cell cytotoxicity through noticeable by naked eyes, the lowest concentration which made yeast cell in high CO₂ condition dead (blue solution) meant that the compound has

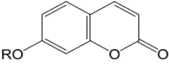
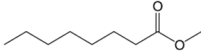
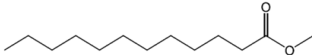
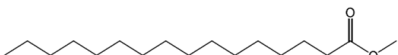
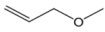
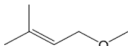
cytotoxicity with yeast cells at that concentration. According to Table 3.40, the most potent compounds were **17** and **35** since they could inhibit the activity of hCA II at the lowest concentration used in this assay ($<0.032 \mu\text{M}$). For compounds **17** and **35**, yeast cells died at concentration of $0.032 \mu\text{M}$; nonetheless still did not know the conditions of cells at lower concentration, in the event of cells alive at lower concentration meant Minimal Effective Dose (MED) was $0.032 \mu\text{M}$, but yeast cells died at lower concentration implied that their MED was less than suggesting that C-8 position side chain of coumarin comprised carbonyl and diminutive groups strongly influenced hCA II inhibitory effect. Interestingly these compounds seemed to show higher activity than a positive control, acetazolamide. Moreover, compound **18** displayed higher activity than a positive control with MED of $0.16 \mu\text{M}$. These three compounds (**17**, **18** and **35**) significantly showed hCA II inhibitory activity, whereas the remaining three compounds (**8**, **9** and **10**) were quite effective hCA II inhibitors, with MED of $0.80 \mu\text{M}$. Compound **35** could express higher potent against hCA II than compounds **36** and **37**. This suggested that long carbon chains decrease activity to inhibit enzyme hCAII which could be used to treat various pathological conditions such as glaucoma.

The anti-human carbonic anhydrase II activity has been researched by Supuran's group, but the activity was tested under *in vitro* conditions. In 2013, Supuran and co-workers [14] collected twenty-seven natural coumarins and evaluated for inhibition of six human CA isozymes (CAs I, II, VII, IX, XII and XIII). The simplest coumarin was a weak inhibitor of CA I and CA II and most obvious was that the natural coumarin was very weak CA II inhibitor. In 2013, Supuran and co-workers [58] synthesized two sulfocoumarins and seventeen sulfocoumarin derivatives and tested for the inhibition of zinc enzyme human carbonic anhydrase. All sulfocoumarins also were ineffective hCA I and II inhibitors.

3.5 Structure-Activity Relationship (SAR) study

The most chemical constituent of *M. paniculata* is coumarin which consist methoxy group at C-7 position. So, i envisioned that further modifications of coumarin functionalities would provide more information concerning the structure–activity relationship of coumarin. Coumarin derivatives which were tested on antihuman carbonic anhydrase II were illustrated in Table 3.41.

Table 3.41 Structures of coumarin derivative showing anti-hCA II activity

Compound	Structure	Anti-hCA II Activity	
		Minimal Effective Dose (μM)	Non-toxic dose (μM)
			
35		< 0.032	20.00
36		N/A	> 500.00
37	R = 	100.00	100.00
38		4.00	100.00
39		100.00	100.00

N/A = No Activity

According to Table 3.41, among ester derivative (**35-37**), the hCA II was excellently inhibited by compound **35** which showed MED < 0.032 μM . This suggested that long carbon chains decrease activity to inhibit enzyme hCA II. In addition, when compare activity of compound **38** and **39** which were ether derivative, the result showed compound **38** exhibited higher activities than compound **39**. This proposed that compound with diminutive group was more suitable for inhibitory activity of hCA II enzyme.

CHAPTER IV

CONCLUSION

The leaves of *M. paniculata* were extracted with hexane, CH₂Cl₂, EtOAc and MeOH furnishing their crude extracts.

The separation of Fractions I, II and III by column chromatography gave 5 compounds (**1**, **2**, **3**, **4** and **5**). Fractions VI-I and VI-II were separated by semi-prep HPLC yielding 24 compounds (**6-7** and **12-33**) including 2,6,2',6'-tetramethoxy-4,4'-bis-(1,2-*trans*-2,3-epoxy-1-hydroxypropyl) biphenyl (**20**) and medioresinol (**21**) which were firstly reported as constituents in *M. paniculata*. Compounds **8**, **9**, **10** and **11** were obtained from recrystallization by petroleum ether, MeOH, MeOH and acetone: petroleum ether, respectively. Among thirty-three isolated constituents, three major compounds were auraptene (**2**), phenalosin (**3**) and murrangatin acetate (**5**). In addition, ester (**34-37**) and ether derivatives of umbelliferone (**38-39**) were prepared by esterification and alkylation. Certain constituents were evaluated for antifeedant, insecticidal, repellent, antibacterial, anti-inflammatory, antioxidant and antihuman carbonic anhydrase II activity.

For antifeedant activity, the MeOH extract showed the highest percentage of larval antifeedant with 62% antifeedant index amongst four crude extracts. For three

major compounds, auraptene (**2**) revealed the highest feeding deterrence of 61 % against *S. litura* larva.

It should be noted at this point that this was the first report on the insecticidal activity of compounds **2**, **3** and **5**. Murrangatin acetate (**5**) exhibited the highest percentage of larval mortality (93%), whereas auraptene (**2**) and phebalosin (**3**) exhibited 83 and 90% at the same concentration, respectively. All three compounds displayed significant insecticidal activity against the 2nd instars of *S. litura*. This strongly implied that those compounds may be responsible as chemical defense to protect the leaves of *M. paniculata* from insects. For repellent activity, phebalosin (**3**) exhibited the best percent repellency on *Ferrisia virgate* (Cockerell) adults with 70%, which was higher than the positive control (lemom glass) at both 2 and 4 h. Compound **3** was further evaluated for repellent activity at various concentrations and found that it had high potent in repellent activity.

For antibacterial activity of compounds **2**, **3** and **5** against *P. acnes*, *S. aureus*, *S. sobrinus*, *S. mutans*, and *S. typhi*, all compounds exhibited weak activity with inhibition zone of 7.00-9.00 mm.

Eighteen compounds (**1**, **2**, **3**, **5**, **6**, **8**, **9**, **10**, **11**, **12**, **15**, **17**, **18**, **25**, **26**, **28**, **29** and **33**) revealed no cytotoxicity against RAW 264.7 cells and appropriate for further biological activity study. Nonetheless, they did not inhibit NO production with 80-140 % NO.

For antioxidant activity, only compound **12** exhibited moderate antioxidant activities with IC_{50} 289 $\mu\text{g/mL}$.

Fourteen compounds (**1-3**, **5**, **8-10**, **17-18** and **35-39**) were tested on antihuman carbonic anhydrase II. Compounds **17** and **35** inhibited hCA II activity at the lowest concentration (0.032 μM). In addition, these two compounds showed higher activity than the positive control, acetazolamide. Furthermore, the inhibitory activity of compounds on human carbonic anhydrase enzyme was primarily tested under *in vivo* conditions.



REFERENCES

- [1] Wu, T.-S., Liou, M.-J., and Kuoh, C.-S. Coumarins of the Flowers of *Murraya paniculata*. Phytochemistry 28(1) (1989): 293-294.
- [2] Ito, C. and Furukawa, H. Constituents of *Murraya exotica* L. Structure Elucidation of New Coumarins. Chemical and Pharmaceutical Bulletin 35(10) (1987): 4277-4285.
- [3] Wu, I. Chondroprotective Evaluation and Docking Study of Two Natural Coumarins: Murrangatin and Murracarpin. Journal of Intercultural Ethnopharmacology 2(2) (2013): 91.
- [4] Kinoshita, T. and Firman, K. Myricetin 5,7,3',4',5'-pentamethyl Ether and Other Methylated Flavonoids from *Murraya paniculata*. Phytochemistry 45(1) (1997): 179-181.
- [5] Barik, B.R., Dey, A.K., Das, P.C., Chatterjee, A., and Shoolery, J.N. Coumarins of *Murraya exotica*-absolute Configuration of Auraptenol. Phytochemistry 22(3) (1983): 792-794.
- [6] Wu, T.-S. Coumarins from the Leaves of *Murraya paniculata*. Phytochemistry 27(7) (1988): 2357-2358.
- [7] Ito, C. and Furukawa, H. Two New Coumarins from *Murraya* plants. Chemical and Pharmaceutical Bulletin 37(3) (1989): 819-820.
- [8] Imai, F., Kinoshita, T., and Sankawa, U. Constituents of the Leaves of *Murraya paniculata* Collected in Taiwan. Chemical and Pharmaceutical Bulletin 37(2) (1989): 358-362.
- [9] Kinoshita, T. and Shimada, M. Isolation and Structure Elucidation of a New Prenylcoumarin from *Murraya paniculata* var. *omphalocarpa* (Rutaceae). Chemical and Pharmaceutical Bulletin 50(1) (2002): 118-120.
- [10] Saied, S., Nizami, S.S., and Anis, I. Two New Coumarins from *Murraya paniculata*. Journal of Asian Natural Products Research 10(5-6) (2008): 515-9.

- [11] Aziz, S.S.S.A., Sukari, M.A., Rahmani, M., Kitajima, M., Aimi, N., and Ahpandi, N.J. Coumarins from *Murraya paniculata* (Rutaceae). The Malaysian Journal of Analytical Sciences 14(1) (2010): 1-5.
- [12] Cuong, N.M., et al. Vasorelaxing Activity of Two Coumarins from *Murraya paniculata* Leaves. Biological and Pharmaceutical Bulletin 37(4) (2014): 694-697.
- [13] Wu, L., Li, P., Wang, X., Zhuang, Z., Farzaneh, F., Xu, R. Evaluation of Anti-inflammatory and Antinociceptive Activities of *Murraya exotica*. Pharmaceutical Biology 48(12) (2010): 1344-1353.
- [14] Davis, R.A., Vullo, D., Maresca, A., Supuran, C.T., and Poulsen, S.A. Natural Product Coumarins that Inhibit Human Carbonic Anhydrases. Bioorganic and Medicinal Chemistry 21(6) (2013): 1539-43.
- [15] Nguyen, C.M., Pham, K.N., Ho, D.V., Bui, T.H., Eun, K.J., and Kim, Y.H. The Soluble Epoxide Hydrolase sEH Inhibitory Activity of Coumarins from the Leaves of *Murraya paniculata*. Current Research in Biological and Pharmaceutical Sciences 3(3) (2014): 1-5.
- [16] Rodanant, P., Khetkam, P., Suksamram, A., and Kuvatanasuchati, J. Coumarins and Flavonoid from *Murraya paniculata* (L.) Jack: Antibacterial and Anti-inflammation Activity. Pakistan Journal of Pharmaceutical Sciences 28(6) (2015): 1947-1951.
- [17] Xu, G., et al. Isomeranzin Suppresses Inflammation by Inhibiting M1 Macrophage Polarization through the NF- κ B and ERK Pathway. International Immunopharmacology 38 (2016): 175–185.
- [18] You, C.-x., et al. Repellent Activity of Compounds from *Murraya alata* Drake against *Tribolium castaneum*. Industrial Crops and Products 95 (2017): 460-466.
- [19] Dai, Y.-G., Li, W.-S., Pedpradab, P., Liu, J.-J., Wu, J., and Shen, L. Thaixylomolins O–R: Four New Limonoids from the Trang Mangrove, *Xylocarpus moluccensis*. The Royal Society of Chemistry 6 (2016): 85978–85984.

- [20] Barik, B.R. and Kundu, A.B. A Cinnamic Acid Derivative and a Coumarin from *Murraya exotica*. Phytochemistry 26(12) (1987): 3319-3321.
- [21] Tjahjandarie, T.S., Saputri, R.D., and Tanjung, M. Oxygeranylated Coumarins from The Root of *Limonia accidisima* L. and Their DPPH Radical Scavenging Activity. Der Pharmacia Lettre 8(20) (2016): 33-36.
- [22] Tantishaiyakul, V., Pummangura, S., and Chaichantipyuth, C. Phebalosin from the Bark of *micromelum minutum*. Journal of Natural Products 49(1) (1986): 180-181.
- [23] Kinoshita, T., Jin-Bin, W., and Feng-Chi, H. The Isolation of a Prenylcoumarin of Chemotaxonomic Significance from *Murraya paniculata* var. omphalocarpa. Phytochemistry 43(1) (1996): 125-128.
- [24] Yu, B.C., Yang, M.C., Lee, K.H., Kim, K.H., Choi, S.U., and Lee, K.R. Two New Phenolic Constituents of *Humulus japonicus* and Their Cytotoxicity Test In Vitro. Archives of Pharmacal Research 30(11) (2007): 1471.
- [25] Li, X., Li, J., Wang, D., Wang, W., and *, Z.C. Chromone and Flavonoids from *Maackia amurensis*. Asina Journal Of Traditional Medicines 4(3) (2009): 98-103.
- [26] Ito, C., Furukawa, H., Ishii, H., Ishikawa, T., and Haginiwa, J. The Chemical Composition of *Murraya paniculata*. The Structure of Five New Coumarins and One New Alkaloid and the Stereochemistry of Murrangatin and Related Coumarins. Journal of the Chemical Society, Perkin Transactions 1 (7) (1990): 2047-2055.
- [27] Darmawan, A., Kosela, S., Kardono, L.B.S., and Syah, Y.M. Scopoletin, a Coumarin Derivative Compound Isolated from *Macaranga gigantifolia* Merr. Journal of Applied Pharmaceutical Science 2(12) (2012): 175-177.
- [28] Naseri, M., Monsef-Esfehani, H.R., Saeidnia, S., Dastan, D., and Gohari, A.R. Antioxidative Coumarins from the Roots of *Ferulago subvelutina*. Asian Journal of Chemistry 25(4) (2013): 1875-1878.
- [29] Joshi, P.C., Mandal, S., Das, P.C., and Chatterjee, A. Two Minor Coumarins of *Boenninghausenia albiflora*. Phytochemistry 32(2) (1993): 481-483.
- [30] Lv, H.N., et al. Anti-inflammatory Coumarin and Benzocoumarin Derivatives from *Murraya alata*. Journal of Natural Products 78(2) (2015): 279-85.

- [31] Xin-Jia, Y., *et al.* A New Biphenyl Neolignan from Leaves of *Patrinia villosa* (Thunb.) Juss. Juss. Phcog Mag 12(45) (2016): 1-3.
- [32] Deyama, T., Ikawa, T., Kitagawa, S., and Nishibe, S. The Constituents of *Eucommia ulmoides* OLIV. V. Isolation of Dihydroxydehydrodiconiferyl Alcohol Isomers and Phenolic Compounds. Chemical and Pharmaceutical Bulletin 35(5) (1987): 1785-1789.
- [33] Kinoshita, T., Wu, J.-B., and Ho, F.-C. Prenylcoumarins from *Murraya paniculata* var. *omphalocarpa* (Rutaceae) : The Absolute Configuration of Sibiricin, Mexoticin and Omphamurin. Chemical and Pharmaceutical Bulletin 44(6) (1996): 1208-1211.
- [34] Bohlmann, F. and Fritz, U. Neue Flavone aus *Heteromma simplicifolium*. Phytochemistry 18(6) (1979): 1080-1081.
- [35] Joshi, B.S. and Kamat, V.N. Isolation of 3,3',4',5,5',7,8-heptamethoxyflavone from *Murraya exotica*. Phytochemistry 9(4) (1970): 889.
- [36] Ferracin, R.J., das G.F. da Silva, M.F., Fernandes, J.B., and Vieira, P.C. Flavonoids from the Fruits of *Murraya paniculata*. Phytochemistry 47(3) (1998): 393-396.
- [37] Shin, H.J., Nam, J.-W., Yoon, U.J., Han, A.-R., and Seo, E.-K. Identification of Three New Flavonoids from the Peels of *Citrus unshiu*. Helvetica Chimica Acta 95(2) (2012): 240-245.
- [38] Passador, E.A.P., das G.F. da Silva, M.F., Fo, E.R., Fernandes, J.B., Vieira, P.C., and Pirani, J.R. A Pyrano Chalcone and a Flavanone from *Neoraputia magnifica*. Phytochemistry 45(7) (1997): 1533-1537.
- [39] Ito, C. and Furukawa, H. Three New Coumarins from Leaves of *Murraya paniculata*. Heterocycles 26(11) (1987): 2959-2962.
- [40] Nour, A.M.M., Khalid, S.A., Kaiser, M., Brun, R., Abdalla, W.I.E., and Schmidt, T.J. The Antiprotozoal Activity of Methylated Flavonoids from *Ageratum conyzoides* L. Journal of Ethnopharmacology 129(1) (2010): 127-130.
- [41] Ito, C., *et al.* Anti-tumor-promoting Effects of 8-substituted 7-methoxycoumarins on Epstein-Barr Virus Activation Assay. Cancer Letters 138(1-2) (1999): 87-92.

- [42] Missau, F.C., et al. Phebalosin and Its Structural Modifications are Active against the Pathogenic Fungal Causing Paracoccidioidomycosis. Medicinal chemistry 4(8) (2014): 581-587
- [43] Janneta, H.B., H-Skhirib, F., Mighria, Z., Simmonds, M.S.J., and Blaney, W.M. Antifeedant Activity of Plant Extracts and of New Natural Diglyceride Compounds Isolated from *Ajuga pseudoiva* Leaves against *Spodoptera littoralis* Larvae. Industrial Crops and Products 14(3) (2001): 213-222.
- [44] Koul, O. Insect Antifeedants. CRC Press, Boca Raton, FL. (2005).
- [45] Susurluk, H., Çalışkan, Z., Gürkan, O., Kırmızıgül, S., and Gören, N. Antifeedant Activity of Some *Tanacetum* species and Bioassay Guided Isolation of the Secondary Metabolites of *Tanacetum cadmeum* ssp. *cadmeum* (Compositae). Industrial Crops and Products 26(2) (2007): 220-228.
- [46] Zapata, N., Budia, F., Viñuela, E., and Medina, P. Antifeedant and Growth Inhibitory Effects of Extracts and Dimeranes of *Drimys winteri* Stem Bark against *Spodoptera littoralis* (Lep., Noctuidae). Industrial Crops and Products 30(1) (2009): 119-125.
- [47] Arivoli, S. and Tennyson, S. Screening of Plant Extracts for Oviposition Activity against *Spodoptera litura* (Fab). (Lepidoptera: Noctuidae). International Journal of Fauna and Biological Studies 1(1) (2013): 20-24.
- [48] Papachristos, D.P., Karamanoli, K.I., Stamopoulos, D.C., and Menkissoglou-Spiroudi, U. The Relationship between the Chemical Composition of Three Essential Oils and Their Insecticidal Activity against *Acanthoscelides obtectus* (Say). Pest Management Science 60(5) (2004): 514-520.
- [49] Carpinella, M.C., Defago, M.T., Valladares, G., and Palacios, S.M. Antifeedant and Insecticide Properties of a Limonoid from *Melia azedarach* (Meliaceae) with Potential Use for Pest Management. Journal of Agricultural and Food Chemistry 51(2) (2003): 369-374.
- [50] Sharma, R., Negi, D.S., Shiu, W.K.P., and Gibbons, S. Characterization of an Insecticidal Coumarin from *Boenninghausenia albiflora*. Phytotherapy Research 20(7) (2006): 607-609.

- [51] Mollah, J.U. and Islam, W. Toxicity of *Murraya paniculata* (L.) Jack Leaf-derived Materials against *Callosobruchus maculatus* (F.) (coleoptera: bruchidae). Pakistan Entomologist 30(1) (2008): 61-64.
- [52] Zheng, W.F., Tan, R.X., Yang, L., Liu, Z.L. Two Flavones from *Artemisia giraldii* and Their Antimicrobial Activity. Planta Medica 62(2) (1996): 160-162.
- [53] Keating, G.J., and O'Kennedy, R. In: O'Kennedy R, Thornes RD, Editors. The Chemistry and Occurrence of Coumarins. West Sussex, England: John Wiley & Sons (1997): 23-64.
- [54] Wu, J., Liu, K., and Shi, X. The Anti-inflammatory Activity of Several Flavonoids Isolated from *Murraya paniculata* on Murine Macrophage Cell Line and Gastric Epithelial Cell (GES-1). Pharmaceutical Biology 54(5) (2016): 868-881.
- [55] Bansal, Y., Sethi, P., and Bansal, G. Coumarin: a Potential Nucleus for Anti-inflammatory Molecules. Medicinal Chemistry Research 22(7) (2013): 3049–3060.
- [56] Hadjipavlou-Litina, D.J., and Litinas KE, K.C. The Antiinflammatory Effect of Coumarin and Its Derivatives. Current Medicinal Chemistry 6(6) (2007): 293–306.
- [57] Naresh, s., Narinder, k., and Rashmi, A. Isolation and Characterization of *Murraya paniculata* Ethanol Seed Extract for Their Antioxidant Components. International Research Journal of Pharmacy 5(9) (2014): 690-694.
- [58] Wang, Z.C., et al. Sulfonamides Containing Coumarin Moieties Selectively and Potently Inhibit Carbonic Anhydrases II and IX: Design, Synthesis, Inhibitory Activity and 3D-QSAR Analysis. European Journal of Medicinal Chemistry 66 (2013): 1-11.



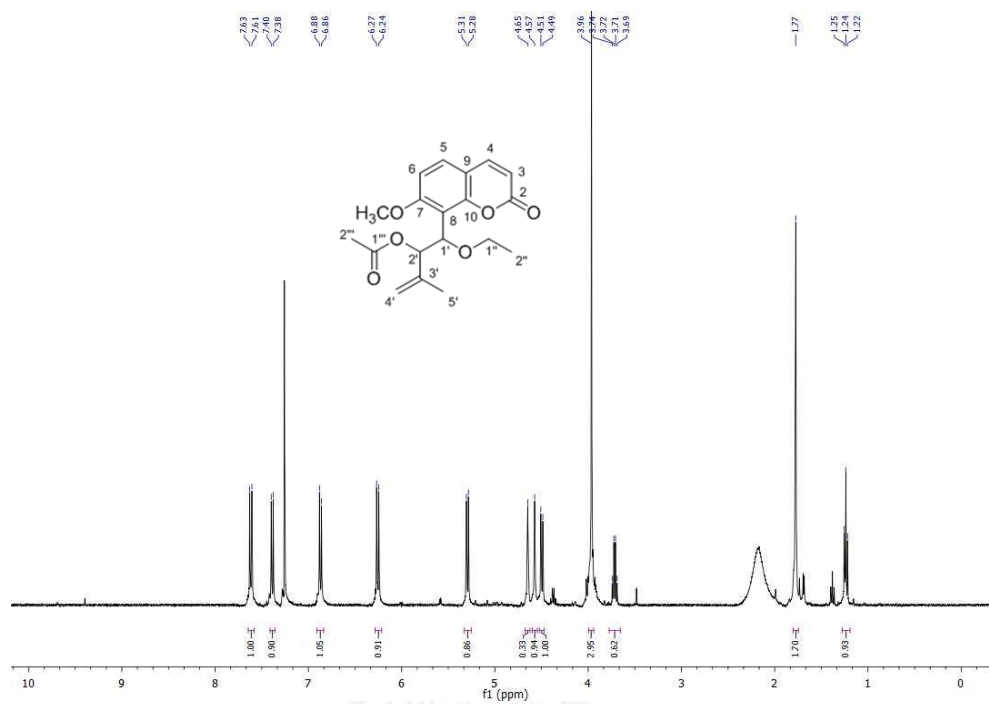


Figure A-1 The ^1H NMR spectrum (CDCl_3) of compound **1**

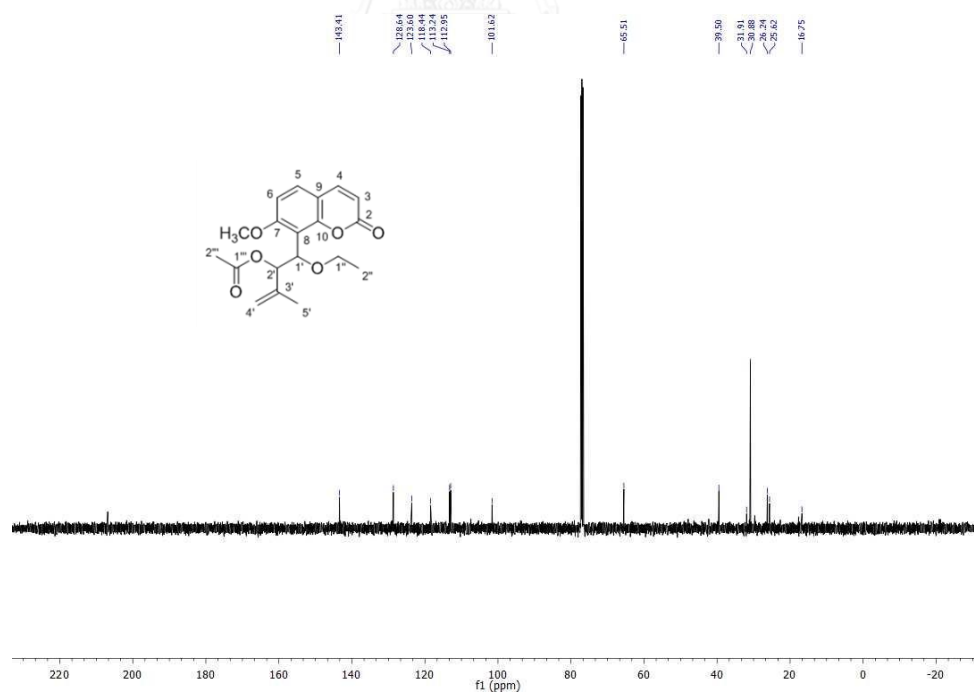


Figure A-2 The ^{13}C NMR spectrum (CDCl_3) of compound **1**

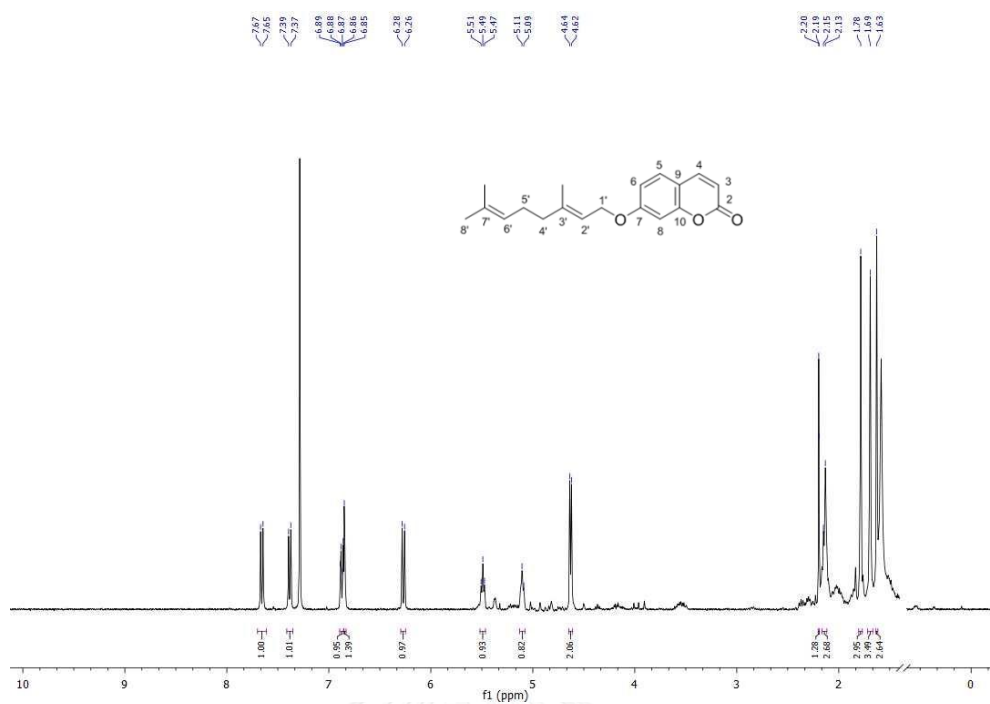


Figure A-3 The ^1H NMR spectrum (CDCl₃) of compound 2

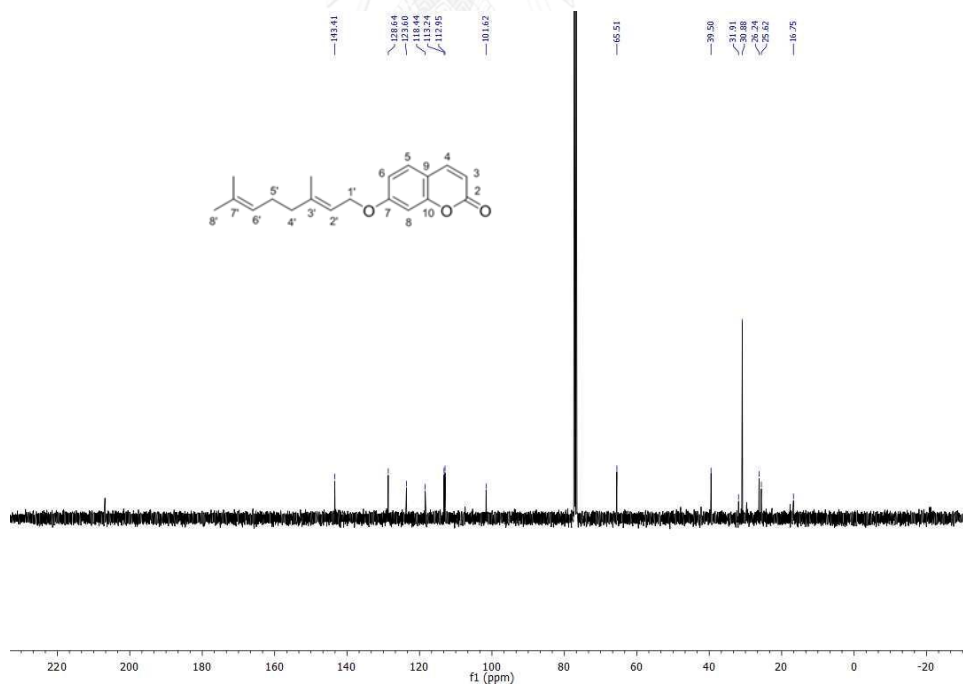


Figure A-4 The ^{13}C NMR spectrum (CDCl₃) of compound 2

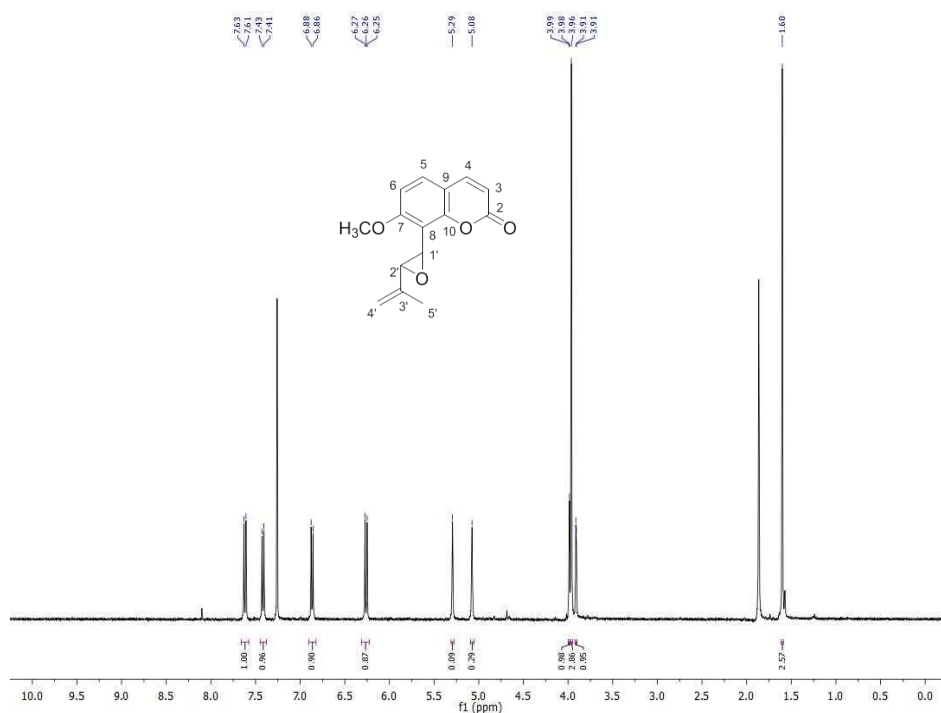


Figure A-5 The ¹H NMR spectrum (CDCl₃) of compound 3

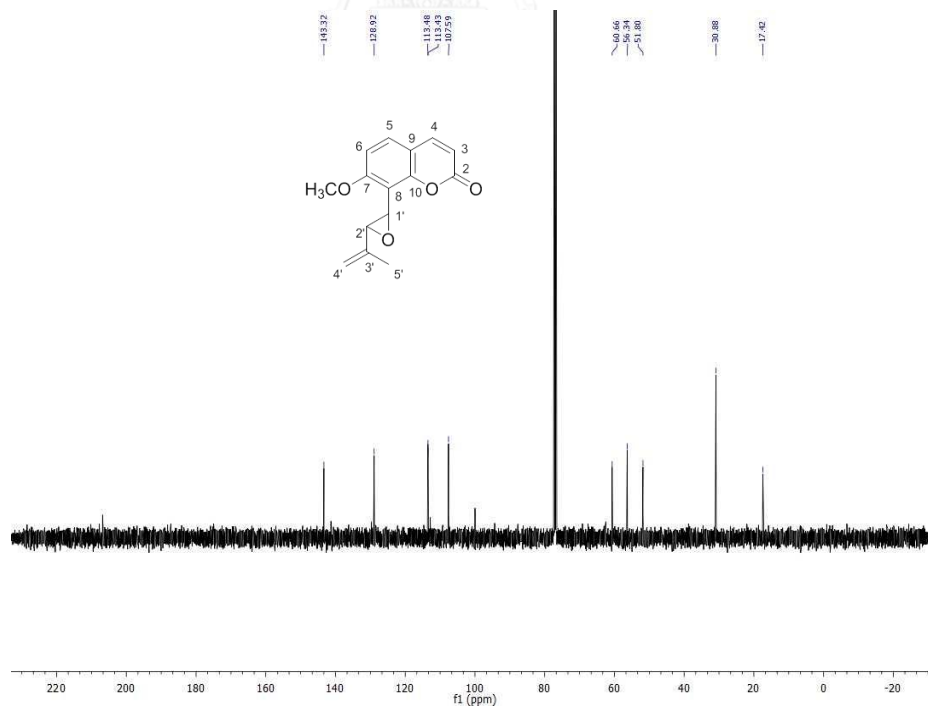


Figure A-6 The ¹³C NMR spectrum (CDCl₃) of compound 3

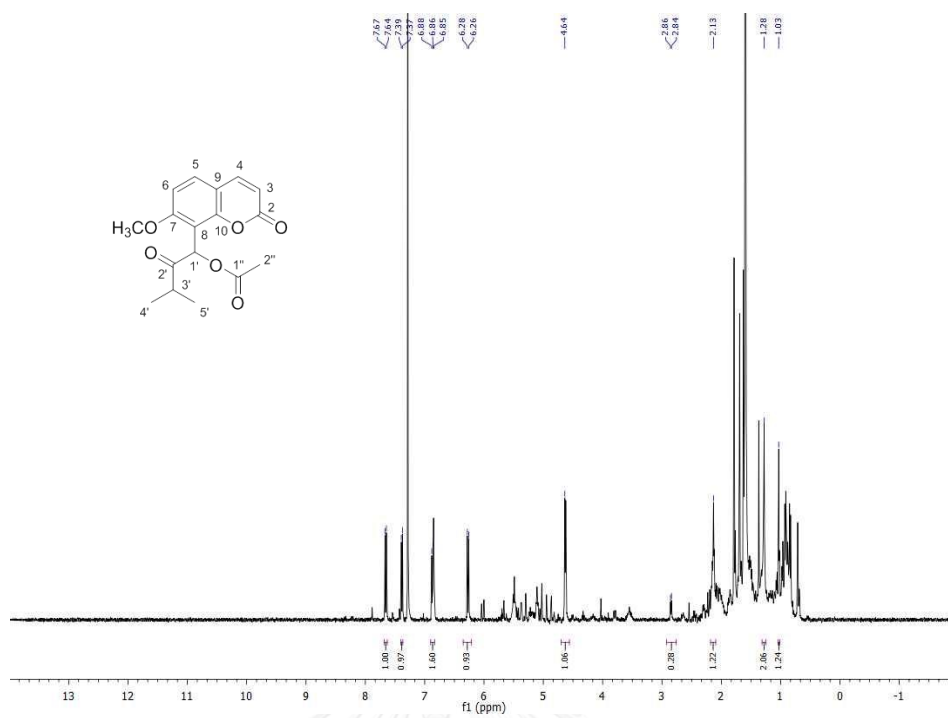


Figure A-7 The ^1H NMR spectrum (CDCl₃) of compound 4

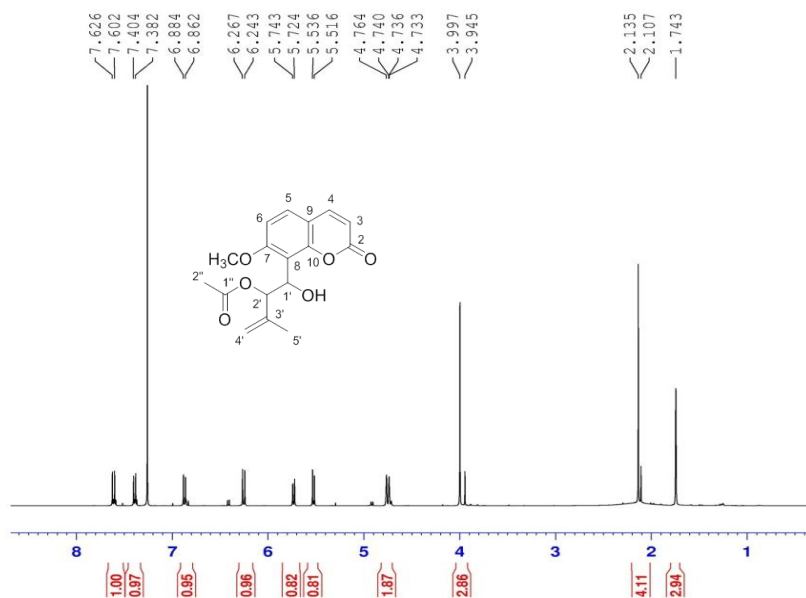


Figure A-8 The ^1H NMR spectrum (CDCl₃) of compound 5

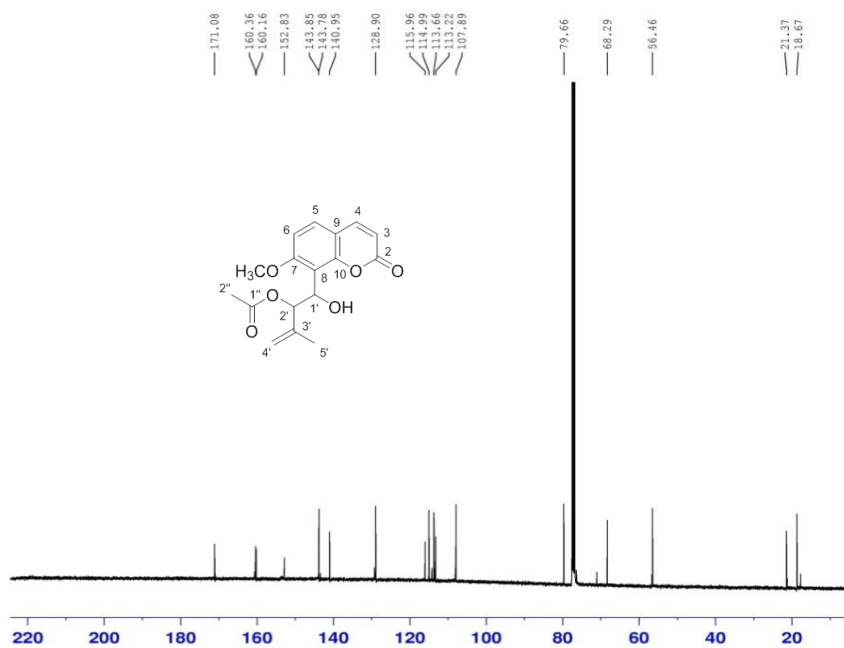


Figure A-9 The ^{13}C NMR spectrum (CDCl₃) of compound 5

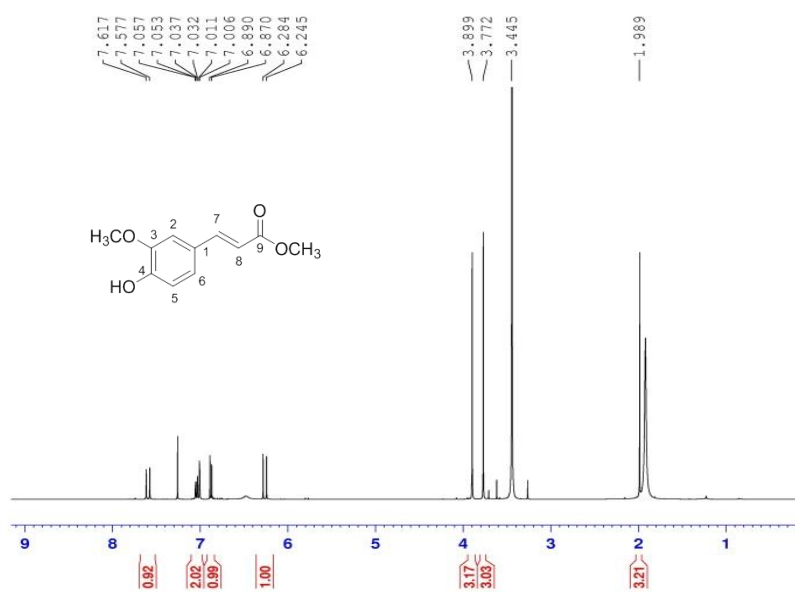


Figure A-10 The ^1H NMR spectrum (CDCl₃) of compound 6

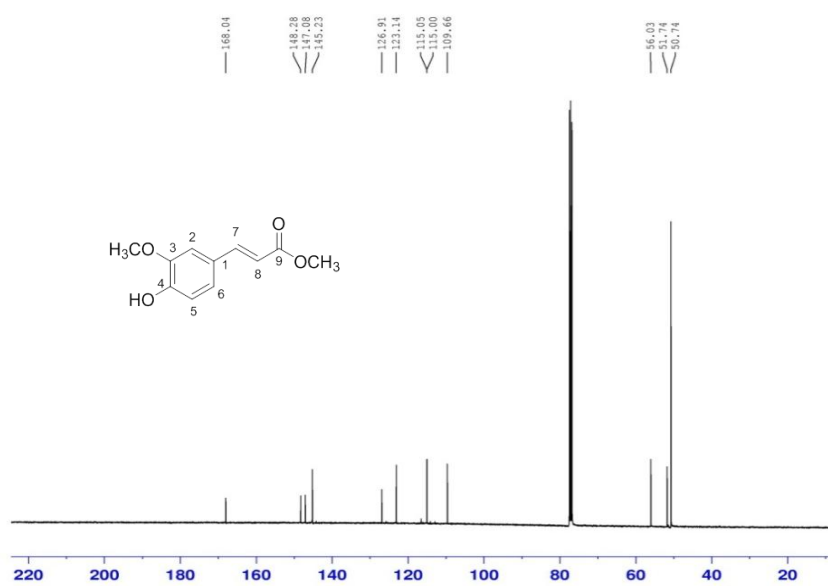


Figure A-11 The ^{13}C NMR spectrum (CDCl₃) of compound 6

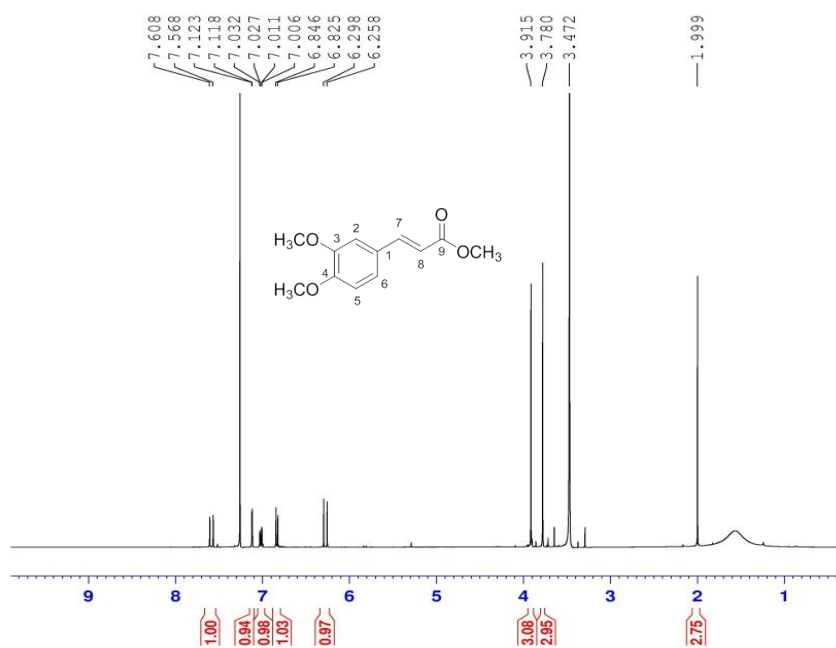


Figure A-12 The ^1H NMR spectrum (CDCl₃) of compound 7

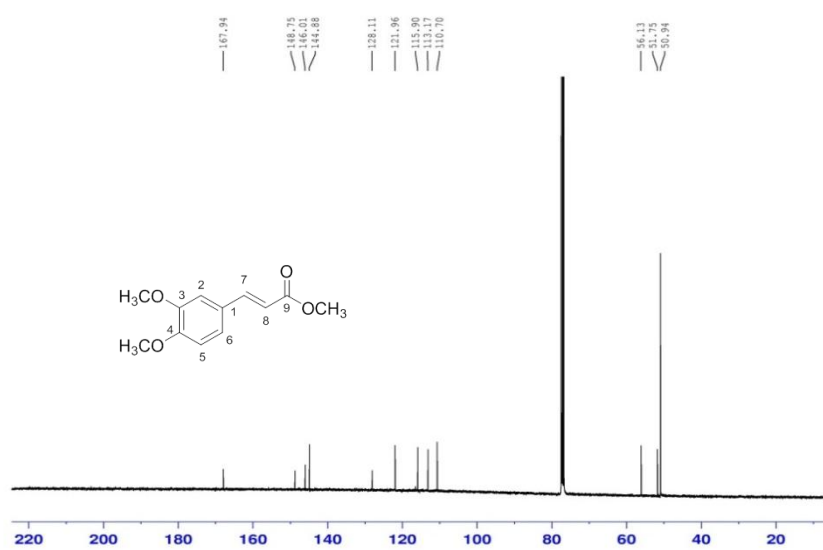


Figure A-13 The ^{13}C NMR spectrum (CDCl₃) of compound 7

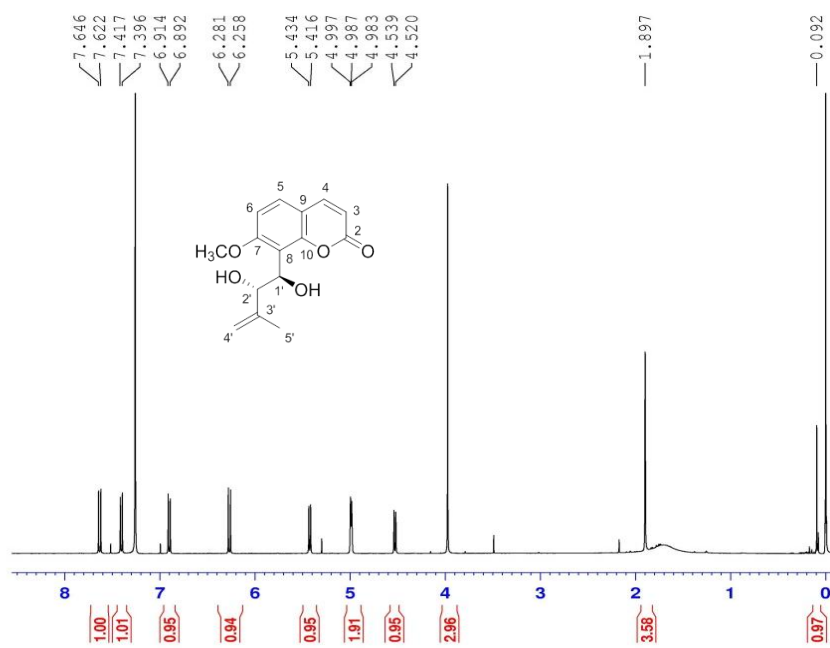


Figure A-14 The ^1H NMR spectrum (CDCl₃) of compound 8

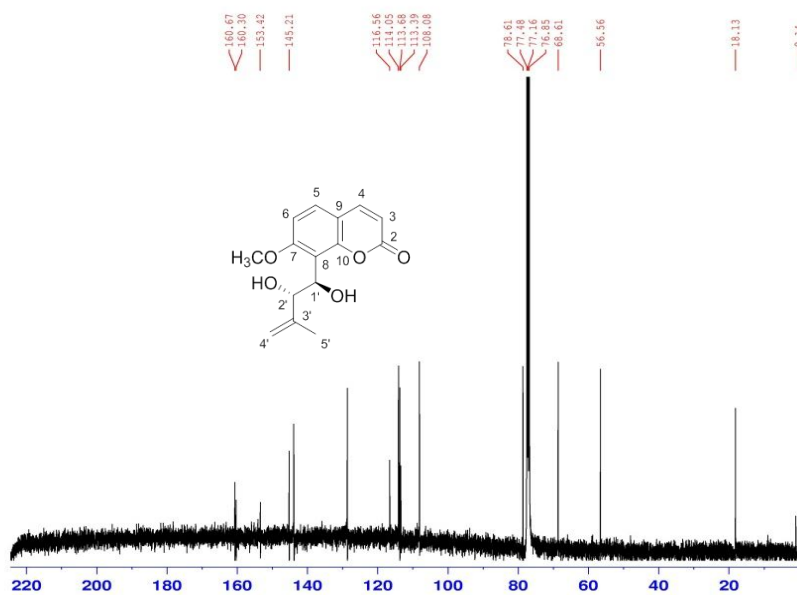


Figure A-15 The ^{13}C NMR spectrum (CDCl₃) of compound 8

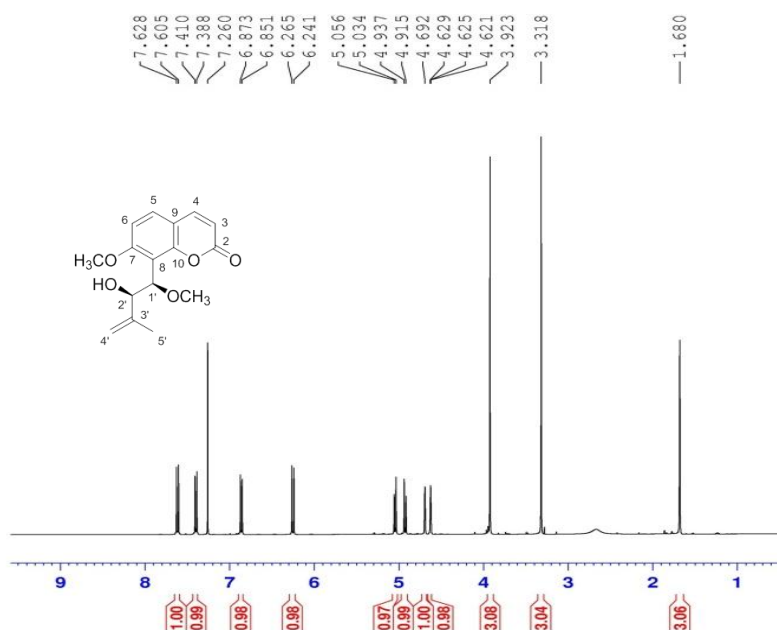


Figure A-16 The ¹H NMR spectrum (CDCl₃) of compound 9

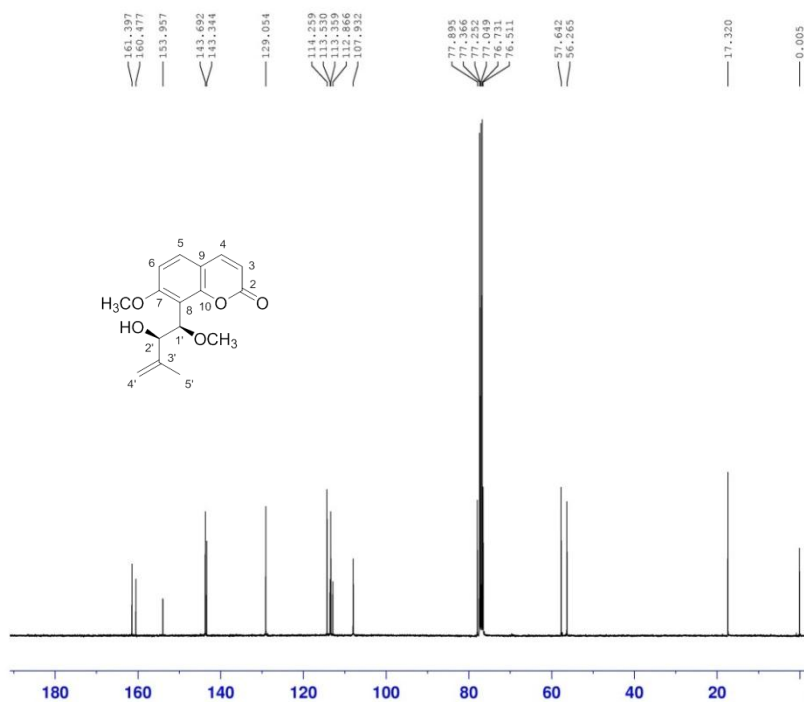


Figure A-17 The ¹³C NMR spectrum (CDCl₃) of compound 9

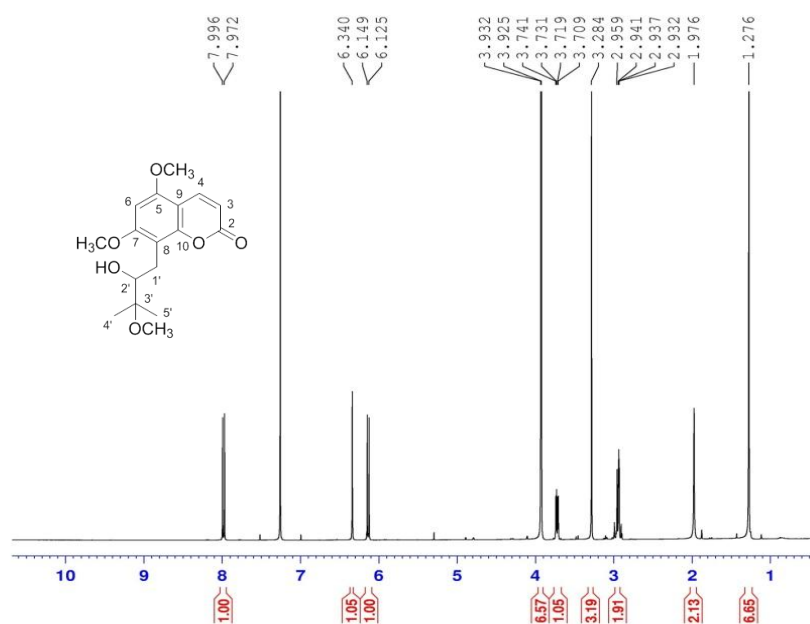


Figure A-18 The ^1H NMR spectrum (CDCl_3) of compound 10

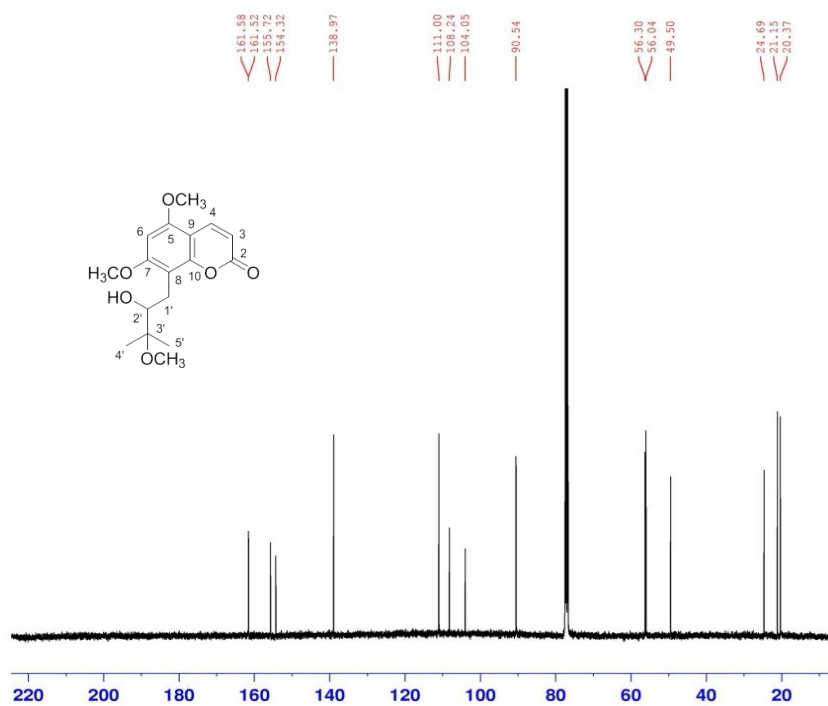


Figure A-19 The ^{13}C NMR spectrum (CDCl_3) of compound 10

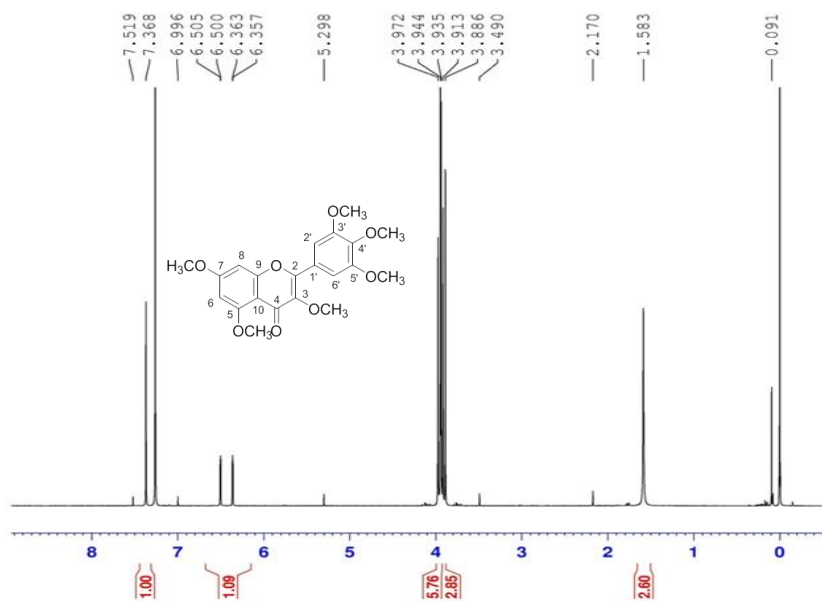


Figure A-20 The ^1H NMR spectrum (CDCl₃) of compound 11

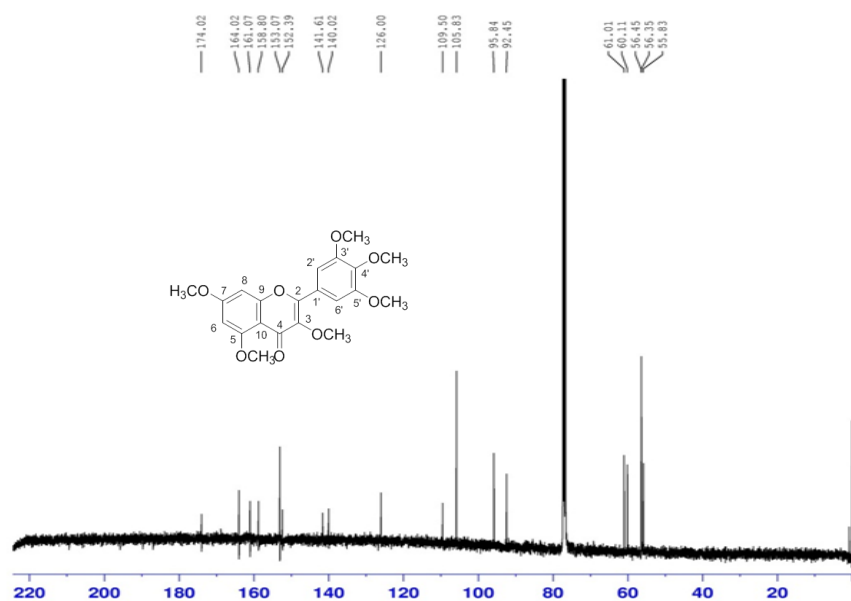


Figure A-21 The ^{13}C NMR spectrum (CDCl₃) of compound 11

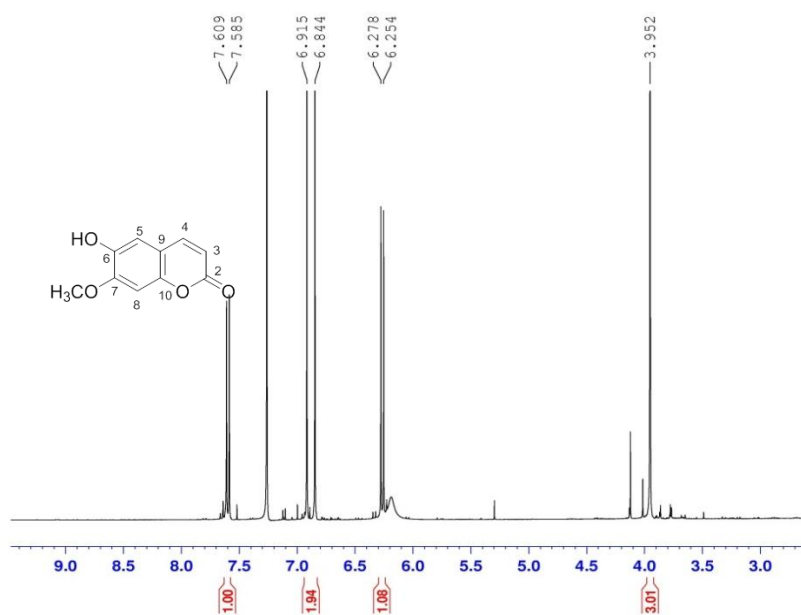


Figure A-22 The ^1H NMR spectrum (CDCl_3) of compound 12

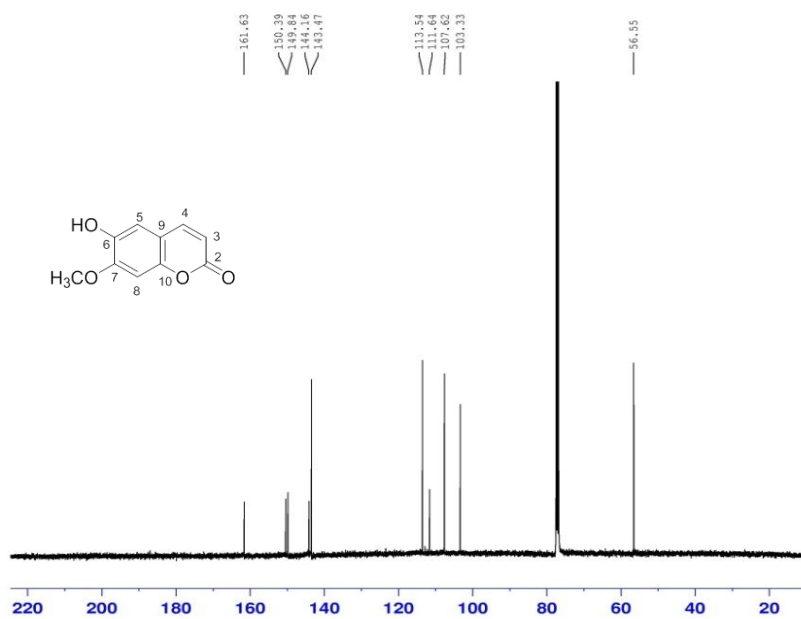


Figure A-23 The ^{13}C NMR spectrum (CDCl_3) of compound 12

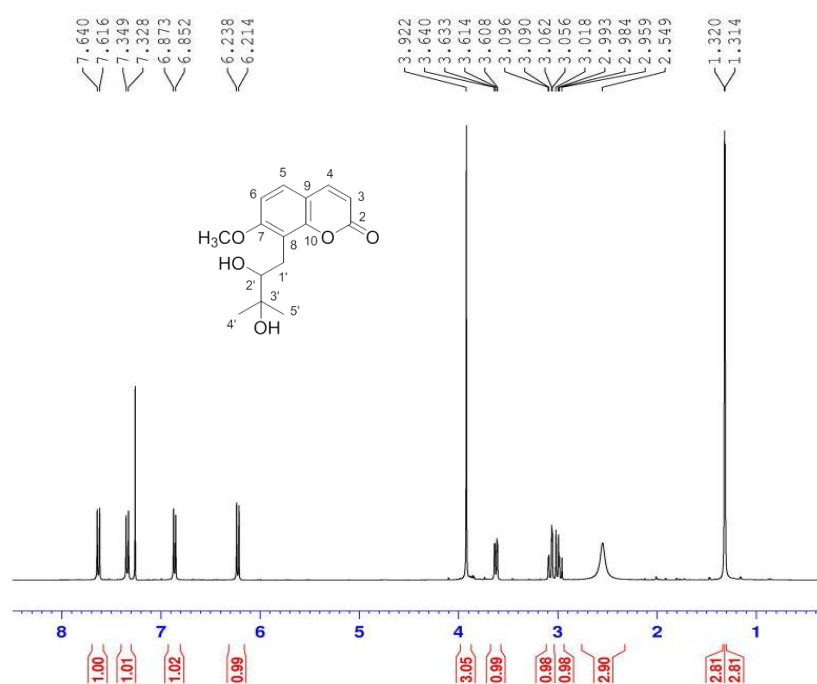


Figure A-24 The ¹H NMR spectrum (CDCl₃) of compound 13

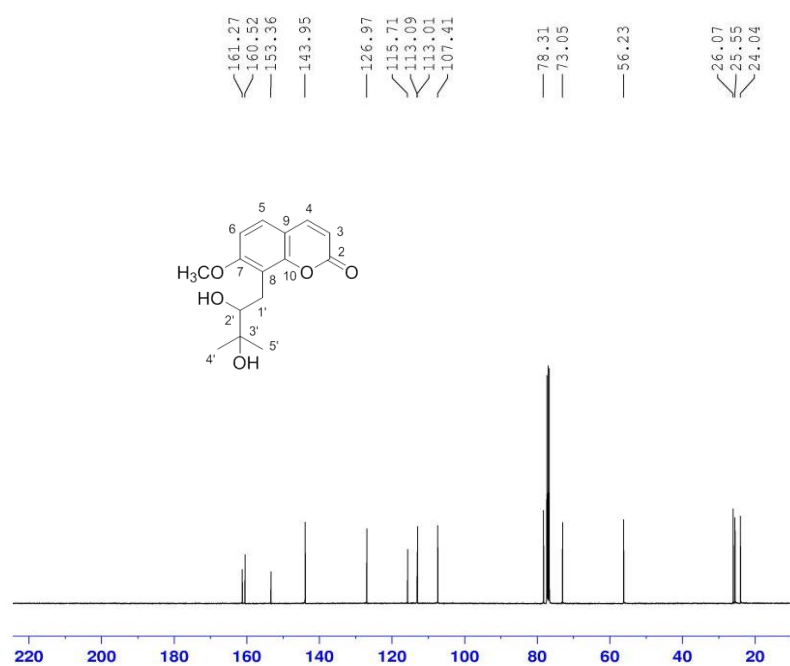


Figure A-25 The ¹³C NMR spectrum (CDCl₃) of compound 13

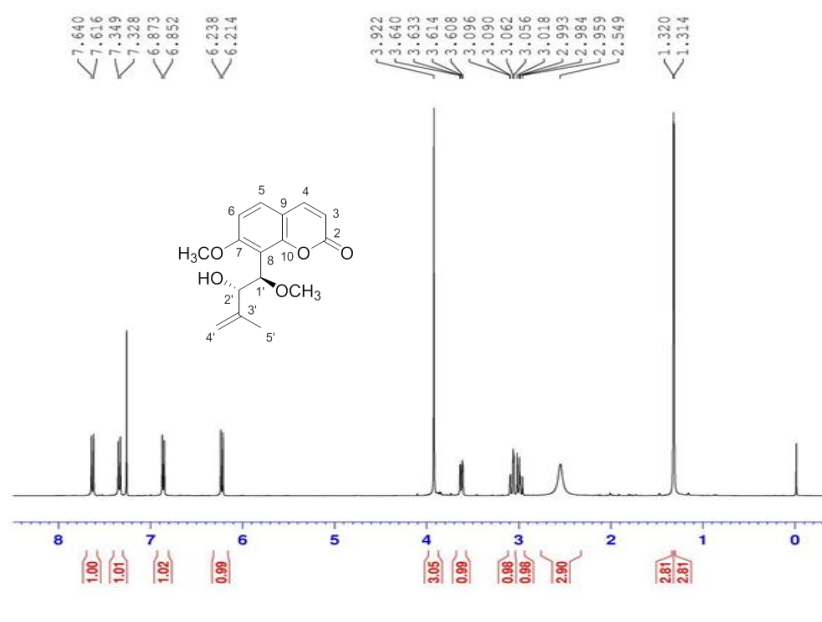


Figure A-26 The ¹H NMR spectrum (CDCl₃) of compound 14

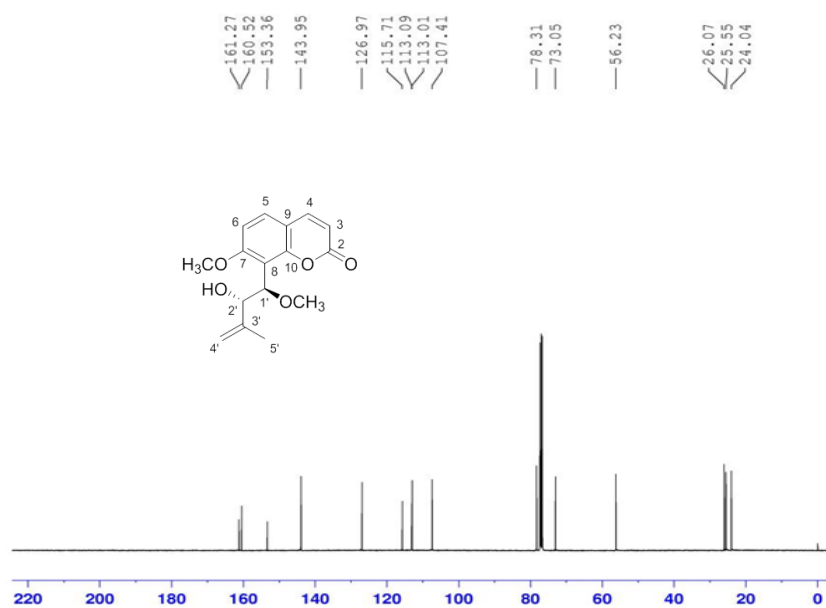


Figure A-27 The ¹³C NMR spectrum (CDCl₃) of compound 14

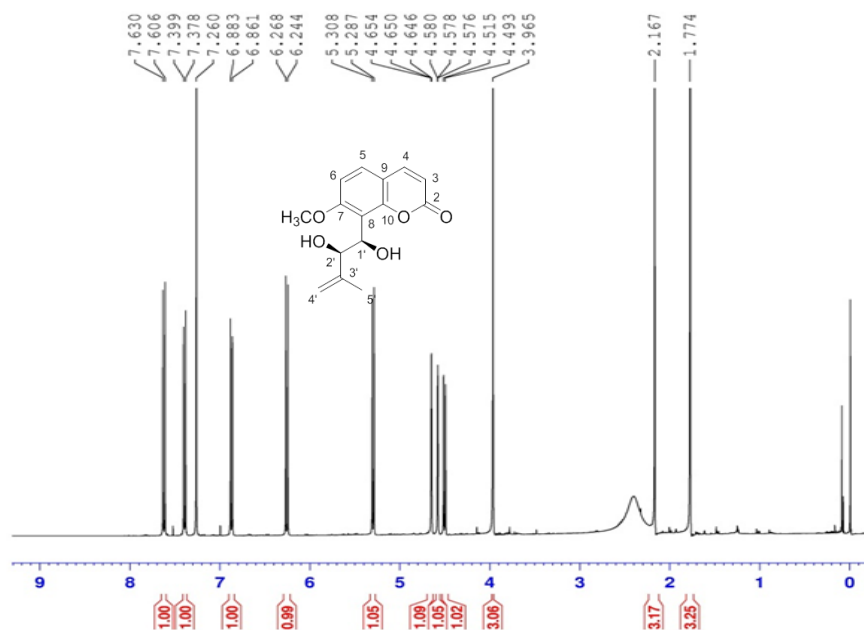


Figure A-28 The ¹H NMR spectrum (CDCl₃) of compound 15

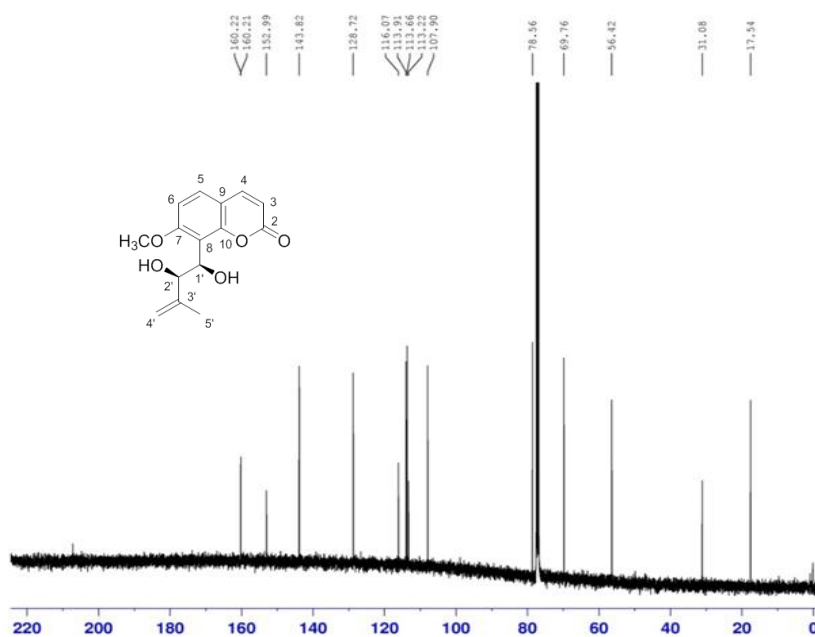


Figure A-29 The ¹³C NMR spectrum (CDCl₃) of compound 15

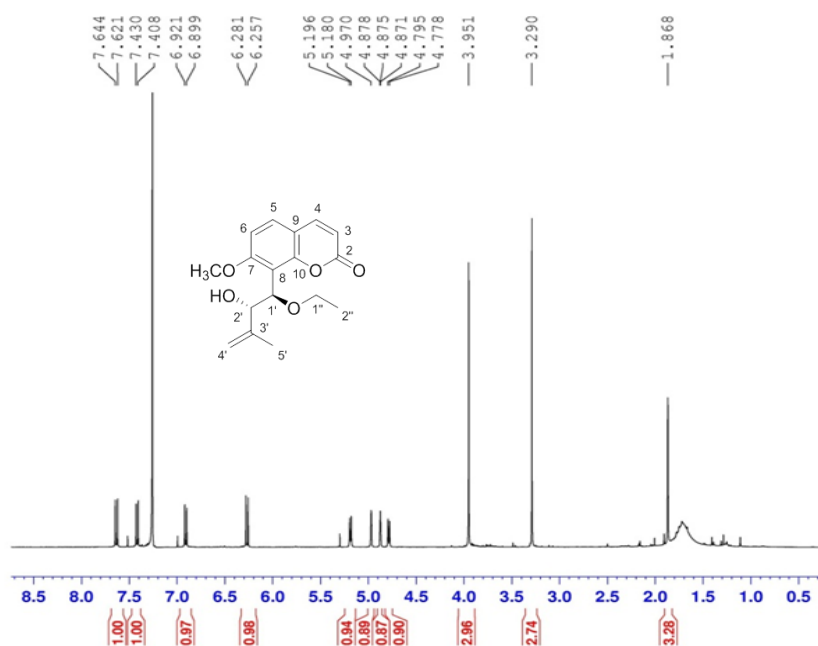


Figure A-30 The ^1H NMR spectrum (CDCl₃) of compound 16

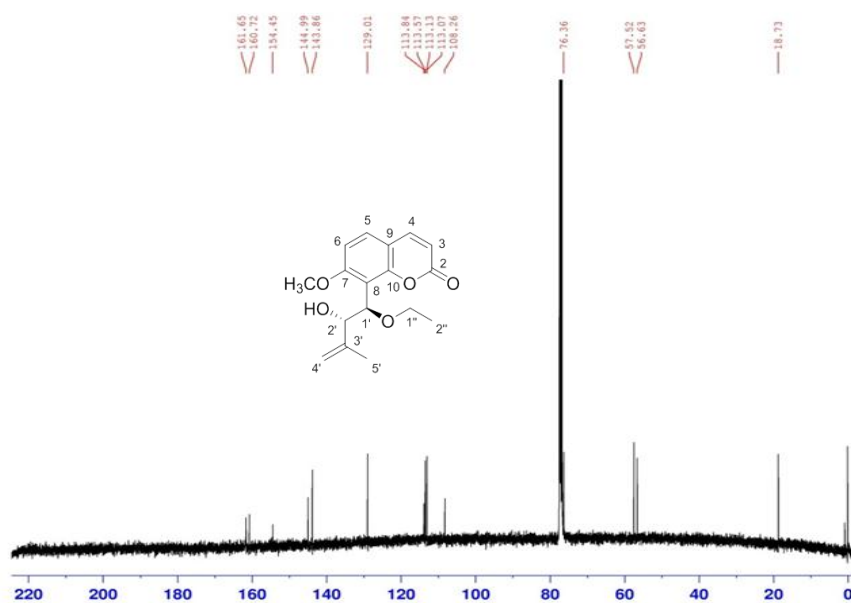
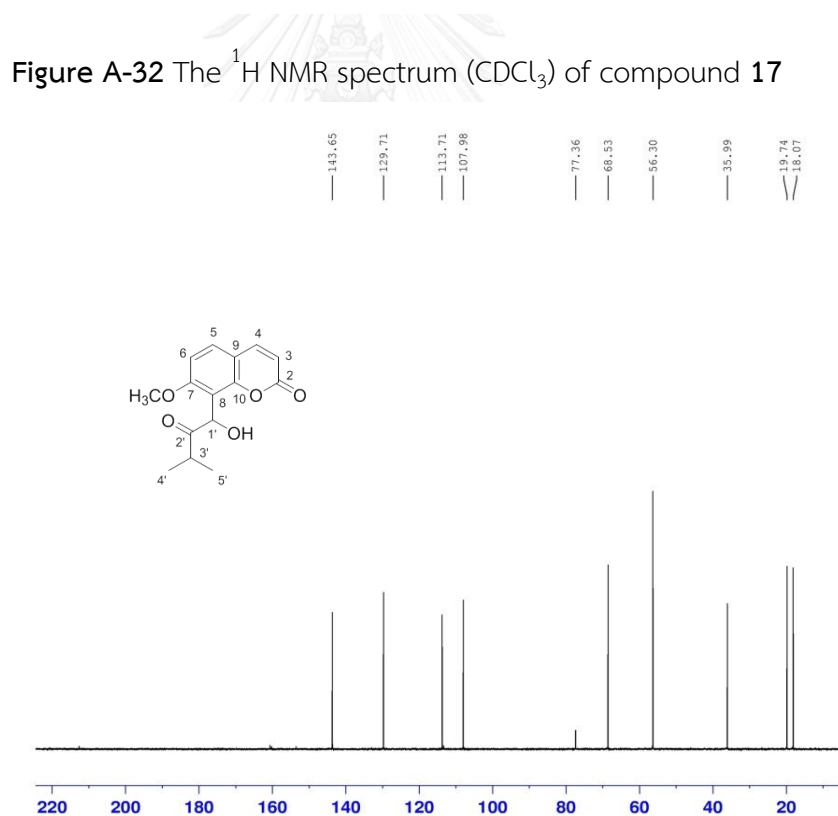
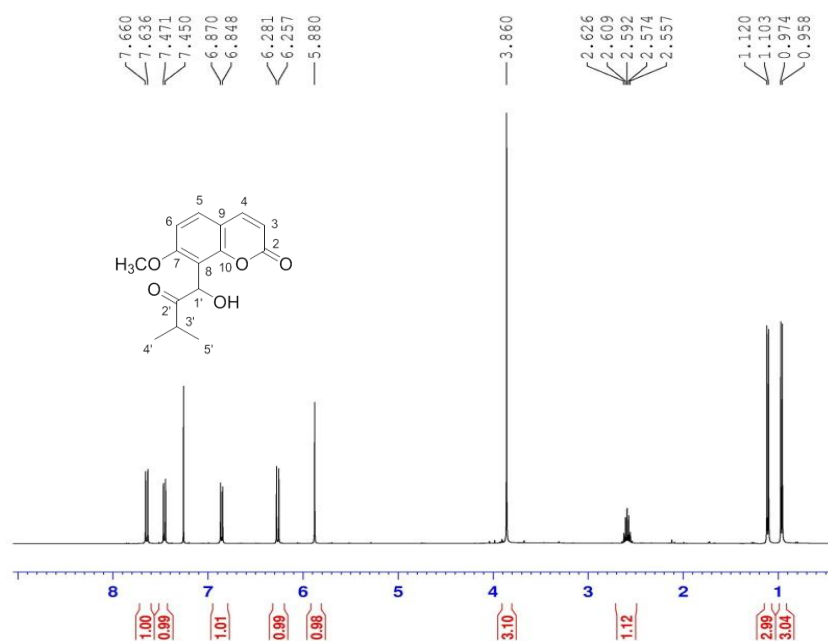


Figure A-31 The ^{13}C NMR spectrum (CDCl₃) of compound 16



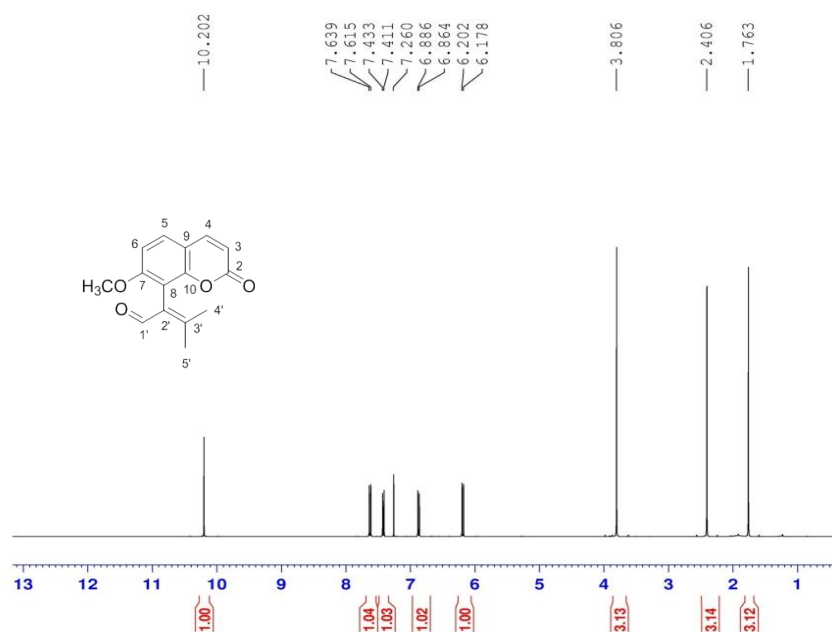


Figure A-34 The ^1H NMR spectrum (CDCl₃) of compound 18

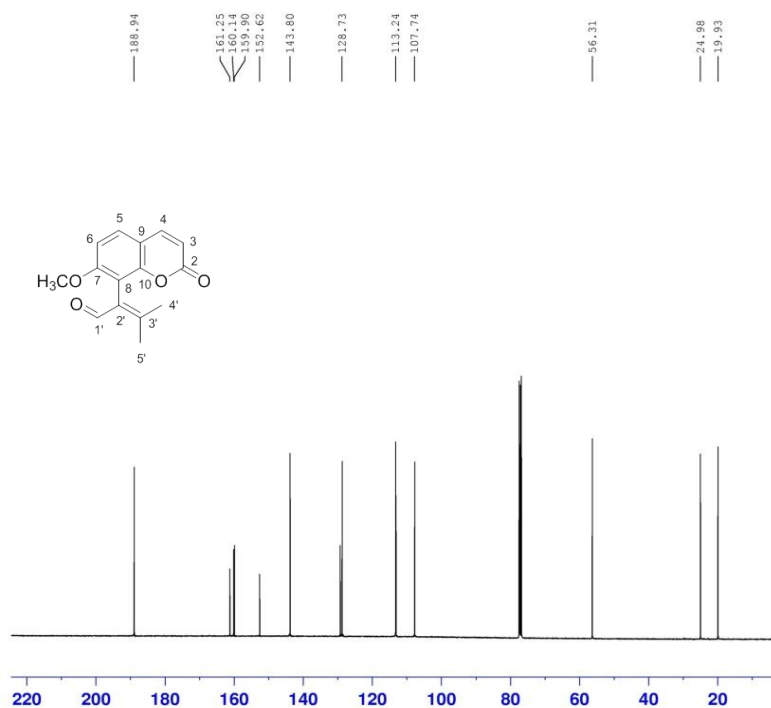


Figure A-35 The ^{13}C NMR spectrum (CDCl₃) of compound 18

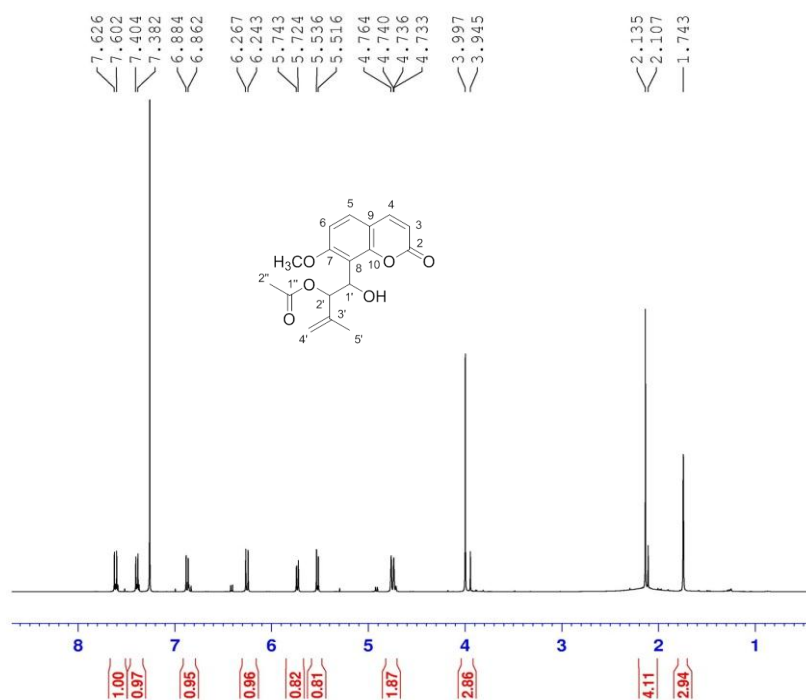


Figure A-36 The ¹H NMR spectrum (CDCl₃) of compound 19

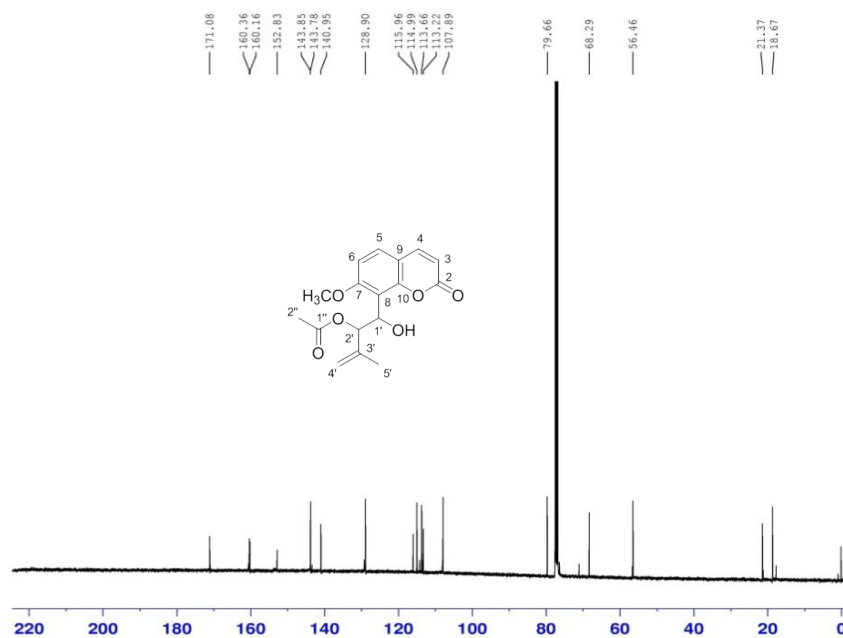


Figure A-37 The ¹³C NMR spectrum (CDCl₃) of compound 19

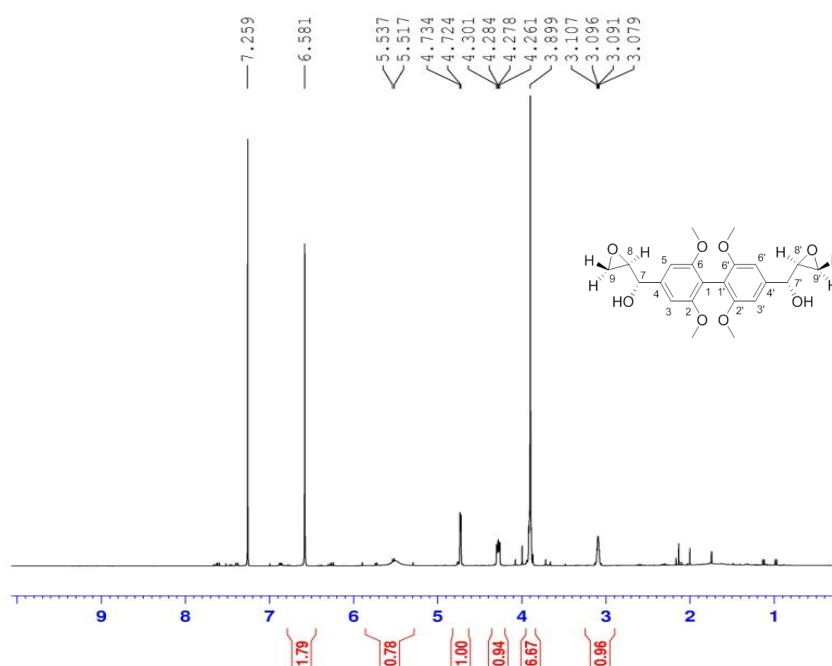


Figure A-38 The ¹H NMR spectrum (CDCl₃) of compound 20

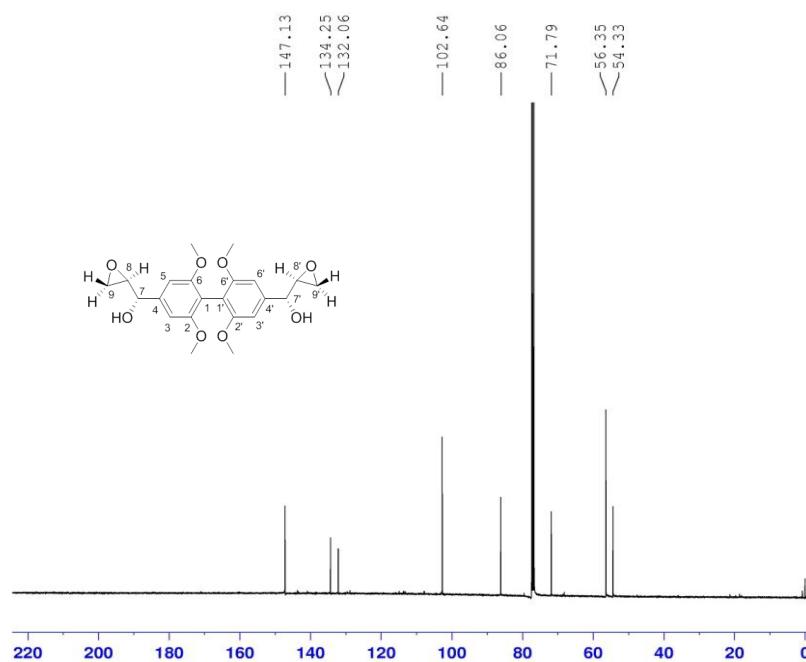


Figure A-39 The ¹³C NMR spectrum (CDCl₃) of compound 20

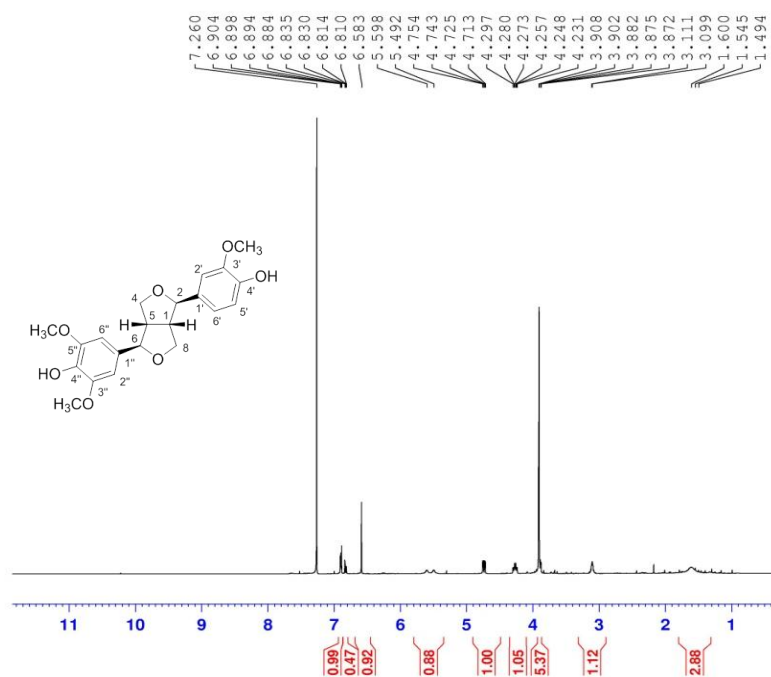


Figure A-40 The $^1\text{H NMR}$ spectrum (CDCl₃) of compound 21

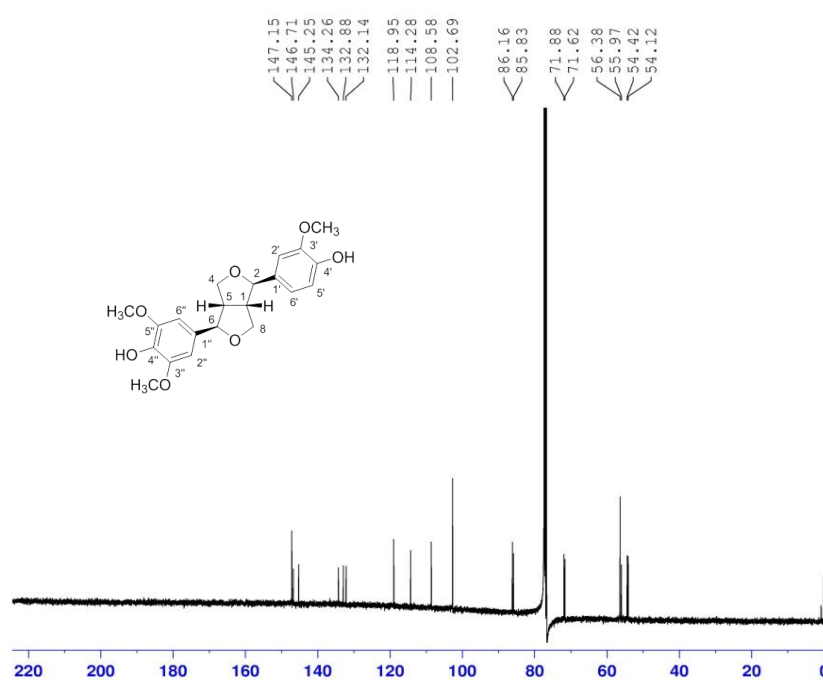


Figure A-41 The $^{13}\text{C NMR}$ spectrum (CDCl₃) of compound 21

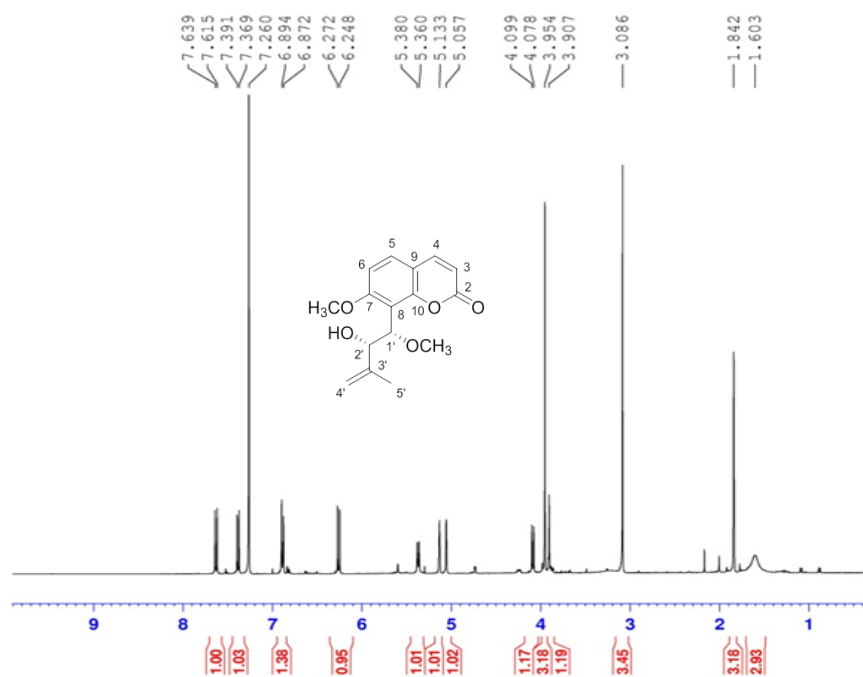


Figure A-42 The ¹H NMR spectrum (CDCl₃) of compound 22

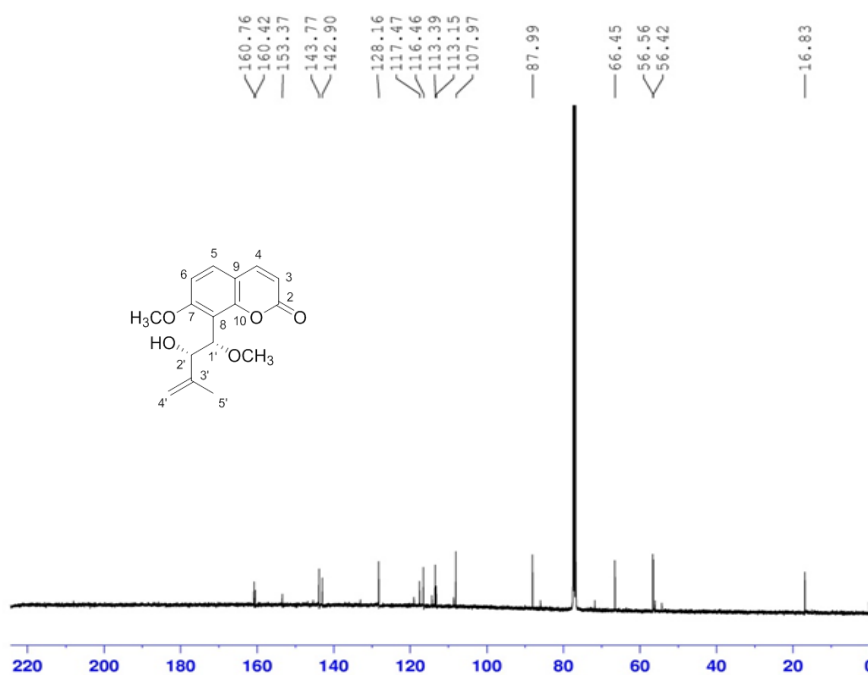


Figure A-43 The ¹³C NMR spectrum (CDCl₃) of compound 22

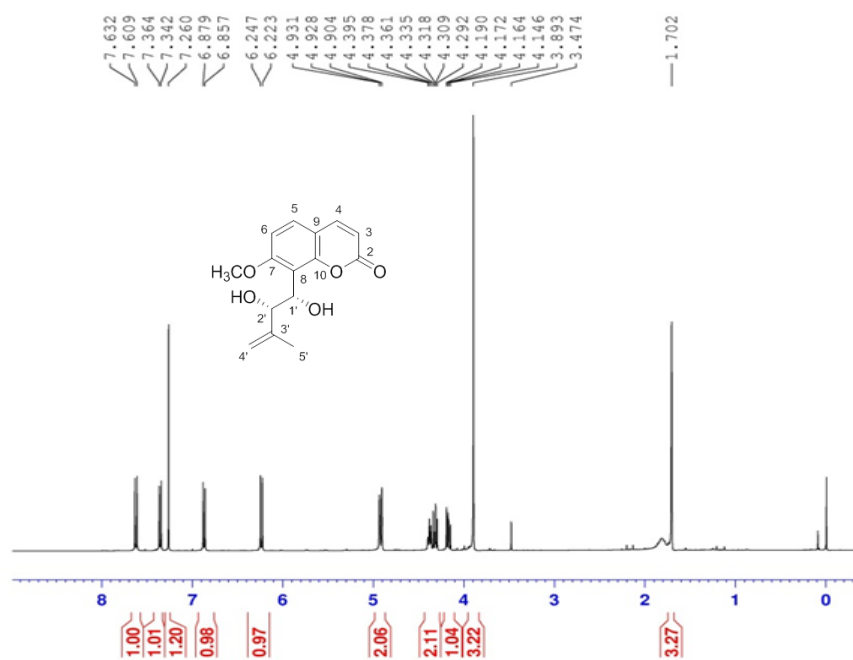


Figure A-44 The ¹H NMR spectrum (CDCl₃) of compound 23

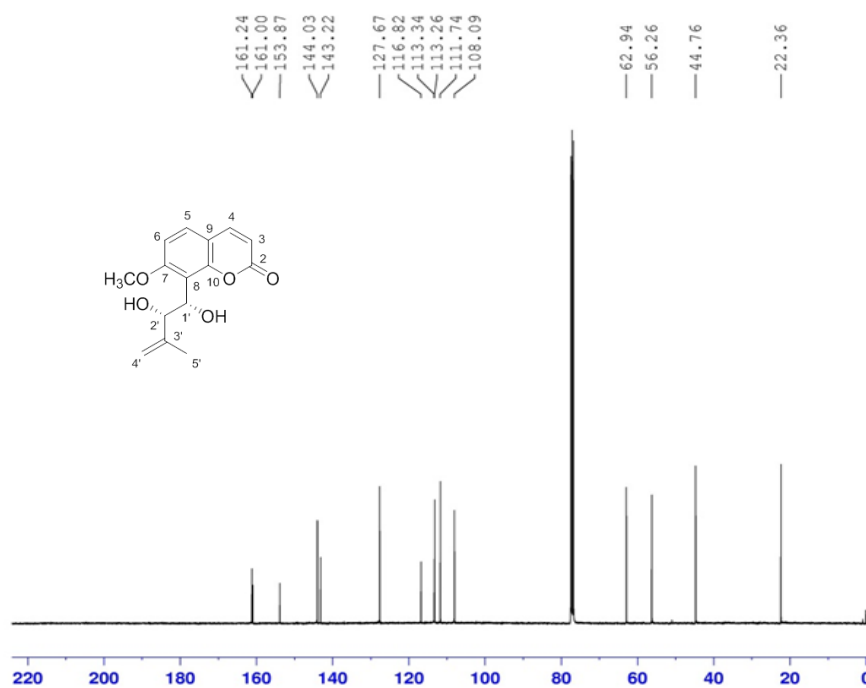


Figure A-45 The ¹³C NMR spectrum (CDCl₃) of compound 23

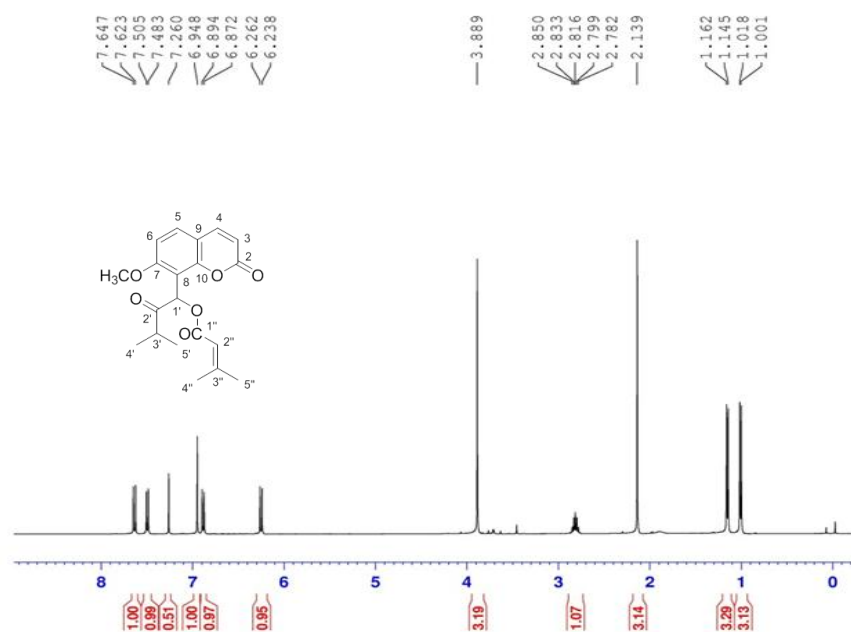


Figure A-46 The ¹H NMR spectrum (CDCl₃) of compound **24**

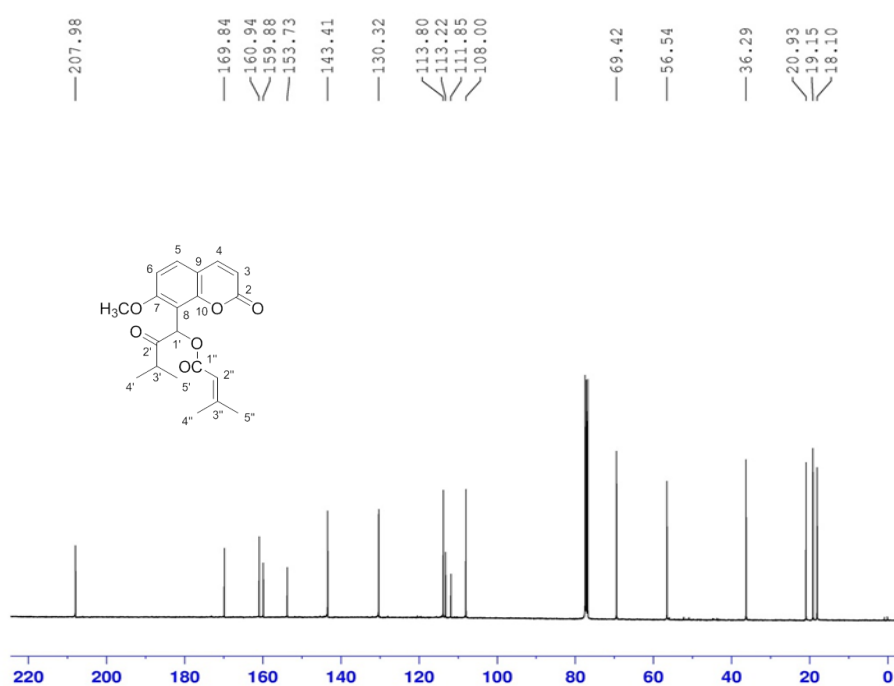


Figure A-47 The ¹³C NMR spectrum (CDCl₃) of compound **24**

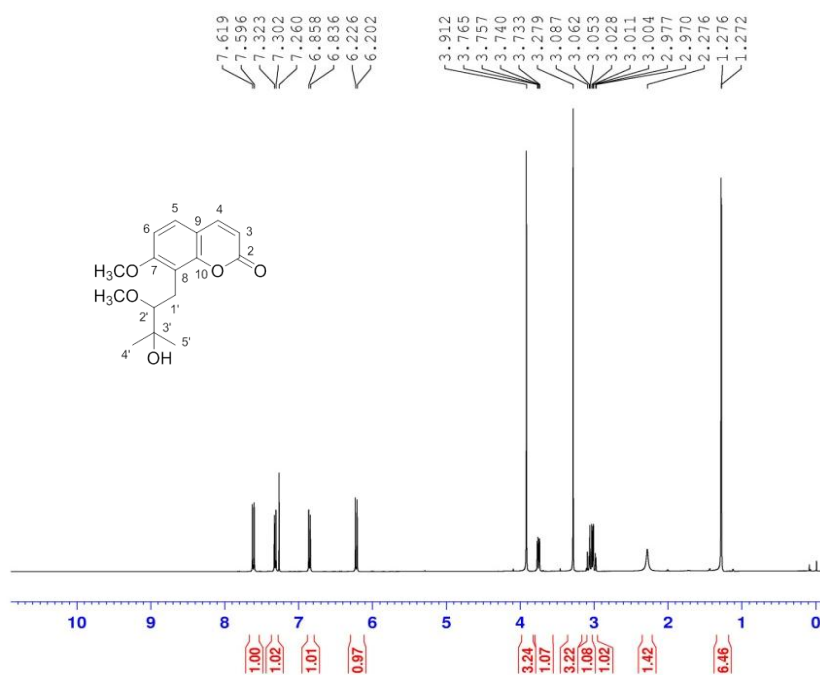


Figure A-48 The ¹H NMR spectrum (CDCl₃) of compound 25

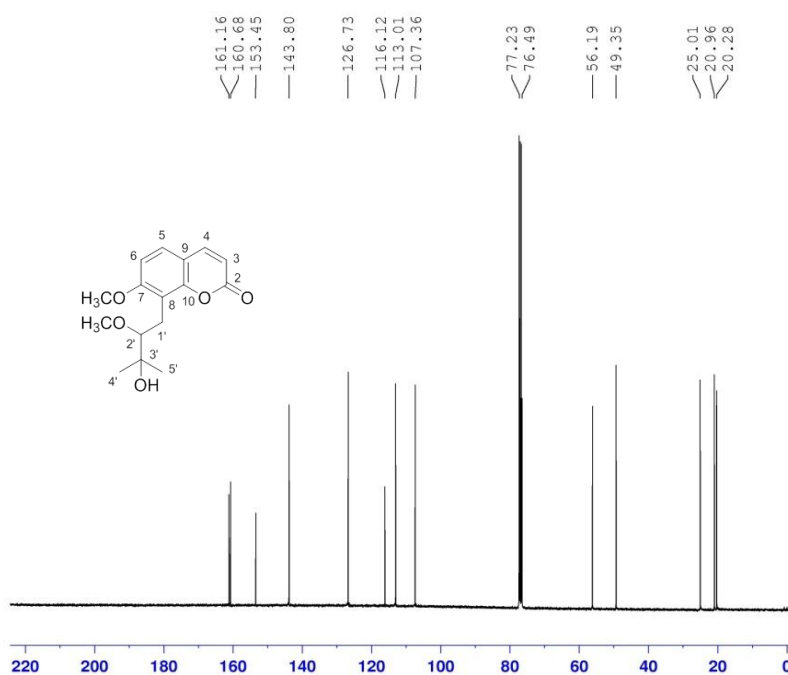


Figure A-49 The ¹³C NMR spectrum (CDCl₃) of compound 25

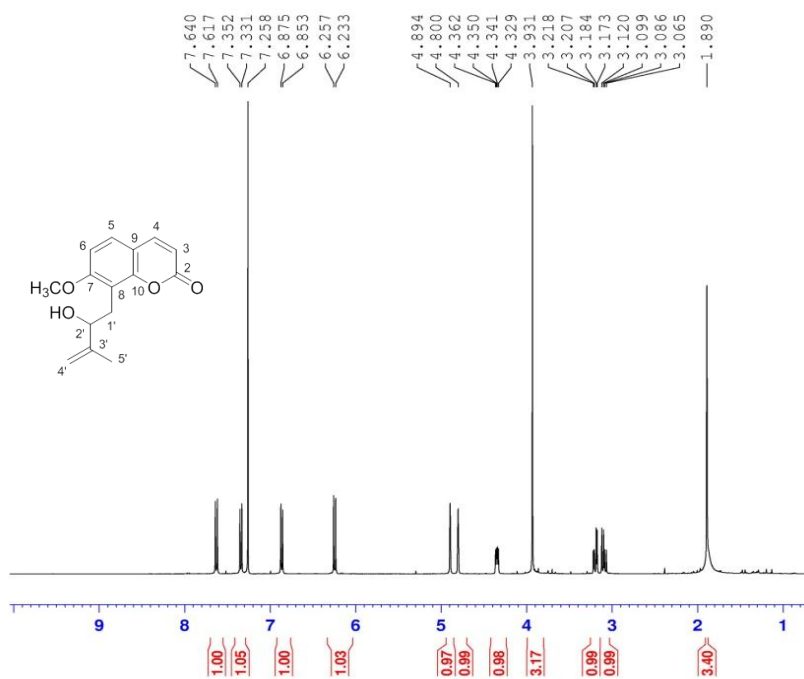


Figure A-50 The ^1H NMR spectrum (CDCl₃) of compound 26

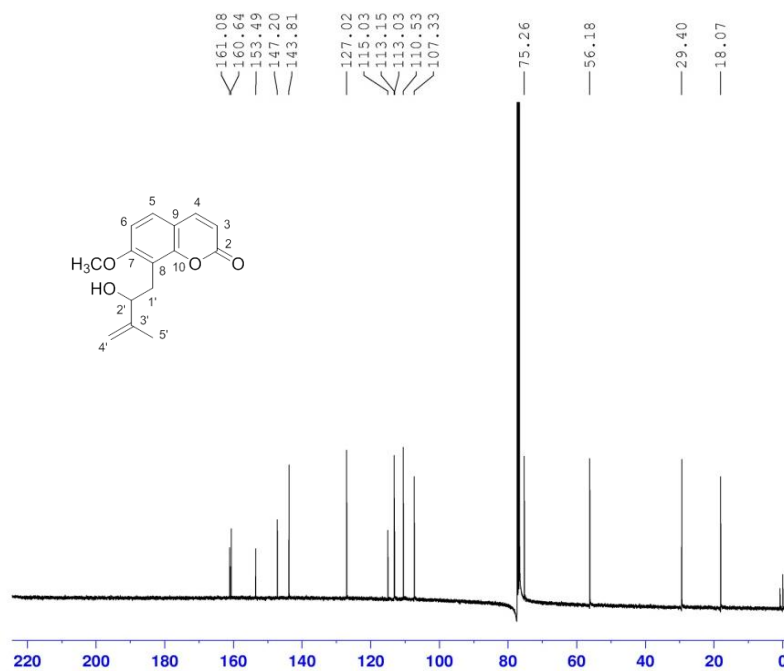


Figure A-51 The ^{13}C NMR spectrum (CDCl₃) of compound 26

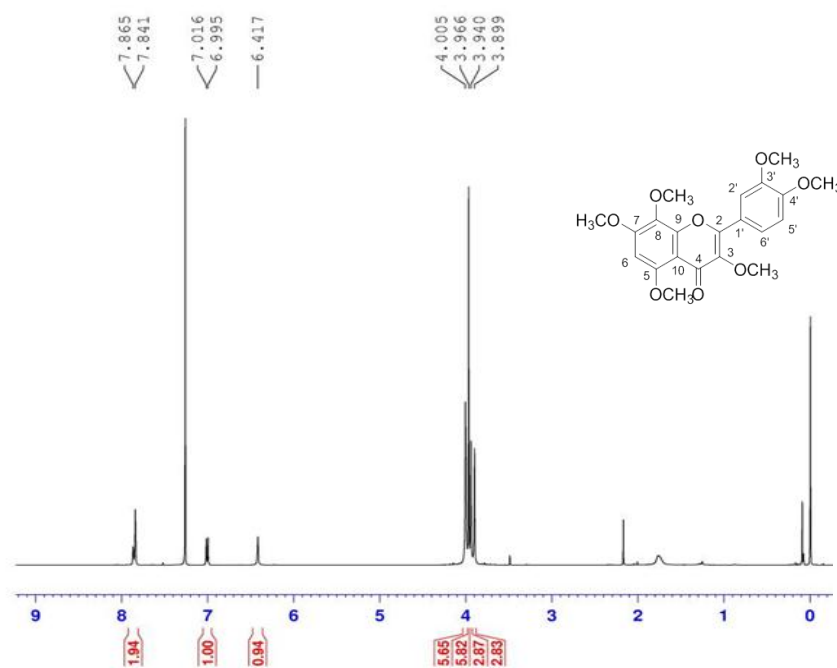


Figure A-52 The $^1\text{H NMR}$ spectrum (CDCl_3) of compound 27

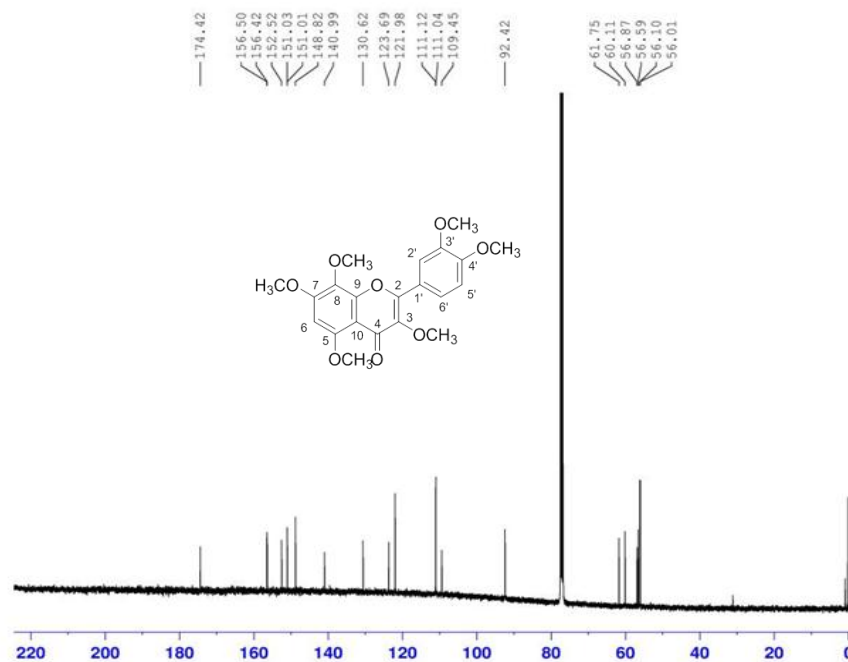


Figure A-53 The $^{13}\text{C NMR}$ spectrum (CDCl_3) of compound 27

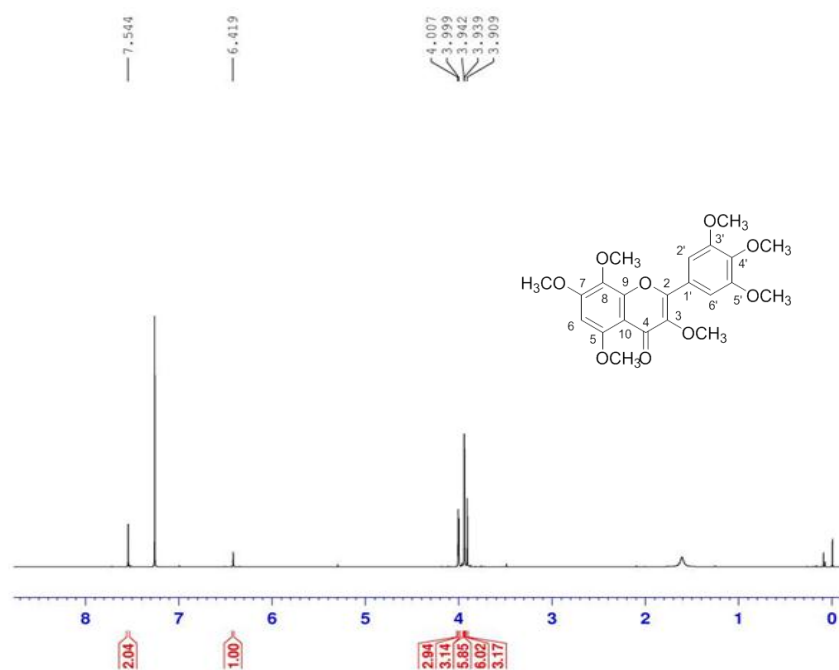


Figure A-54 The ^1H NMR spectrum (CDCl₃) of compound 28

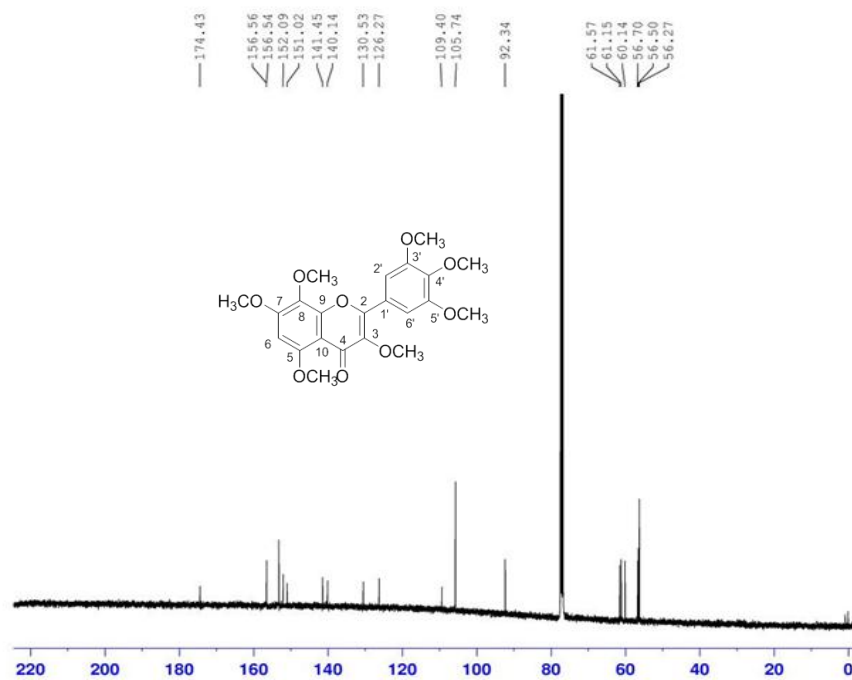


Figure A-55 The ^{13}C NMR spectrum (CDCl₃) of compound 28

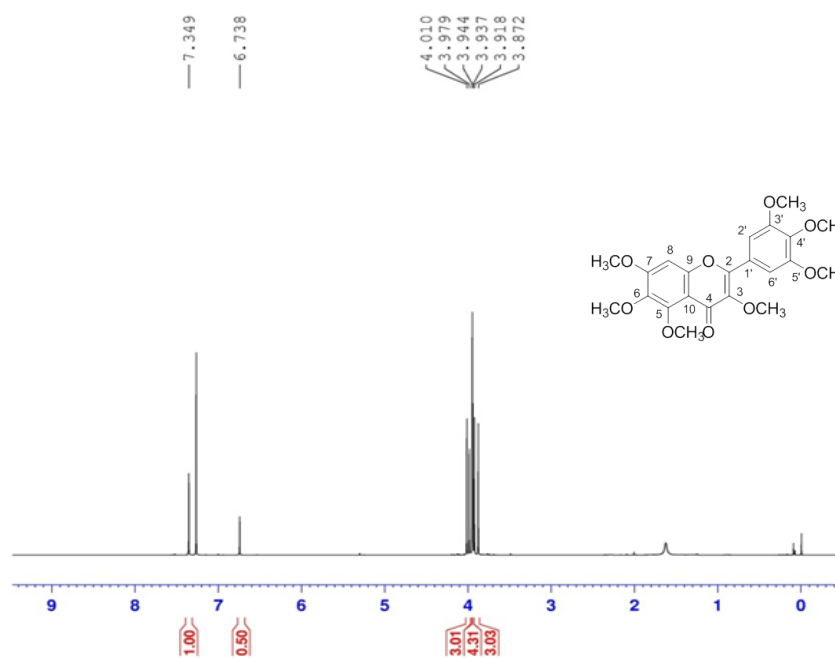


Figure A-56 The ^1H NMR spectrum (CDCl₃) of compound 29

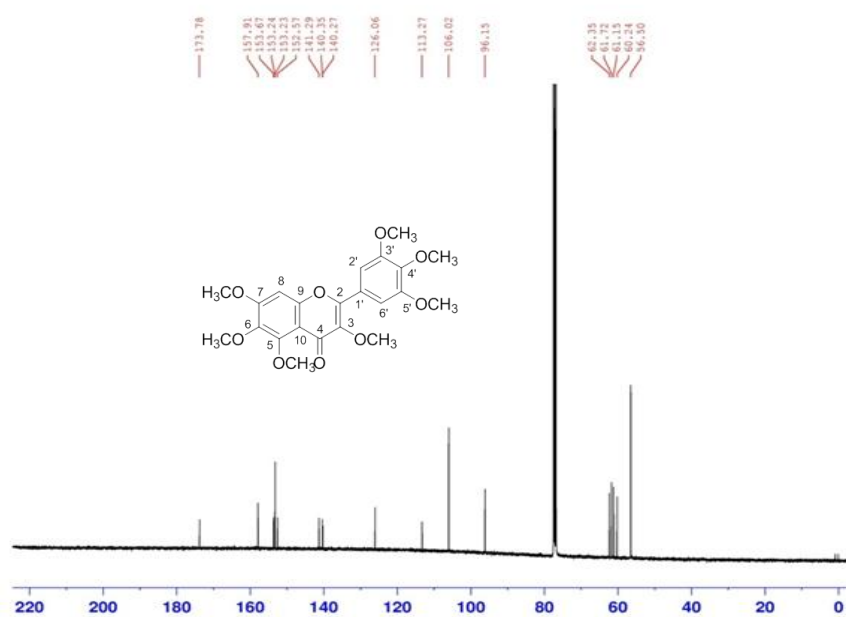


Figure A-57 The ^{13}C NMR spectrum (CDCl₃) of compound 29

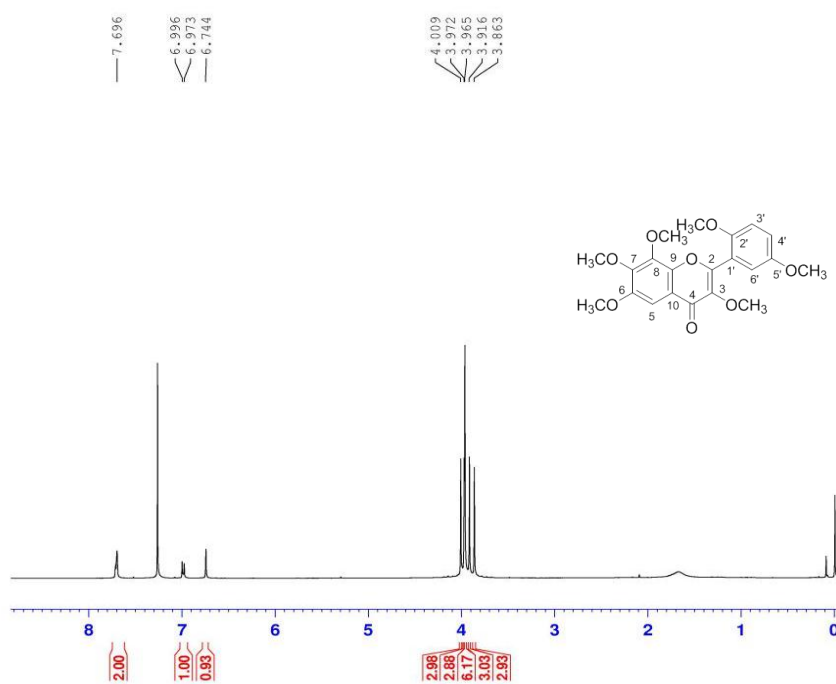


Figure A-58 The ^1H NMR spectrum (CDCl₃) of compound 30

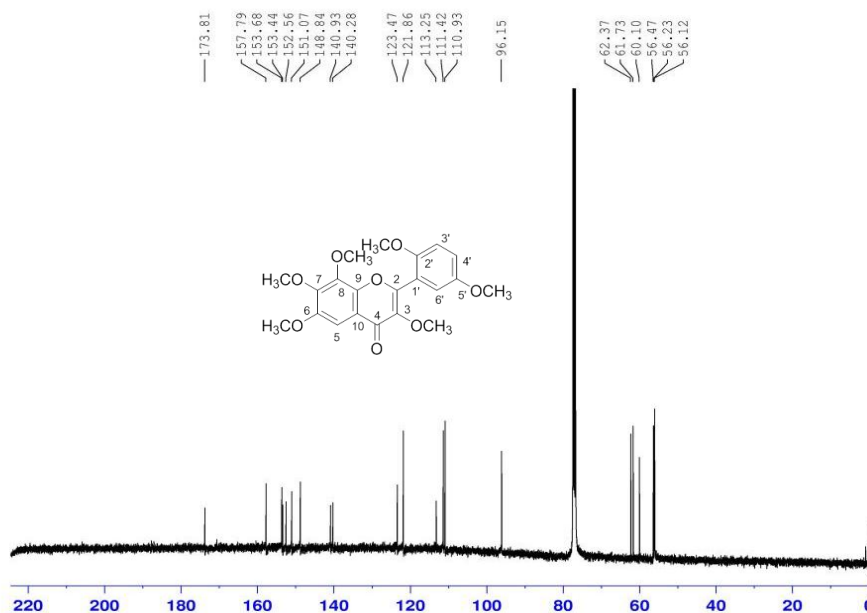


Figure A-59 The ^{13}C NMR spectrum (CDCl₃) of compound 30

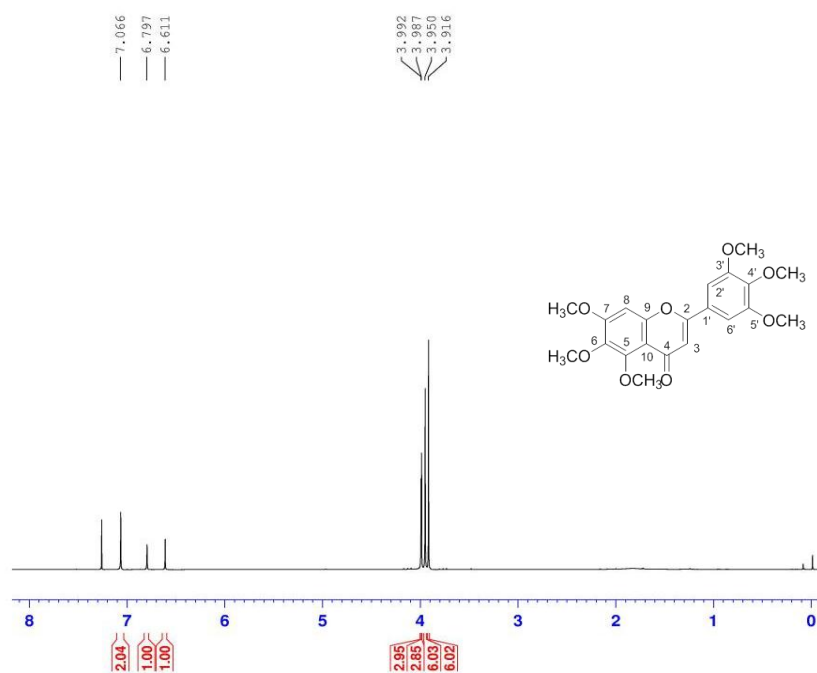


Figure A-60 The ¹H NMR spectrum (CDCl₃) of compound **31**

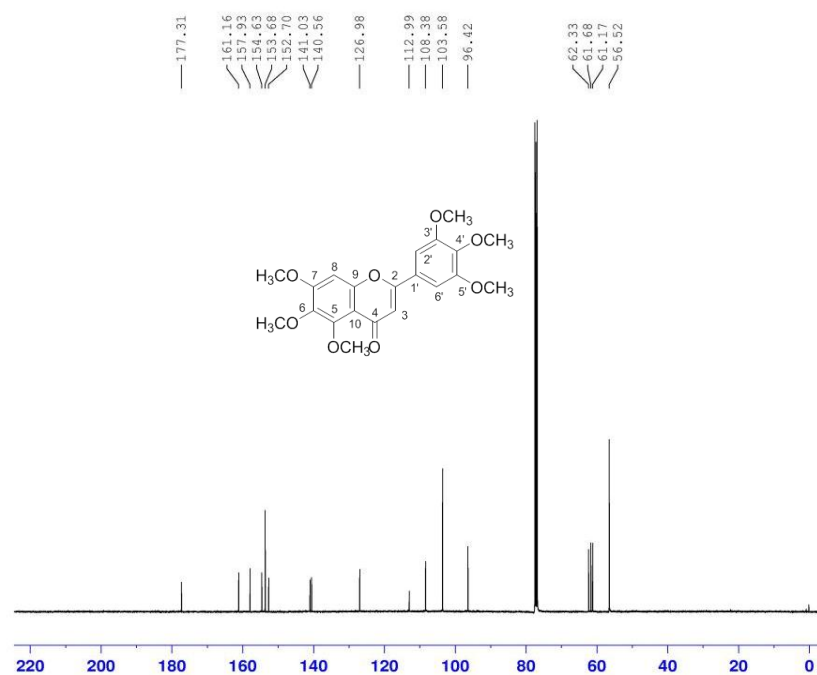


Figure A-61 The ¹³C NMR spectrum (CDCl₃) of compound **31**

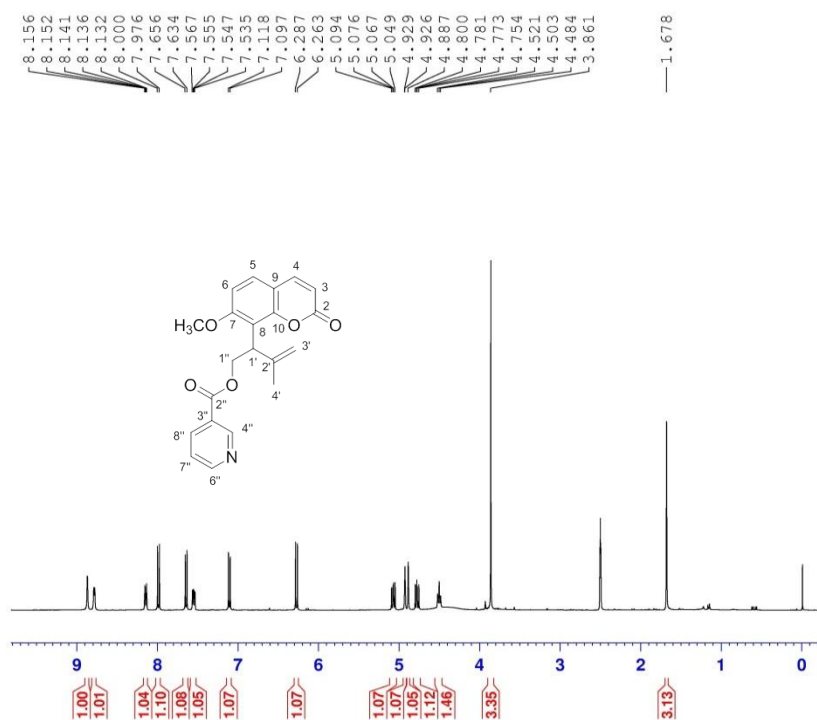


Figure A-62 The ¹H NMR spectrum (CDCl₃) of compound 32

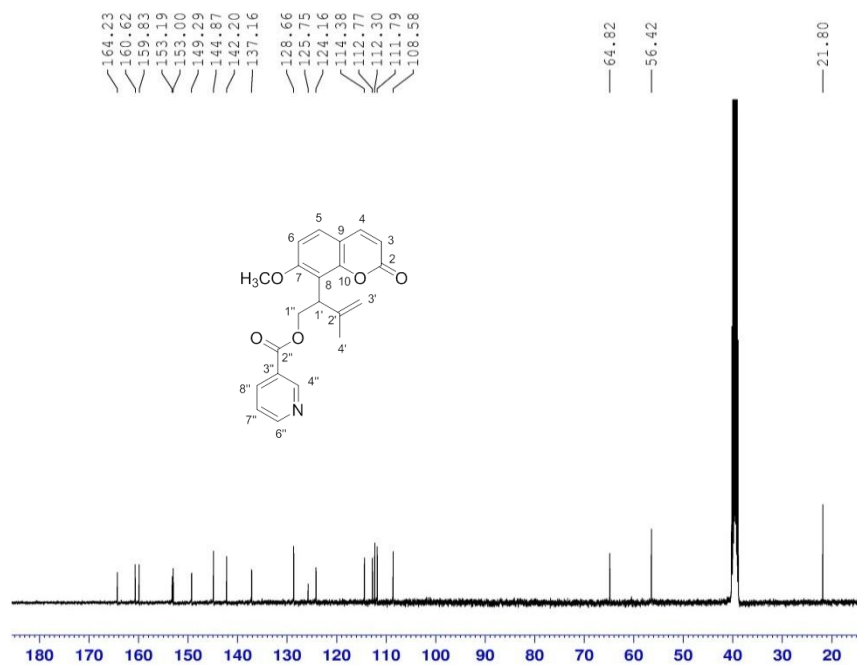


Figure A-63 The ¹³C NMR spectrum (CDCl₃) of compound 32

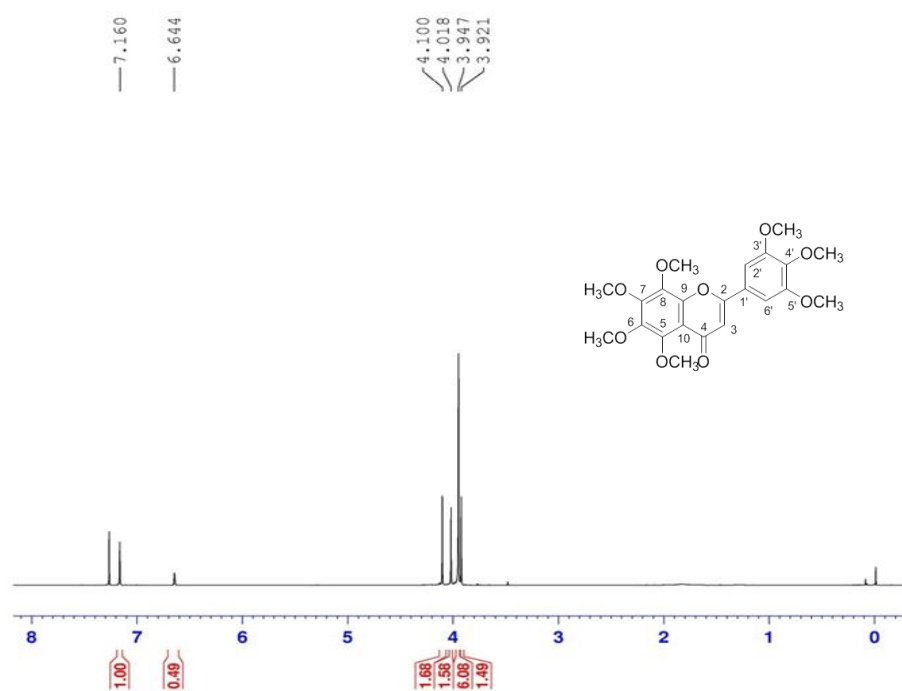


Figure A-64 The ^1H NMR spectrum (CDCl₃) of compound **33**

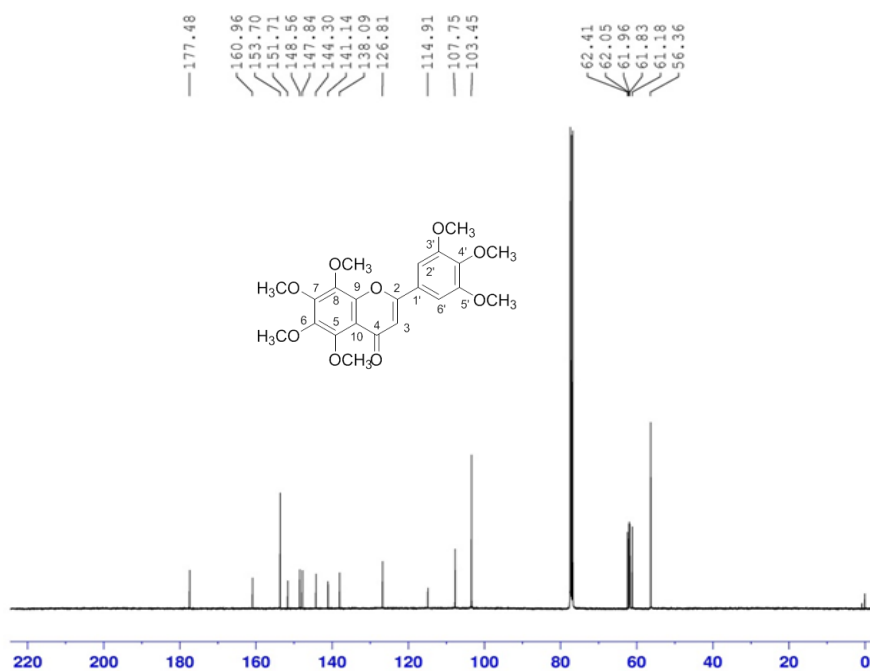


Figure A-65 The ^{13}C NMR spectrum (CDCl₃) of compound **33**

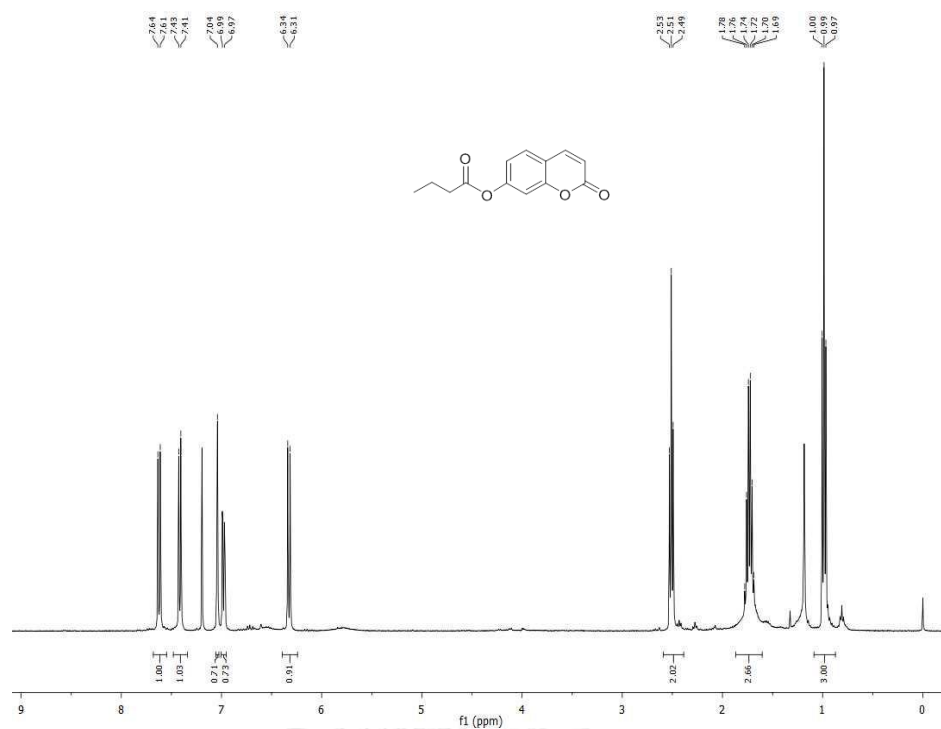


Figure A-66 The ^1H NMR spectrum (CDCl_3) of compound 34

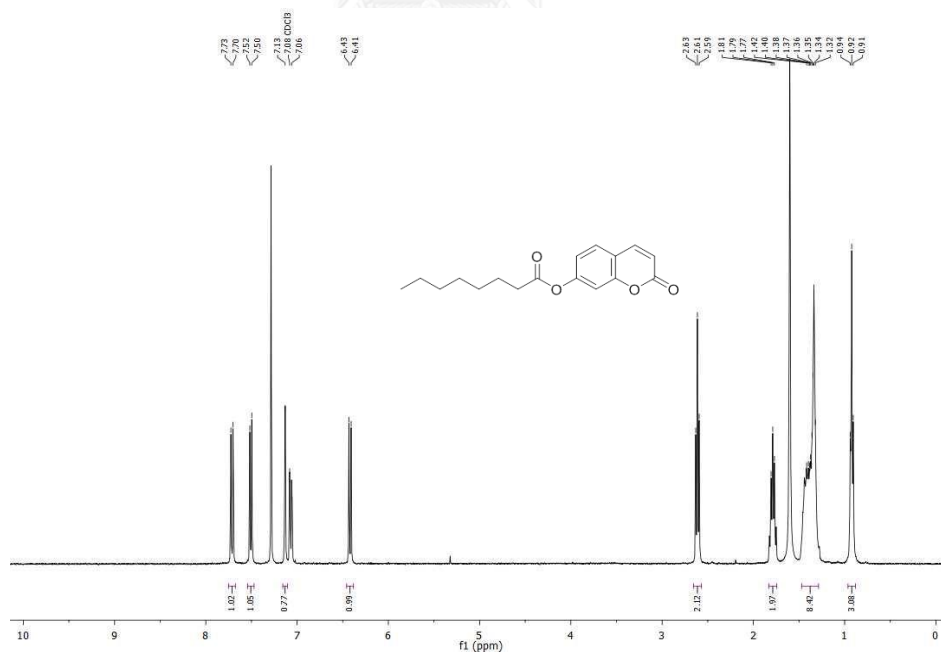


Figure A-67 The ^1H NMR spectrum (CDCl_3) of compound 35

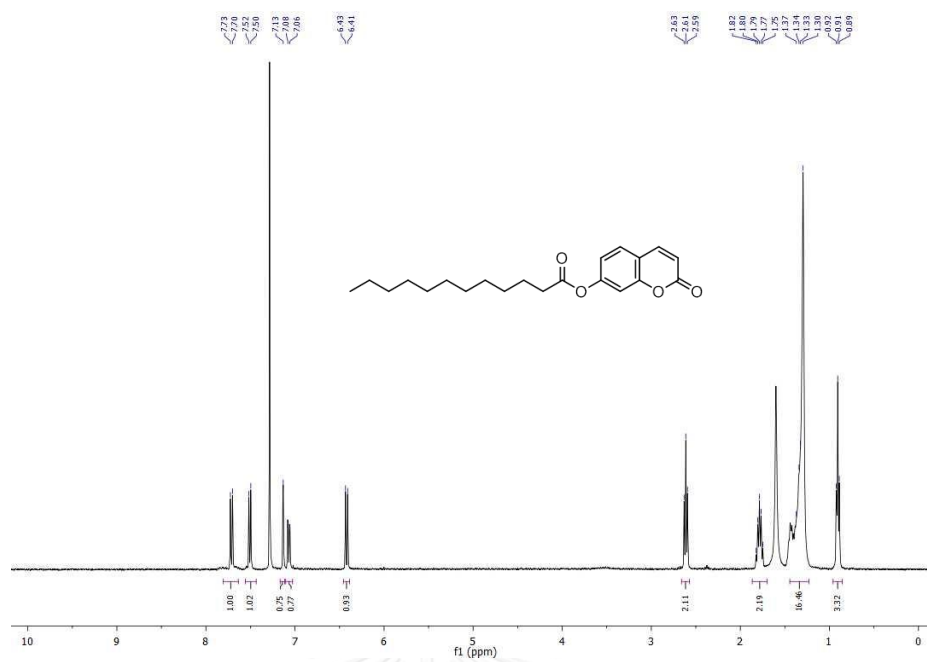


Figure A-68 The ^1H NMR spectrum (CDCl_3) of compound 36

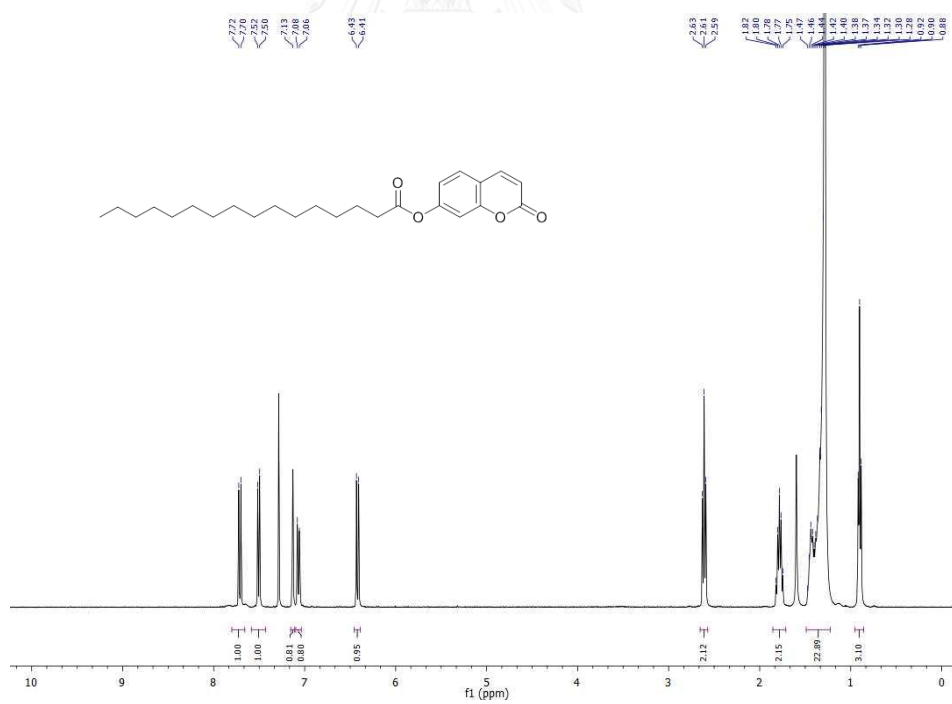


Figure A-69 The ^1H NMR spectrum (CDCl_3) of compound 37

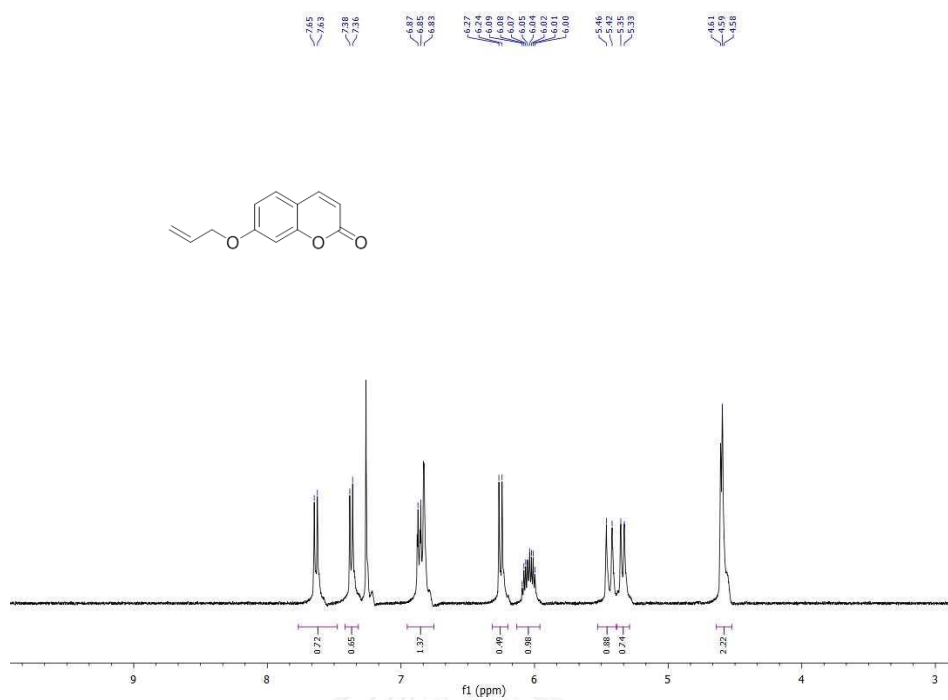


Figure A-70 The ¹H NMR spectrum (CDCl₃) of compound 38

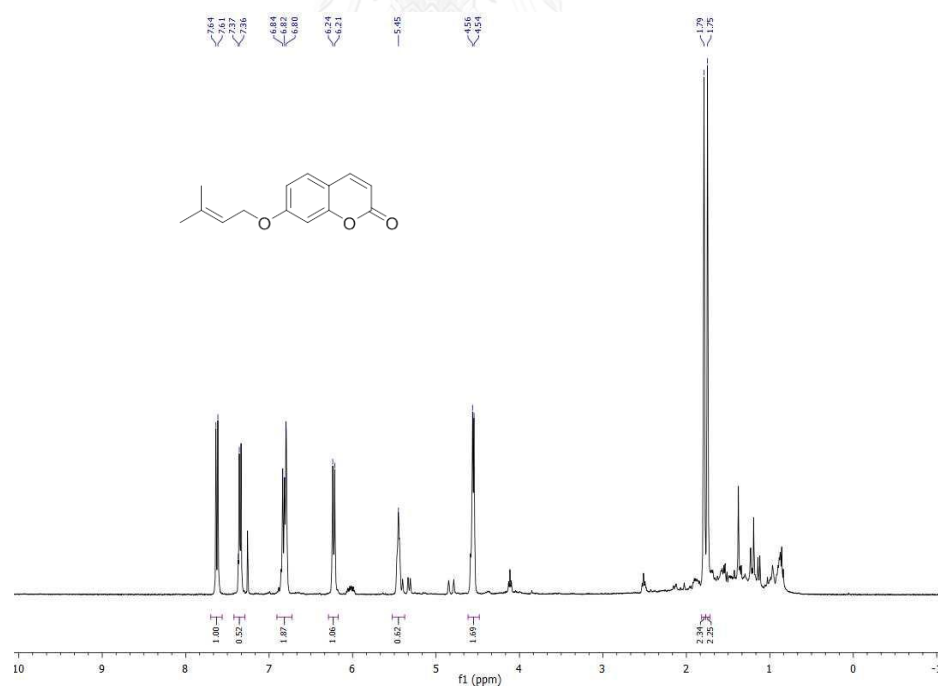


Figure A-71 The ¹H NMR spectrum (CDCl₃) of compound 39

VITA

Miss Nawara Samritsakulchai was born on November 24, 1991 in Nakhon Phanom, Thailand. She graduated with Bachelor's Degree of Science in Chemistry from Ubon Ratchathani University in 2014. After that, she continued her study for a master degree of Science in Organic Chemistry at the Department of Chemistry, Chulalongkorn University. During her study, she received a grant fund from Research Professional Development Project under the Science Achievement Scholarship of Thailand and Overseas Research Experience Scholarship for Graduate Student, Chulalongkorn University, Thailand. Her permanent address is 94 Thatphanom, Thatphanom, Nakhon Phanom, 48110, Thailand. E-mail: lichypeach@gmail.com

